



**Assessing the influence of time-since-death:  
Pilot scale kraft and thermomechanical pulping  
of beetle-killed lodgepole pine**

Barbara Dalpke, Ashif Hussein, Surjit Johal, Bernard Yuen,  
Darwin Ortiz and Paul Watson

**Mountain Pine Beetle Working Paper 2008-26**

Pulp and Paper Research Institute of Canada

3800 Wesbrook Mall

Vancouver BC  
Canada V6S 2L9

MPBI Project # 8.65

Natural Resources Canada  
Canadian Forest Service  
Pacific Forestry Centre  
506 West Burnside Road  
Victoria BC V8Z 1M5  
2008

© Her Majesty the Queen in Right of Canada 2008  
Printed in Canada

**Library and Archives Canada Cataloguing in Publication**

**Assessing the influence of time-since-death : pilot scale kraft and thermomechanical pulping of beetle killed lodgepole pine / Barbara Dalpke ... [et al.].**

**(Mountain pine beetle working paper ; 2008-26)**

**"MPBI Project # 8.65".**

**Includes bibliographical references: p.**

**Includes abstract in French.**

**ISBN 978-1-100-11466-8**

**Cat. no.: Fo143-3/2008-26E**

**1. Wood-pulp--British Columbia--Quality control. 2. Wood chips --British Columbia--Quality control. 3. Pulping--Economic aspects--British Columbia. 4. Lodgepole pine--Diseases and pests--Economic aspects--British Columbia. 5. Mountain pine beetle--Economic aspects--British Columbia. I. Dalpke, Barbara, 1973- II. Pacific Forestry Centre III. Series: Mountain Pine Beetle Initiative working paper 2008-26**

**SB945 M78 A86 2008**

**676'.121**

**C2008-980396-5**

## Abstract

Pilot plant kraft and mechanical pulping trials were carried out for a well controlled sample set to determine the influence of TSD of mountain pine beetle (MPB)-killed lodgepole pine on pulping and pulp quality. Samples included trees of red, grey and late grey attack stages as well as unattacked trees and sample sites were established in three different biogeoclimatic subzones in British Columbia, thus accounting for natural variability. Prior to pulping, samples were tested for wood and fibre properties as well as chip quality. Kraft and thermomechanical (TMP) pulping parameters were monitored, pulp quality was determined, and sheet structure was evaluated by scanning electron microscopy.

Wood and fibre quality showed little measurable influence from TSD other than a significant drop in moisture. Kraft pulping and pulp quality was also independent of TSD, although some influence on kink index was seen which could suggest a greater susceptibility to mechanical damage for fibres from MPB-killed wood. For TMP pulp, MPB-killed wood showed lower sheet density and possibly higher sheet roughness when compared to unattacked wood. Preliminary calendering and lintering tests also resulted in some differences, suggesting that runnability and printing quality of TMP paper may be affected.

The results of this study suggest that MPB-killed wood is an acceptable source of fibre for kraft pulping even at grey and late grey stages. However there are operational issues, including impacts on chemical recovery, that are being addressed in other projects. For TMP, such wood can be used with little penalty regarding pulping and strength parameters, however some effect on sheet structure and surface structure may exist which would be important in the printing paper sector. Thus, TMP results should be followed up with a more detailed study of printing behaviour of MPB-killed wood.

Keywords: mountain pine beetle, lodgepole pine, shelf life, fibre properties, pulp quality, chip quality, kraft and mechanical pulping, lintering

## Résumé

Des essais du procédé Kraft et de la réduction en pâte mécanique ont été réalisés dans une usine-pilote, pour un ensemble d'échantillons bien contrôlés, afin d'établir l'influence du temps écoulé depuis la destruction du pin de Murray par le dendroctone du pin ponderosa (DPP) sur la fabrication de la pâte à papier et la qualité de celle-ci. Les échantillons étaient composés d'arbres aux stades rouge, gris, à la fin du stade gris et d'arbres intacts. Des sites d'échantillonnage ont été créés dans trois différentes sous-zones biogéoclimatiques en Colombie-Britannique, afin de refléter la variabilité naturelle. Avant la fabrication de la pâte à papier, les propriétés du bois et des fibres des échantillons ont été testées, de même que la qualité des copeaux. Les paramètres du procédé Kraft et du procédé thermomécanique ont été surveillés, la qualité de la pâte établie et la structure de la feuille évaluée au moyen de la microscopie électronique à balayage.

Le temps écoulé depuis la destruction a eu une influence quasi impossible à évaluer sur la qualité du bois et de la fibre, si ce n'est la diminution considérable du taux d'humidité. Le temps écoulé depuis la destruction n'a pas non plus eu d'incidence sur le procédé Kraft et la qualité de la pâte, même s'il a quelque peu influencé l'indice de plissement, ce qui pourrait vouloir dire que les fibres du bois détruit par le DPP sont davantage sensibles aux dommages mécaniques. Pour la pâte fabriquée au moyen du procédé thermomécanique, la densité des feuilles fabriquées à partir de bois détruit par le DPP était inférieure et elles étaient plus rugueuses, comparativement au bois intact. Les tests préliminaires de calandrage et de piquetage se sont également traduits par des différences, suggérant que l'aptitude au passage sur machine et la qualité d'impression du papier produit au moyen du procédé thermomécanique pourraient être modifiées.

Les résultats de cette étude suggèrent que le bois détruit par le DPP est une source acceptable de fibres pour le procédé Kraft, même au stade gris et à la fin du stade gris. Il existe toutefois des problèmes opérationnels, notamment sur le plan du procédé de récupération chimique, lesquels sont abordés dans d'autres projets. Pour le procédé thermomécanique, il est possible d'utiliser ce bois sans que cela nuise trop à la fabrication de la pâte et à la résistance de celle-ci. Toutefois, ce bois pourrait endommager la structure des feuilles et de la surface, un facteur important pour les fabricants de papier d'impression. Par conséquent, il faudrait mener une étude approfondie pour établir la mesure dans laquelle le bois détruit par le DPP se répercute sur la qualité du papier destiné à l'impression.

Mots-clés: dendroctone du pin ponderosa, pin de Murray, durée de conservation, propriétés des fibres, qualité de la pâte, qualité des copeaux, procédé Kraft, réduction en pâte mécanique, piquetage

## Table of Contents

1	Introduction.....	1
2	Material and Methods .....	2
	2.1 Sampling.....	2
	2.1.1 Sampling matrix.....	2
	2.1.2 Field sampling.....	2
	2.2 Wood core testing.....	3
	2.2.1 Fibre quality analysis (FQA).....	3
	2.2.2 Moisture Content and Wood Density.....	3
	2.2.3 SilviScan Analysis.....	4
	2.2.4 Extractives.....	4
	2.2.5 Predictions from NIR measurements.....	4
	2.3 Pulping.....	5
	2.3.1 Harvesting and chipping.....	5
	2.3.2 Dendrochronology.....	5
	2.3.3 Kraft pulping.....	6
	2.3.4 Thermomechanical (TMP) pulping.....	6
	2.4 Pulp testing.....	7
	2.4.1 Pulp and handsheet testing of kraft pulps.....	7
	2.4.2 Pulp and handsheet testing of thermomechanical (TMP) pulps.....	7
	2.4.3 Calendering of thermomechanical (TMP) handsheets.....	7
	2.4.4 Linting evaluation of thermomechanical (TMP) pulps.....	7
	2.5 Microscopy work .....	8
3	Results and Discussion .....	9
	3.1 Sampling sites.....	9
	3.2 Core evaluation.....	10
	3.2.1 Fibre quality analysis.....	10
	3.2.2 Moisture Content and Wood Density.....	13
	3.2.3 SilviScan Analysis.....	15
	3.2.4 Extractives.....	18
	3.2.5 Near infrared range (NIR) measurements.....	19
	3.3 Selection of sites and trees for pulping trials.....	20
	3.4 Influence of attack stage on wood and fibre properties of selected sites.....	23
	3.5 Exact kill date determination for harvested trees.....	25
	3.6 Chip quality.....	26
	3.7 Kraft pulping.....	28
	3.7.1 Pulping parameters.....	28
	3.7.2 Pulp quality.....	30
	3.8 Thermomechanical (TMP) pulping.....	35
	3.8.1 Energy-freeness relationship.....	35
	3.8.2 Pulp quality.....	35
	3.8.3 Calendering and calendered handsheets quality.....	42
	3.8.4 Linting.....	47

4	Conclusions.....	50
5	Acknowledgements.....	52
6	Literature Cited.....	53
7	Contacts: .....	56
8	Appendices.....	57
	Appendix A.....	57
	Appendix B.....	63
	Appendix C.....	64
	Appendix D.....	70
	Appendix E.....	75

## List of Tables

Table 1. Sampling matrix of required sites for harvesting of pulp wood	2
Table 2. New sample sites and their characteristics.	9
Table 3. Sample sites for pulping trials.	21
Table 4. Density and fibre properties of individual trees selected for harvest and comparison to site averages.	21
Table 5. Main effect ANOVA analysis of site and attack stage-influence on wood and fibre properties.	23
Table 6. Time-since-death estimates compared to actual TSD as determined by dendrochronology.	25
Table 7. Fibre quality data for kraft fibres	31
Table 8. Univariate results from main effect ANOVA analysis showcasing the influence of site attribute and attack stage on kraft fibre quality.	31
Table 9. Selected fibre morphology values and resulting collapse index as represented by $G/E_T$ .	33
Table 10. ANOVA analysis for TMP pulp and handsheet properties with site attribute and attack stage as main effects.	36
Table 11. Required nip loads to reach set target PPS roughness values.	44
Table 12. Fibre morphology of R-14 and R-14/28 fractions for pulps from dry subzone sites at 100 ml CSF.	46
Table 13. PLPI numbers for samples from dry subzones at approximately 100 ml CSF.	47
Table 14. Results from Paplint testing for dry site samples.	48

## List of Figures

Figure 1. Map of interior British Columbia with sample site locations.)	10
Figure 2. Average length weighted fibre length of trees from new samples sites.	11
Figure 3. Average fibre coarseness of trees from new samples sites.	11
Figure 4. Fibre coarseness versus length weighted fibre length (LWFL) for samples from Trent et al. 2006 and this study.	12
Figure 5. Fibre coarseness versus length of individual trees, distinguished by site attributes.	13
Figure 6. Average wood density of trees from new sample sites.	14
Figure 7. Average moisture content of trees from new sample sites.	14
Figure 8. Moisture content versus TSD for all sample sites from Trent et al. 2006 and from this study.	15
Figure 9. Comparison of <i>G</i> -factor, as an important parameter for fibre conformability, of trees from new sample sites.	16
Figure 10. Average wood fibre coarseness of trees from new sample sites.	16
Figure 11. Average microfibril angle of wood fibres of trees from new sample sites.	17
Figure 12. Wood density of trees of new sites as measured by SilviScan averaged over age rings 60 – 80.	18
Figure 13. Average extractive content of trees from new sample sites.	19
Figure 14. Wood core moisture contents of green and red trees at site 18-01 as predicted from NIR measurements.	20
Figure 15. Average fibre length at sites selected for pulping trial compared by subzone.	24
Figure 16. Basic density of chip samples by subzone attribute.	26
Figure 17. Chip dry solids content for all chip samples.	27
Figure 18. Chip size distribution by Gradex classification.	27
Figure 19. Chip size distribution by Rader classification.	28
Figure 20. Kappa number versus H-factor for all pulp samples.	28
Figure 21. H-factor at kappa 30 for all pulp samples, grouped by subzone.	29
Figure 22. Pulp yield at kappa 30 for all pulp samples, sorted by site attribute.	29
Figure 23. Tensile index of kraft pulps at CSF = 400 ml grouped by subzone.	30
Figure 24. Cross-section and surface images of selected kraft handsheets before and after PFI mill refining.	34
Figure 25. Freeness versus energy relationship for all pulp samples.	35
Figure 26. BauerMcNett R-28 fraction as a function of CSF for all samples.	37
Figure 27. Fines (BauerMcNett P-200 fraction) at 100 ml CSF compared by subzones.	37
Figure 28. Sheet density as a function of CSF.	38
Figure 29. Tensile index as a function of CSF (a), and of apparent sheet density (b)	39
Figure 30. Brightness of TMP handsheets at 100 ml CSF.	39
Figure 31. ISO opacity of TMP handsheets at 100 ml CSF.	40
Figure 32. Scattering coefficient of TMP handsheets at 100 ml CSF.	40
Figure 33. Surface roughness of smooth sides of TMP handsheets at 100 ml CSF.	41
Figure 34. Surface and cross-section images taken with the ESEM of unattacked and red attack samples from the “dry” site.	42
Figure 35. Handsheet smoothing with increasing calendering nip load for samples from the dry subzone sites.	43
Figure 36. Sheet density as a function of PPS roughness for dry site samples.	45



Figure 37. Tensile index as a function of PPS roughness for dry site samples.	45
Figure 38. Opacity as a function of PPS roughness for dry site samples.	46
Figure 39. Accumulated fibre length $L_{AT}$ of linting material for dry site samples.	49
Figure 40. Lint material of the “dry”, late grey sample (site 01-01) calendered to 3.5 $\mu\text{m}$ PPS S10 roughness.	50
Figure 41. Average wood fibre diameter of trees from new sample sites (60 – 80 year age class), measured by SilviScan.	57
Figure 42. Average fibre wall thickness of trees from new sample sites (60 – 80 year age class), measured by SilviScan.	57
Figure 43. Total acetone extractives found at all sample sites of MPBI projects 8.15 and 8.65, as a function of TSD as estimated from tree appearance (extractive values shown are site averages).	58
Figure 44. Basic wood density for the 60 – 80 years age class of sites selected for pulping trials, determined by SilviScan.	58
Figure 45. Wood fibre diameter for the 60 – 80 years age class of sites selected for pulping trials, determined by SilviScan.	59
Figure 46. Wood fibre cell wall thickness for the 60 – 80 years age class of sites selected for pulping trials, determined by SilviScan.	59
Figure 47. Wood fibre coarseness for the 60 – 80 years age class of sites selected for pulping trials, determined by SilviScan.	60
Figure 48. Specific surface area for the 60 – 80 years age class of sites selected for pulping trials, determined by SilviScan.	60
Figure 49. Microfibril angle for the 60 – 80 years age class of sites selected for pulping trials, determined by SilviScan.	61
Figure 50. Collapsibility geometrical factor $G$ for the 60 – 80 years age class of sites selected for pulping trials, determined by SilviScan.	61
Figure 51. Fibre coarseness after maceration for the 60 – 80 years age class of sites selected for pulping trials, determined by FQA.	62
Figure 52. Pulp yield as a function of kappa number for all pulp samples.	64
Figure 53. Consumed effective alkali as a function of kappa number for all pulp samples	64
Figure 54. Fibre length distribution (length weighted fibre length) of all pulp samples at kappa 30 and before PFI mill refining.	65
Figure 55. Fibre width distribution of all pulp samples at kappa 30 and before PFI mill refining.	65
Figure 56. Surface and cross-section images of TMP sheets from “wet” sites.	75
Figure 57. Surface and cross-section images of TMP sheets from “moist” sites.	76
Figure 58. Surface and cross-section images of TMP sheets from “dry” sites.	77



## **1 Introduction**

The question of paramount importance in the handling of the mountain pine beetle (MPB)-killed wood resource in British Columbia is that of shelf-life, being defined as the time span that dead wood can still be harvested and utilized without compromising product quality and process economics. The sheer volume of dead timber from the mountain pine beetle epidemic could supply the forestry sector in B.C. with raw material for many years to come, provided the trees retain their economic value. In order to direct future harvest efforts efficiently, information is needed regarding the maximum allowable time infested trees can remain unharvested before loss in economic value due to irreversible loss of quality occurs. Such questions regarding the shelf-life of dead standing timber need a differentiated approach, as requirements regarding the quality of wood and thus shelf-life, differ by forestry sector and end-use application. Research is underway to address shelf-life estimates for MPB-killed timber for the solid wood sector, where moisture content and checking are the most pressing issues. This work presents a similar effort to identify shelf-life issues concerning the pulp and paper industry, which forms an important part of B.C.'s integrated forestry sector. The use of wood that has exceeded its shelf-life would result in lower pulp quality, thus diminishing market access for B.C.'s pulp and paper industry. The ensuing economic impacts cannot be tolerated and therefore such wood has to be diverted from pulping operations. The answers to shelf-life questions with regards to both solid wood and pulp and paper sectors can be combined and will form the basis for future harvest planning based on sound economics, allowing for the most effective harvesting of MPB-killed timber over the long term.

An initial study to clarify some of the shelf-life issues related to the pulp and paper industry was undertaken by Paprican in previous work (Trent et al. 2006). Wood and fibre qualities that are important to pulping operations were determined for MPB-killed trees from different biogeoclimatic zones, thus accounting for the ecological diversity of the province of B.C., and of different times since death. However, no direct linkage of these fibre properties with pulp quality was investigated. Also, little is known about the influence of changing wood and fibre quality on the pulping process itself.

To better understand such an influence on the pulping process and the mechanism of pulp quality deterioration with time-since-death (TSD) for MPB-killed wood, and to be able to link pulp quality deterioration to variables investigated in previous work, pilot kraft and thermomechanical (TMP) pulping trials and related pulp quality testing were undertaken. A well designed sampling scheme of four different TSD categories by three different biogeoclimatic zones was used to establish influence of TSD on pulp properties while also accounting for natural variability related to ecological conditions. Pulp quality was evaluated through wood fibre and handsheet testing. Pulping variables were monitored to establish any changes in pulping behaviour. Additional testing including a microscopic evaluation of sheet structure, and tests of the linting propensity of TMP pulps were employed to further understand and explain the observations from handsheet testing.

## 2 Material and Methods

### 2.1 Sampling

#### 2.1.1 Sampling matrix

A sampling matrix was established that includes four different stage-of-attack categories and three different groups of sites with attributes that provide different growth conditions. With such a sampling scheme, the influence of TSD of MPB-killed lodgepole pine on pulp properties can be established, while the effect of natural variability is also included. The sampling matrix is shown in Table 1 To take advantage of sample sites that have been established in previous work (Trent et al. 2006, and Dalpke et al. 2007), the subzones were selected to maximize the number of existing sample sites while at the same time providing meaningful differences between growth conditions of the three site groups. As a result, the sampling matrix includes four sites established as part of Trent et al. 2006, two sites for which the pulping data is available from the related project Dalpke et al. 2007, and five sites that had to be newly established (three of them were sites with unattacked trees which have not been included in any previous projects). A late grey stage site in a wet, cool subzone could not be established due to the dynamics of the mountain pine beetle infestation, which has affected such subzones only in recent years.

**Table 1.** Sampling matrix of required sites for harvesting of pulp wood

	Dry, cold climate Low site productivity	Moist, cold climate Medium site productivity	Wet, cool climate Medium site productivity
Green trees (unattacked)	New site	New site	New site
Red attack	New site	Existing pulping data	Existing pulping data
Early grey stage	Established site	New site	Established site
Late grey stage	Established site	Established site	Not found

The four stage-of-attack categories were chosen according to the following criteria. Red attack refers to trees with needles turned red but having at least some foliage remaining, grey stage includes trees that lost all needles and may start to loose small branches, late grey stage refers to trees that lost all needles as well as almost all small branches. The four categories are supposed to represent different TSD brackets, however it is well known that outer tree characteristics are not always a good indicator of TSD (Lewis et al. 2006). Actual kill dates of trees that were used in the pulping trials were determined later by dendrochronology, but this data was not available when selecting sample sites.

#### 2.1.2 Field sampling

Initial sample site selection was done with the help of local contractors according to the criteria outlined in Table 1 using forest stand composition and BEC maps, taking also into account beetle spread history over the last years. Intact stands within the SBS (sub boreal spruce) and SBPS (sub boreal pine-spruce) zones (Banner et al. 1993, DeLong, 2003, Steen and Coupé 1997) composed of mature pine as the leading species were targeted. Site accessibility was another criterion. Potential sample sites were checked in

the field and ten sites (two for each required new samples site) were established across the Vanderhoof, Williams Lake, Fort St. James and Nadina forest districts in B.C.

At each site, the plot centre location was marked with either a stake or by marking a tree as plot centre, and global positioning system (GPS) co-ordinates were recorded (GPS co-ordinates were recorded in decimal degrees using the WGS\_84 datum) (Snyder 1987). Ten mature, dominant or co-dominant lodgepole pine trees (*Pinus contorta* Dougl. Ex Loud. var. *latifolia* Engelm.) were marked at each site and two, 12-mm increment cores were taken from breast height (1.3 m) through the pith from bark to bark of each tree. Height and diameter were measured for each tree. A biogeoclimatic classification to the site series level was completed, which includes determination of soil moisture and nutrient regimes, measuring of site data and shrub, herb and graminoid vegetation attributes. Site productivity was quantified using SIBEC (site index using biogeoclimatic ecosystem classification, with site index a measure of potential site productivity based on tree height at 50 years of age). A preliminary determination of TSD of the beetle-killed trees was done based on tree appearance (amount of needle, bark and small branches lost) and general information about time of beetle attack in the area.

## **2.2 Wood core testing**

All increment cores that had been collected from newly established sites were tested for wood and fibre properties by fibre quality analysis (FQA) and SilviScan analysis. Also, wood moisture, density, extractives, decay and blue stain were determined.

In addition to the cores from new sites, cores were taken from trees that were harvested from sites established in previous projects. These cores were analyzed for extractives, moisture, decay and blue stain only. It was shown by Trent et al. (2006) that other wood and fibre properties are not influenced by TSD, thus the core data (FQA and SilviScan) of 10 trees of each site that were determined previously in the respective projects can be used.

### **2.2.1 Fibre quality analysis (FQA)**

For FQA of wood cores, annual growth rings were counted and three age classes were cut out. These age classes represented mature wood sections from each stem and include ranges of 40 to 60 years, 60 to 80 years and 80 to 120 years.

Each section was first cooked in water for a period of four hours at a temperature of 120°C. Following this, the sections were macerated in a solution of equal parts hydrogen peroxide and glacial acetic acid for a period of 48 hours at a temperature of 70°C. The resultant pulp was dispersed using a Hamilton Beach mixer and diluted to a target consistency. Each sample was analyzed in duplicate on the standard FQA Fibre Quality Analyzer (OpTest Equipment Inc.) to determine length weighted fibre length (LWFL) and fibre coarseness (Allen 1999).

### **2.2.2 Moisture Content and Wood Density**

Green and oven-dried (o.d.) mass was measured for all cores, and moisture content (MC) was calculated as percent moisture of green wood (Equation 1).

$$\text{MC [\%]} = [1 - (\text{o.d. mass}/\text{green mass})] * 100 \quad (\text{Equation 1})$$

Average wood density was determined volumetrically by estimating green core volume based on measured core length and a 12-mm core radius as given by the core borers. Density is given as basic density, which is based on o.d. mass:

$$\text{Basic density [kg/m}^3\text{]} = \text{o.d. mass [kg]}/\text{green core volume [m}^3\text{]} \quad (\text{Equation 2})$$

### **2.2.3 *SilviScan Analysis***

The SilviScan system is a suite of instrumentation designed for the rapid and non-destructive assessment of wood and fibre properties on solid wood, using image analysis, x-ray densitometry and diffraction to measure fibre diameter, wood density and microfibril angle from wood cores (Lawrence and Woo 2005). Cell wall thickness and coarseness are calculated assuming a constant cell wall density of 1500 kg/m<sup>3</sup>. Properties are measured as profiles over the length of a core with a resolution of 25 µm. These profiles can be used as measured, or they can be averaged to create mean values for the whole core or specific core section. For this report, we report values averaged over the 60 – 80 year age rings unless stated otherwise.

For sample preparation, the cores were ethanol dehydrated directly upon receipt to prevent fungal growth and to minimize fibre collapse and internal checking. After air-drying, the cores were debarked and shipped to CSIRO in Australia for additional preparation and SilviScan analysis. A more detailed description of the SilviScan techniques and measurements used for MPB-related projects at Paprican can be found in Trent et al. (2006).

### **2.2.4 *Extractives***

Total acetone extractive content was obtained using a modified version of TAPPI standard method T280 pm-99. The core samples were placed into Soxhlet thimbles and extracted for 6 hours with 200 ml of acetone after which the extracts were concentrated down to approximately 10 ml using a rotary evaporator. The extracts were filtered through a Pasteur pipette packed with glass wool, into a pre-tared scintillation vial. Further concentration of the extract residue was performed by passing a stream of nitrogen gas into the vial while warming (40-45°C), resulting in 1 ml of residue. This was freeze-dried to eliminate any remaining moisture and weighed to obtain the total content of extractives present in the core sample.

### **2.2.5 *Predictions from NIR measurements***

Near-infrared range (NIR) data was obtained on the cores at 1 cm increments, using a LabSpec Pro vis-NIR spectrometer equipped with a straight probe (3 mm aperture, creating a 5-mm diameter measuring spot size). The NIR data were used to predict decay and blue stain extent, based on a chemometric PLS1 model developed in related work. Detailed experimental procedures as well as information about the model are given in Hsieh et al. 2006. The model also provides moisture and density predictions. The laboratory NIR measurements were chosen over the use of an in-field probe as they provide more accurate predictions. The standard error in prediction (SEP) for the site

averaged predicted decay values is 2.6%, compared to a 2% error cited for the reference method (a 1% caustic solubility method according to TAPPI Standard T212 om-9). Moisture can be predicted with a SEP of 1.7% (compared to 1.3% of the standard method), and bluestain, given as D-b\*, with a SEP of 2.4 (TAPPI standard: 0.4). Only density predictions show a much larger error of 45 kg/m<sup>3</sup>, compared to 5.6 kg/m<sup>3</sup> for the TAPPI standard method. For the moisture predictions, it should be noted that the model was only validated up to 28% moisture content; values above may be used to discuss trends, but should not be seen as absolute values.

## **2.3 Pulp**

### ***2.3.1 Harvesting and chipping***

Based on results from site and core evaluation, five of the ten newly established sample sites were selected for harvesting. For these five sites plus the four sites established in previous work, three trees per site were selected for harvesting based on wood and fibre properties determined from the wood cores. The trees were selected to represent average tree properties on each site. For some sites (sites of the moist/cold site series), up to ten trees per site were selected as the wood was also used in related work (Hu et al. 2007A), however care was taken to exclude trees that deviated noticeably from stand average properties.

Trees were harvested, bucked into 1.2 m length pieces, and the lowest three to six pieces of each tree were transported back to the Vancouver laboratory. From each tree, a sample disc was taken before trees were debarked by hand and slabbed on a portable woodmizer<sup>TM</sup> sawmill to separate juvenile from mature wood. Only the mature wood (> 40 years) of each tree was chipped using a 36-inch 10-knife C.M.&E. disc chipper, representing the sawmill residual chip supply of most pulp operations in B. C. For each site, equal amount of chips from each tree were well mixed creating a total of nine samples.

### ***2.3.2 Dendrochronology***

Before debarking, disc samples were taken from harvested trees and shipped to the University of Northern B.C. for determination of kill date by crossdating (Lewis et al. 2006). Samples included discs from all harvested dead trees plus three discs from live trees for validation of the method. Discs were prepared following standard dendrochronology techniques (Stokes and Smiley 1968). Individual ring-width series were measured to the nearest 0.001 mm using the Velmex System (Velmex, Inc. 1992) and MeasureJ2X (VoorTech Consulting 2004). Series were crossdated by matching ring-width patterns against ring-width chronologies developed for lodgepole pine within the study area. The computer program COFECHA (Holmes 1983) was used and each sample was inspected to detect measurement and crossdating errors. After each tree was dated, it was assumed that the outer ring was the last ring formed prior to mortality if the bark was intact, or if the sapwood was present and firm. Confidence in the mortality dates were rated in four categories, including: (1) not datable; (2) dated but highly suspect; (3) dated with some concerns and; (4) dated with no concerns. Of all samples, four samples were

considered not datable, one was dated but highly suspect, eight were dated with slight concerns and 20 were dated with no concerns.

### **2.3.3 Kraft pulping**

For kraft pulping, aliquots from each of the nine samples were air-dried to about 90% solid content. Chip size distribution of each sample was classified using a Gradex chip classifier and the method described by Hatton (1979). Chips were also classified for their thickness range using the Rader chip thickness classifier, and later screened in a Wennberg chip classifier to obtain accept chips in the thickness range of 2 – 6 mm. Accept chips were well mixed before representative samples were taken for kraft pulping. Chip densities were determined on whole chip samples by a modified PAPTAC (Pulp and Paper Technical Association of Canada) method A.1H.

Three representative aliquots of accept chips from each of the nine samples were kraft cooked in bombs (50 gram, o.d. charge) within a B-K micro-digester assembly (Keays and Bagley 1970) to determine kappa number versus H-factor.

The cooking conditions were as follows:

Time to maximum temperature	:	135 minutes
Maximum cooking temperature	:	170°C
Effective alkali, % o.d. weight of wood	:	16
% Sulphidity	:	25
Liquid to wood ratio	:	4.5:1
H - Factor	:	900 - 1500

All the pulps produced were washed, o.d. and weighed to determine pulp yield. Pulp kappa number and residual effective alkali were determined by standard procedures. From these results the optimum cooking conditions required to produce kraft pulps at  $30 \pm 1$  kappa number were estimated by fitting regression lines through each set of data ( $R^2 > 0.95$ ). Large quantities of kraft pulp were subsequently produced in a 28L Weverk laboratory digester.

### **2.3.4 Thermomechanical (TMP) pulping**

For TMP pulping, aliquots from each of the nine original chip samples were screened on a Burnaby Machinery and Mill Equipment Ltd. two-deck laboratory chip classifier to remove oversize ( $>32$  mm) and fine ( $<8$  mm) material, and chip solid content was determined. The samples were then refined in a 30.5 cm Sunds Defibrator TMP 300 single-disc laboratory refiner. A Labview 6.02 PC system was used to control and/or monitor the refining variables. Pertinent first-stage refining conditions are shown below:

Plates	rotor, No. 3809 modified stator, No. 3804 modified
Preheater pressure	152 kPa



Refiner housing pressure	179-193 kPa
Chip presteaming time	10 min (atmospheric pressure)
Preheater residence time	10 min
Prex compression ratio	3:1
Refining consistency	24 to 27% o.d. pulp (cyclone exit)

The high freeness first-pass pulps were given one to three further passes in a 30.5 cm Sprout Waldron open-discharge laboratory refiner equipped with type D2A507 plates at 17 to 25% refining consistency. Pulps at three different energy/freeness levels were produced from each of the nine different chip furnishes in the Canadian standard freeness range from 62 to 205 ml CSF.

## **2.4 Pulp testing**

### ***2.4.1 Pulp and handsheet testing of kraft pulps***

The kraft pulps produced were disintegrated, washed, screened through an 8-cut screen plate and thickened in a centrifuge for storage. Fibre properties, including distributions of fibre length and diameter, of kraft pulps at 30-kappa number were analyzed using the new high resolution FQA Fibre Quality Analyzer. Four point beating curves were constructed using PFI mill runs of 0, 3,000, 6,000 and 12,000 revolutions according to PAPTAC standard C7. Canadian standard freeness was determined for each point according to PAPTAC standard C1. Handsheets were formed and tested for physical and optical properties using PAPTAC standard methods.

### ***2.4.2 Pulp and handsheet testing of thermomechanical (TMP) pulps***

After latency removal, each of the 27 pulp samples was screened on a 6-cut laboratory flat screen and screen rejects were determined. Bauer-McNett fibre classifications were determined on screened pulps. Fibre lengths of screened pulps were also determined on the standard FQA instrument using representative samples from each of the pulp. Handsheets were prepared with white water recirculation to minimize the loss of fines and tested for structural, mechanical and optical properties using PAPTAC standard methods. Handsheet roughness was measured by a Sheffield instrument and the values obtained are expressed in Sheffield Units (SU).

### ***2.4.3 Calendering of thermomechanical (TMP) handsheets***

Handsheets were calendered in a hard-nip laboratory calender at 50 m/min machine speed and a roll temperature of 50°C. The circular handsheets were trimmed to rectangular strips and then fed through the calender. Calibration curves for roughness versus nip load for each sample were obtained by calendering at a range of nip loads from 0 to 200 kN/m (three sheets per point). From the calibration curves, required nip loads to reach the target roughness of 3.5 and 4.0 µm PPS S10 roughness (PAPTAC standard) are calculated. A larger number of handsheets were then calendered to target roughness for use in the Paplint test, as well as for determining handsheet properties of calendered sheets.

### ***2.4.4 Linting evaluation of thermomechanical (TMP) pulps***

Linting is defined as the removal of loosely bonded particles from the surface of the sheet when paper is in contact with water based ink on the printing press. It was shown by

Wood and Karnis (1992) that linting is caused by particles with low specific surface area. These particles also have low bonding potential. Both fines content and long fibre development (external and internal delamination) affect the specific surface area of mechanical pulps. The majority of low specific surface particles in mechanical pulps are fibre fragments, shives and ray cells. The bonding potential of these particles is weak, thus, if found on the surface of the paper, they are easily removed in the printing process, causing linting.

Two different methods were used to evaluate the linting propensity of a subset of the collected samples. The PLPI test is a fractionation of the pulp suspension based on specific surface area. Linting propensity is quantified based on the assumption that the low surface area fraction may cause linting. It is thus an indirect test of linting propensity. The Paprican lint test (Paplint) is a direct method of measuring linting propensity by feeding a paper sample through a laboratory scale press nip using an ink of certain tackiness and measuring the amount of material that is removed.

#### ***Pulp linting propensity index (PLPI) test***

Pulp linting propensity index (PLPI) is measured using the technique developed by Wood and Karnis (1992). The principle of the PLPI technique is to fractionate the pulp in a series of hydrocyclones to remove the low specific surface area fraction of the pulp. The specific surface area of the particles is then determined by measuring turbidity at a known consistency (Wood and Karnis 1996). The PLPI, which is the fraction of the material with a specific surface below a defined limit of  $4 \text{ m}^2/\text{g}$ , is then calculated based on the amount and specific surface area of the low specific surface material.

#### ***Paprican lint test***

The Paprican lint test (Paplint) is described in detail in PAPTAC Useful Method L.5U. An IGT Model AIC2-5 printability tester was used to perform the tests. A layer of  $5 \text{ g/m}^2$  Paprican lint test oil, containing 12% resins, was applied to the 5-cm wide printing disc of the tester. This oil represents a commercial ink, however without the pigment. A strip of paper is attached to the press and printed at 2.5 m/s and a pressure of 3.6 MPa. The fibres are washed from the printing disc and collected on an 8 micron pore size Millipore filter. This was repeated three times. The surface area of one print is  $0.0054 \text{ m}^2$ , thus the total surface area per test was  $0.01622 \text{ m}^2$ . Per sample, an average of four tests were done and averaged for reporting.

The collected material is then analyzed in a high resolution FQA instrument with a lower length limit of 40 microns. Fibres and fines particles are counted and measured and results are summarized to report the average length, total length and number of fines, medium length fibres and long fibres that were removed during printing.

## **2.5 Microscopy work**

An environmental electron microscope (Quanta FEG 400) was used to obtain images of kraft and uncalendered TMP handsheets. Lint material collected from the Paplint test was viewed in transmitted light using a Nikon Microphot-FX microscope equipped with a Diagnostics Imaging Spot RT-Slider digital camera.

Images of handsheets were taken to visualize possible changes in sheet structure and fibre morphology that may explain possible differences in pulp and handsheet properties between samples. Surface as well as cross-section images were obtained. For surface images, samples were mounted on aluminium stubs with the rough side (that had not been in contact with the drying plate) up and coated with 60:40 Gold:Palladium. Cross-sections were also mounted in sample holders, embedded in epoxy and then coated.

Selected samples of the lint material that had been picked off the paper surface during the Paplint test were prepared by depositing the lint material onto a glass slide (heated to approximately 60°C to facilitate evaporation of the water) and allowing it to dry completely. Images of the selected samples were taken and compared to evaluate whether samples contained different types of linting material.

### 3 Results and Discussion

#### 3.1 Sampling sites

Of the ten new sample sites that were established, six are in the SBS zone and four in the SBPS zone. Table 2 provides subzone specification, site series, site index for lodgepole pine, moisture and nutrient regime information, as well as attack stage according to tree characteristics for these sites. Sites 14-01, 14-02, 15-01 and 15-02 are in a moist climate zone, sites 16-01 and 16-02 are in a wet climate zone, and sites 17-01, 18-01 green, 18-01 red and 18-02 are in a dry climate zone. Throughout this report we will distinguish the groups of zones by these attributes and simply refer to “dry”, “moist” and “wet” sites, but note that this refers to the climate and not to the soil moisture regime at a given site.

**Table 2.** New sample sites and their characteristics.

Site	BEC Subzone (variant)	Site Series	Pine Site Index (m)	Moisture	Nutrient	Attack stage
14-01	SBSmc2	01/04-05	18	4/5	C	Early grey
14-02	SBSmc2	01/04-05	18	4	C	Early grey
15-01	SBSmc2	01	18	4	C	Green
15-02	SBSmc2	01	18	3/4	C/D	Green
16-01	SBSwk3	04	18	4	C	Green
16-02	SBSwk3	04	18	4	C	Green
17-01	SBPSxc	01	15	3/4	C	Green
18-01 green	SBPSxc	01	15	3/4	C/D	Green
18-01 red	SBPSxc	01	15	3/4	C/D	Red
18-02	SBPSxc	01	15	3	C	Red

Figure 1 shows a map with sample site locations of new samples sites as well as some previously established sample sites.

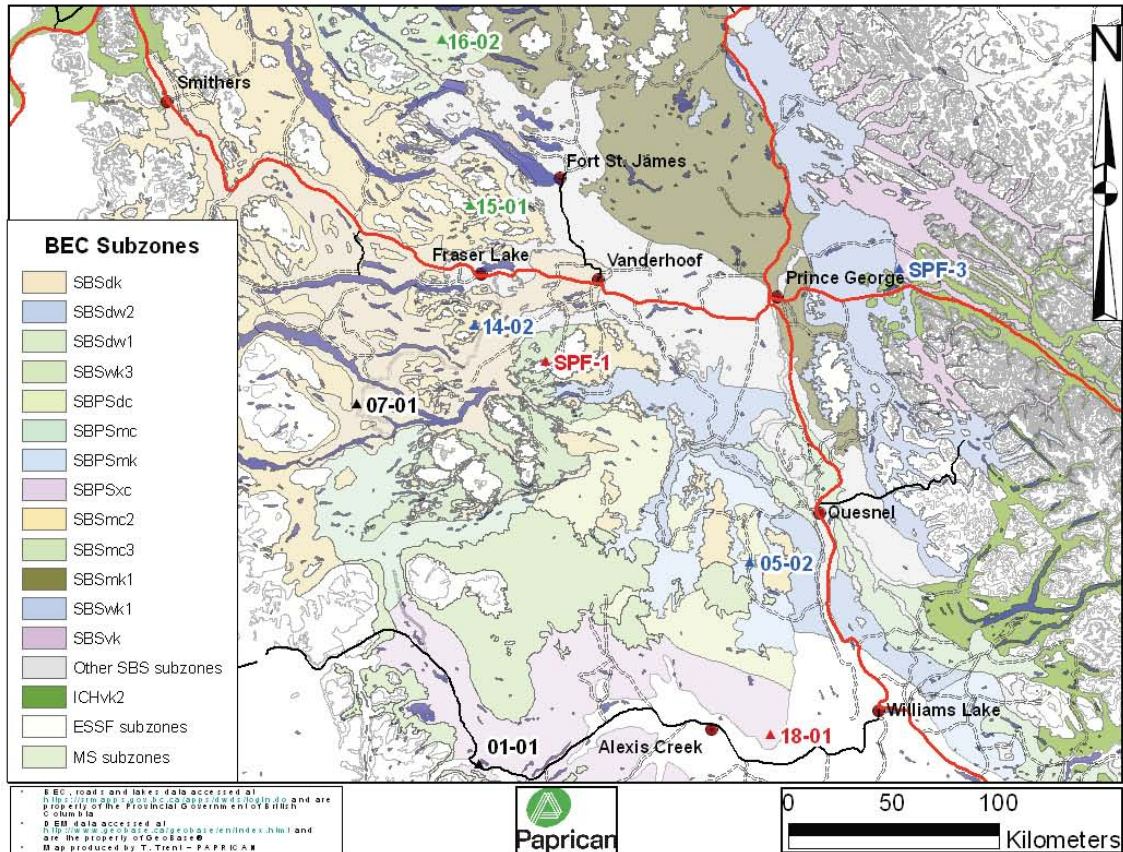


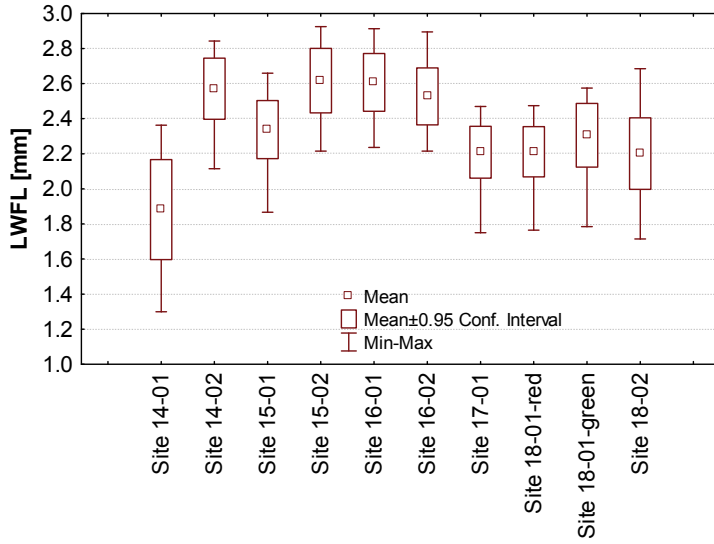
**Figure 1.** Map of interior British Columbia with sample site locations. Site numbers are colour coded (green = unattacked sites, red = red stage sites, blue = grey stage sites and black = late grey stage sites).

## 3.2 Core evaluation

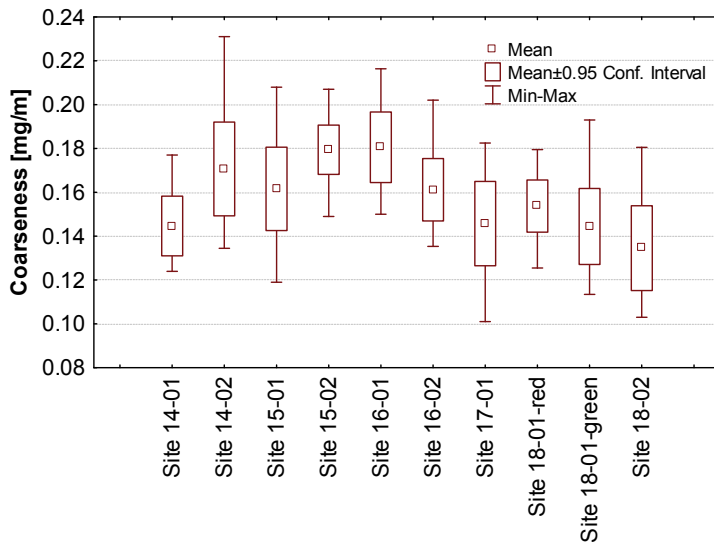
The detailed core analysis of selected samples enables a comparison and discussion of average wood and fibre properties of different sample sites. This information is used to exclude sites from sampling that show abnormal characteristics, which may be due to particular site conditions that are non-representative or due to uncharacteristic disturbance events. After selecting five of the ten new sites for harvesting, individual core data of trees is then used to choose a number of trees that are representative for the site, thus are used for the pulping study.

### 3.2.1 Fibre quality analysis

Average fibre length of mature wood from the new samples sites is 2.2 to 2.6 mm, and coarseness 0.14 to 0.18 mg/m (Figure 2 and Figure 3). These values lie within the normal range for lodgepole pine (Isenberg 1980, Hatton et al. 1992), although the coarseness values are at the lower end of the range. Site 14-01 presents an exception with a fibre length of less than 2 mm and higher variation in fibre length. The fibre length is unusually short for lodgepole pine and site 14-01 was therefore not considered for inclusion in the actual pulping study.

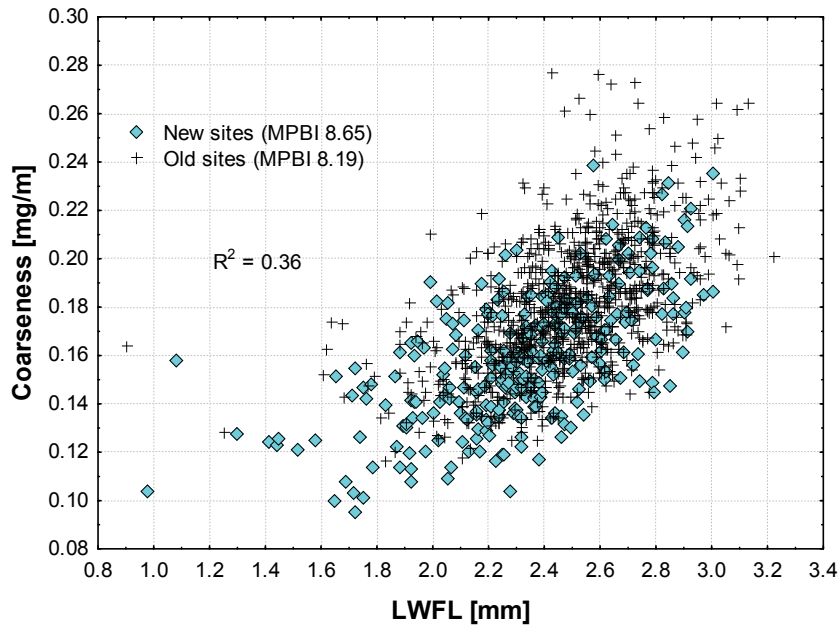


**Figure 2.** Average length weighted fibre length of trees from new samples sites.



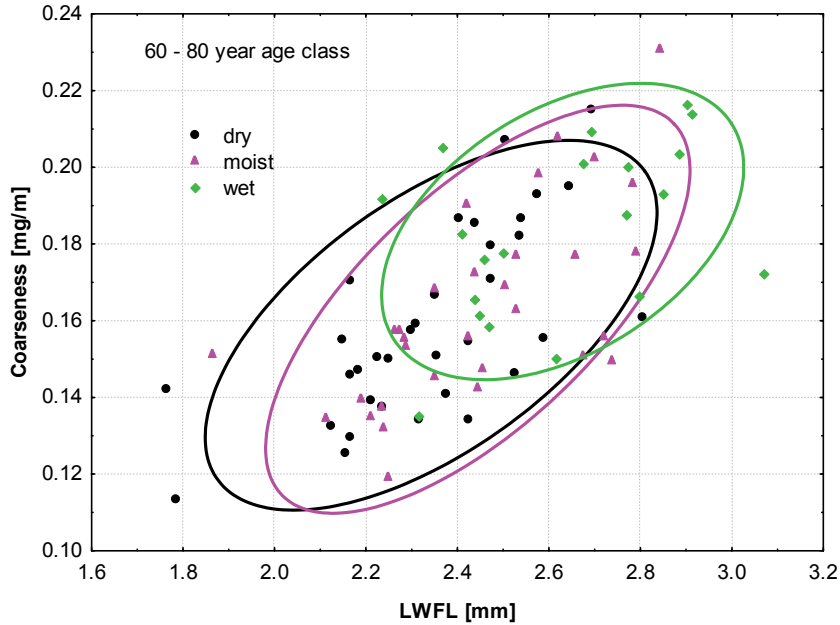
**Figure 3.** Average fibre coarseness of trees from new samples sites.

Figure 2 and Figure 3 also show that fibre length and coarseness at dry sites (sites 17-xx and 18-xx) is lower than at the moist and wet sites. This agrees with previous work that has shown a positive correlation between fibre length and coarseness (Pitts et al. 2001). Figure 4 illustrates this correlation for all sites sampled as part of this or the previous shelf-life study (Trent et al. 2006).



**Figure 4.** Fibre coarseness versus length weighted fibre length (LWFL) for samples from Trent et al. 2006 and this study. Data shown include three age classes (40 – 60, 60 – 80, 80 – 120 years).

The shorter and less coarse fibres observed for dry sites are also in agreement with findings from previous work that looked at the influence of site index on fibre length. Sites with lower site index (as is the case for the dry sites) were shown to produce shorter fibres (Pitts et al. 2001). The influence of growth conditions on fibre length and coarseness is emphasized in Figure 5 which shows a plot of fibre coarseness versus length for the 60 to 80 year age class for individual trees sampled for this work, distinguished by site attributes. The wet sites produce the longest and coarsest fibres, while the dry sites produce the shortest and least coarse fibres.



**Figure 5.** Fibre coarseness versus length of individual trees (60 – 80 year age class), distinguished by site attributes (sites in dry, moist and wet climate zones).

### 3.2.2 *Moisture Content and Wood Density*

Wood density and moisture of whole cores are presented in Figure 6 and Figure 7. For basic wood density, differences between sites exist but there is no common trend for sites in different subzones. However, some sites (18-02, 14-01, 15-02) show larger within-site variations than others. These sites were not selected for harvesting.

Figure 7 shows that moisture content is strongly affected by mountain pine beetle attack. The moisture content of trees from green, unattacked sites (sites 15-01, 15-02, 16-01, 16-02, 17-01 and 18-01-green) far exceeds the moisture content of trees from sites that have been killed by the beetle. The relationship between moisture and TSD has been shown previously (Trent et al. 2006). Using the TSD estimates that are based on tree appearance (this is done to be consistent with the previous study) for new sites, data from Trent et al. 2006 and the current study can be combined to clearly illustrate the effect of TSD on moisture content (Figure 8).

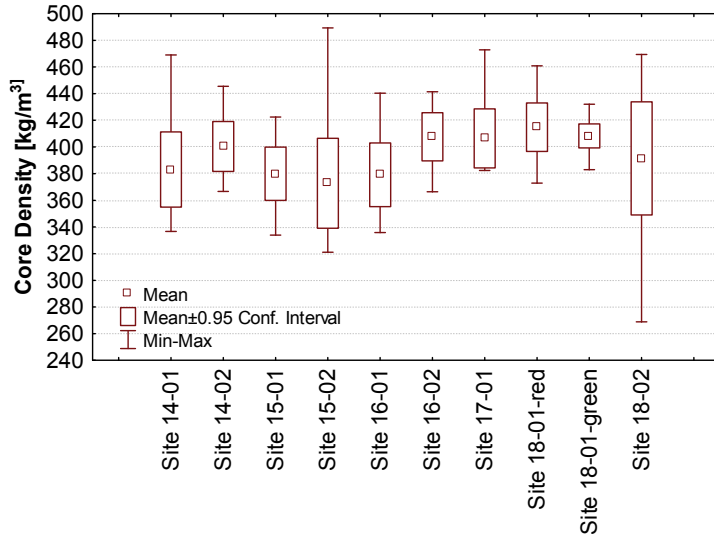


Figure 6. Average wood density of trees from new sample sites.

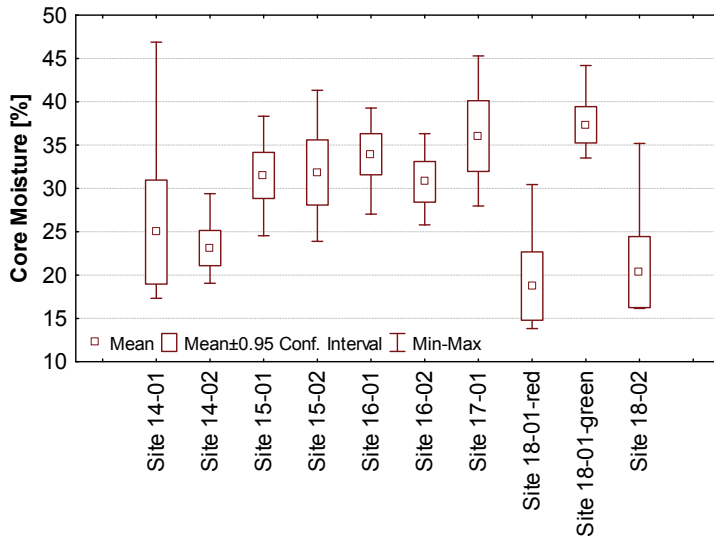


Figure 7. Average moisture content of trees from new sample sites.



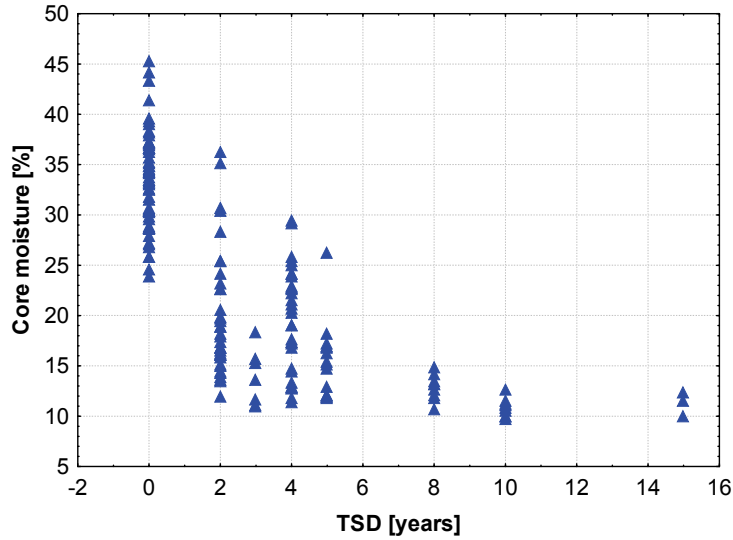


Figure 8. Moisture content versus TSD for all sample sites from Trent et al. 2006 and from this study.

### 3.2.3 *SilviScan Analysis*

All numbers shown in this section are for the 60 – 80 year age class of cores. Being able to compare certain age classes is a major advantage of measuring core profiles as done by the SilviScan instrumentation, as wood and fibre properties can differ with age within a tree. Particularly juvenile and mature wood often show differences. Trees sampled for this project differ in age (tree ages were between 60 and 205 years), thus comparing selected age classes will eliminate the bias that exists when comparing whole core averages.

Fibre dimensions measured with the SilviScan instrumentation include fibre wall thickness and fibre diameter; the latter is here reported as the equivalent circular diameter based on radial and tangential width of the rectangular wood fibres. Fibre diameter and wall thickness are important parameters. Fibres with larger diameter and thinner fibre walls tend to collapse easier. The principle of collapsibility index (Jang and Seth 1998) is used to express this fibre conformability, which is an important parameter in pulp and papermaking as fibres with good conformability promote inter-fibre bonding, thus form stronger sheets. While wood fibre collapsibility is not the same as pulp fibre collapsibility, it is nevertheless useful to look at this parameter for a relative comparison of different wood sources. Collapsibility index is a function of the mechanical properties of the fibre wall, and fibre geometry as defined by a geometric factor  $G$ . For wood fibres, only the geometrical factor  $G$  can be estimated:

$$G = \frac{LP}{2\pi T} \tag{Equation 3}$$

With  $LP$  Inner lumen perimeter [ $\mu\text{m}$ ]  
 $T$  Wood fibre cell wall thickness [ $\mu\text{m}$ ]

A comparison of  $G$  for all new sites is shown in Figure 9. While differences of  $G$  between sites exist, none of the sites show an exceptionally high or low  $G$ . Also, as expected,  $G$  does not seem to depend on attack stage. Interestingly, the wood fibres of trees from dry sites do not show a higher  $G$ -factor on average, even though the coarseness of these fibres is lower than from moist and wet (more productive) sites (Figure 10). Coarseness is often assumed to represent an equal measure of fibre conformability, but these results show that  $G$ -factor is a better measure as it includes fibre diameter and wall thickness. Plots of fibre diameter and wall thickness as underlying parameters for the  $G$ -factor are shown in Appendix A. Fibre diameters are in the range of 32 to 38  $\mu\text{m}$  and are, on average, slightly lower for samples from dry sites, while the average fibre wall thicknesses are in the range of 2.4 to 2.8  $\mu\text{m}$  with no trend for different site groups.

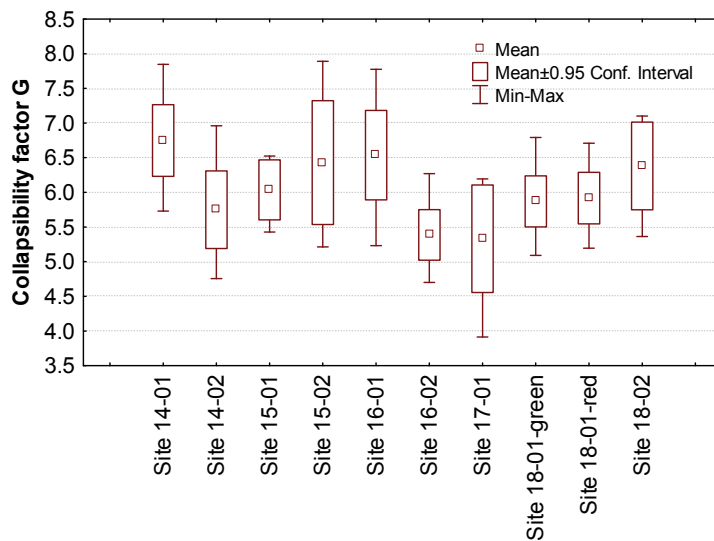


**Figure 9.** Comparison of  $G$ -factor, as an important parameter for fibre conformability, of trees from new sample sites (60 – 80 year age class).

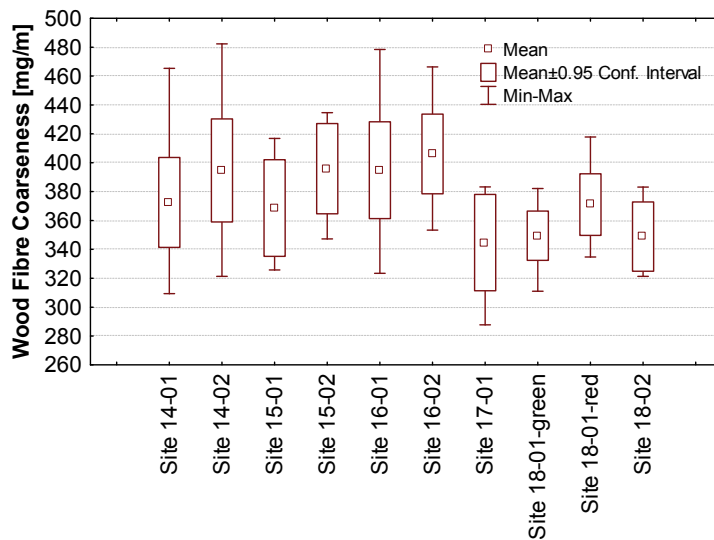


**Figure 10.** Average wood fibre coarseness of trees from new sample sites (60 – 80 year age class).

Besides fibre geometry, SilviScan also determines microfibril angle, another important parameter for fibre collapsibility that influences the fibre wall mechanical properties. Average microfibril angles at new sample sites are compared in Figure 11. In general, microfibril angles are low as is typical for Northern softwoods, and lie within the natural variability range for lodgepole pine. As expected, microfibril angle of green trees does not obviously differ from dead trees.

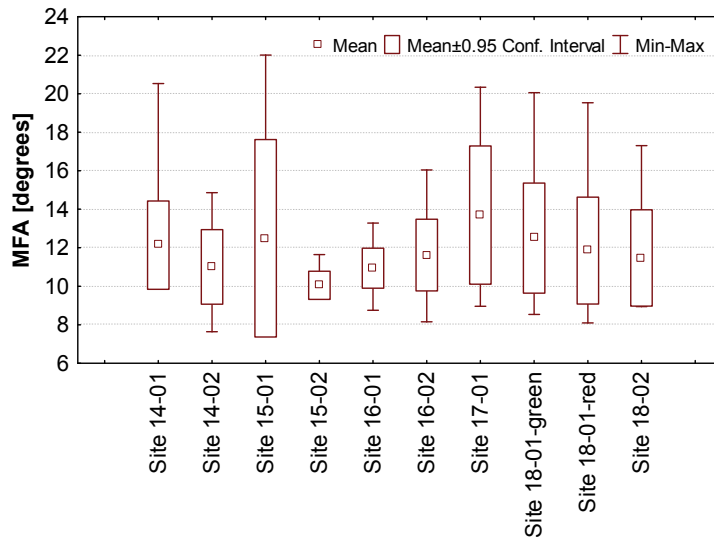


**Figure 11.** Average microfibril angle of wood fibres of trees from new sample sites (60 – 80 year age class).

Lastly, wood density profiles were determined and complement the volumetrically determined whole core data. For comparison between sites, averages are again given for the 60 – 80 year age class (Figure 12). Differences between sites show roughly the same distribution as the data for whole cores in Figure 6, however density of the 60 – 80 year class at some sites is higher than for whole cores, owing to the generally higher density of mature wood compared to juvenile wood.

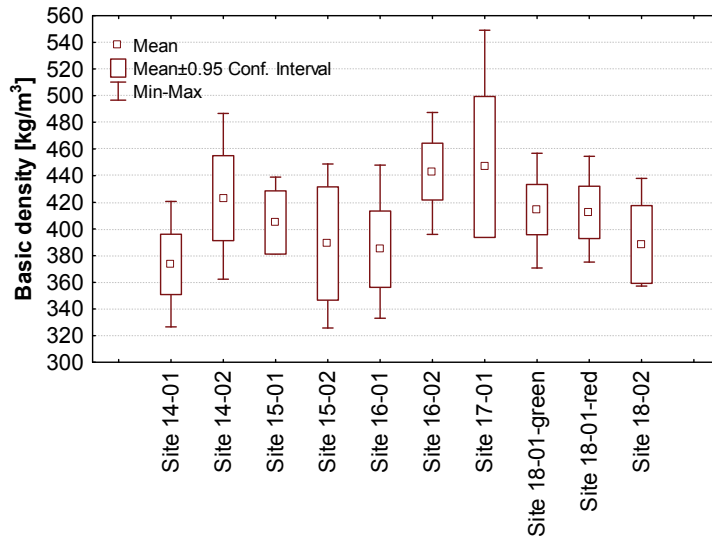


**Figure 12.** Wood density of trees of new sites as measured by SilviScan averaged over age rings 60 – 80 (data is corrected to basic wood density).

### 3.2.4 Extractives

The average extractives content (Figure 13) of all sites lies within the range of 2 to 6% reported for lodgepole pine (Shrimpton 1972, 1973, Woo et al. 2005). For the ten sites of this study, no obvious influence of attack stage on extractives content is apparent, although site 18-02, which is a red stage site, shows a slightly elevated extractive content when compared to other sample sites. While it is sometimes assumed that trees at the red stage attack show elevated extractive content, a plot of extractive contents of all sample sites from Trent et al. 2006 and from the current study shows no relationship between extractives and TSD (Appendix A), although extractives of trees from MPB-killed sites are, on average, slightly higher than extractives of green trees from unattacked sites. The lack in relationship of extractives and TSD (once trees are killed) is consistent with the earlier finding of Trent et al. 2006. In Figure 13 some sites show greater variation and differences between minimum and maximum extractive content. Large variability in extractive content within as well as between sample sites has been reported (Shrimpton 1973, Hatton and Hunt 1991).

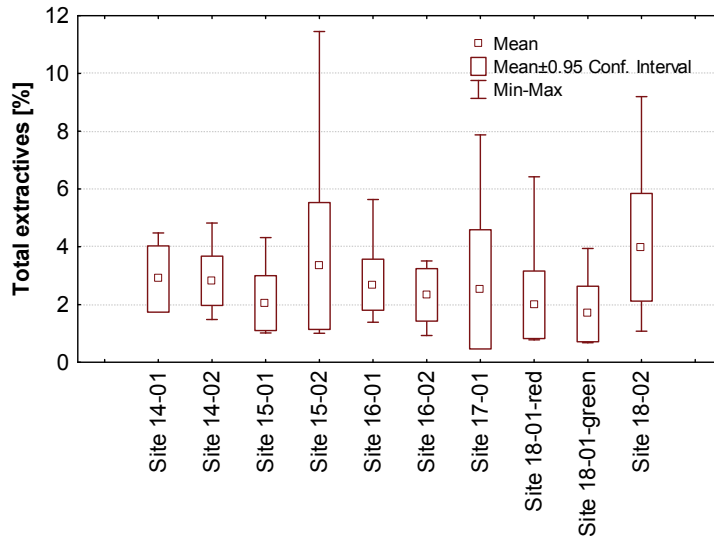


**Figure 13.** Average extractive content of trees from new sample sites (given as % of o.d. wood).

### 3.2.5 *Near infrared range (NIR) measurements*

Predictions from NIR measurements showed that only very few samples contained decay. Of the 100 cores from the new samples site, only three showed some decay that extended over a maximum of 2 cm core length. Harvey (1986) in a study of MPB-killed trees in Oregon also found little decay up to 11 years TSD, with only 13.7% of sampled trees showing some decay. Lewis et al. (2006) found saprot in 46% of samples they took from different heights of lodgepole pine trees that had been killed two years prior, but penetration depths were negligible.

Blue stain predicted by NIR was extensive in dead trees, with most of the red and grey samples showing blue stain that extended over a distance of 1 to 5 cm from the bark. Previous studies also showed that most of the staining occurs within the first year after tree death (Reid 1961), and penetration depths are related to tree diameter (Lewis et al. 2006).

The NIR measurements also provide moisture profiles. Profiles of green trees show much higher moisture contents towards the bark, which drop off towards the centre of the tree. This is related to the difference between sapwood and heartwood and is expected. The moisture profiles of dead trees show a very even distribution, with approximately constant moisture content below the fibre saturation point all along the core. The drop in sapwood moisture is fast, very low moisture contents are already seen in red stage trees. Figure 14 shows the differences in moisture profiles of green and red trees that were both sampled at site 18-01. While density can also be predicted from NIR measurements, we instead used the very accurate density profiled obtained from SilviScan.

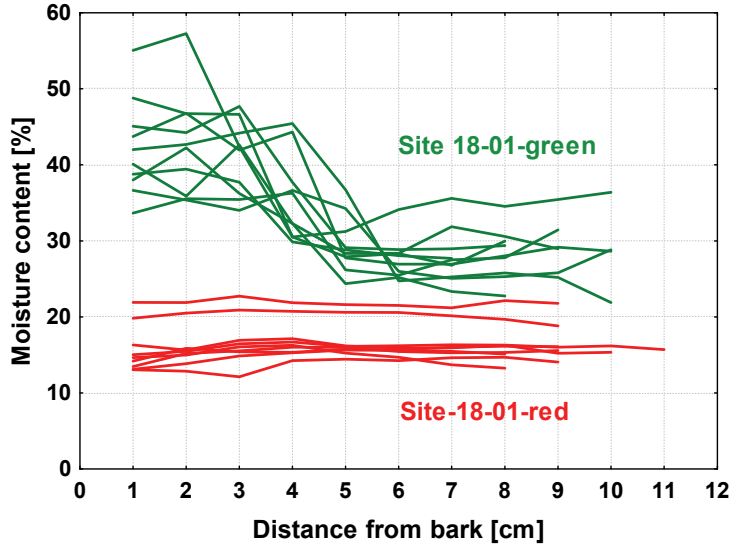


**Figure 14.** Wood core moisture contents of green and red trees at site 18-01 as predicted from NIR measurements.

### 3.3 Selection of sites and trees for pulping trials

Based on results from core analysis as well as consideration of field notes and tree ages, five of the newly established sites were selected for harvesting. In addition, four of the sites established in previous projects were revisited for harvesting. Also, the sample matrix includes two more sites that had been harvested previously and used for pulping trials. As core and pulping data for these two sites were available, they were not revisited. A list of the sites selected to fill the desired sample matrix is shown in Table 3..

While it was not possible to find completely similar sites within a group, the differences in site characteristics within a group are small. It is thus assumed that growth conditions of sites within a group are similar; and environmental variability is thus minimized. The differences in growing conditions between sites are much larger. While the moist and wet sites both have the same site index, the environmental conditions are nevertheless very different (moist and cold versus wet and cool climate), thus wood and fibre quality of these groups should still differ.

**Table 3.** Sample sites for pulping trials.

Site	BEC Subzone (variant)	Site Series	L.Pine Site Index (m)	Moisture	Nutrient	Attack stage
“Dry” sites						
18-01 green	SBPSxc	01	15	3/4	C/D	Green
18-01 red	SBPSxc	01	15	3/4	C/D	Red
05-02	SBPSdc	05	15	5	D	Early grey
01-01	SBPSxc	01	15	4	C	Late grey
“Moist” sites						
15-01	SBSmc2	01	18	4	C	Green
SPF-1	SBSmc3	01	18	4	B	Red
14-02	SBSmc2	01/04-05	18	4	C	Early grey
07-01	SBSmc2	01	18	5	C	Late grey
“Wet” sites						
16-01	SBSwk3	04	18	4	C	Green
SPF-3 red	SBSvk1	02	18	2	B	Red
SPF-3	SBSvk1	02	18	2	B	Early grey

Note: For SPF-1 and SPF-3 red, data from pulping trials in 2004 were available thus included in the reporting, but no harvesting of these sites took place for this project specifically. The testing of wood in 2004 was more limited, thus for these sample sites data are available only for selected wood, fibre and pulp properties.

Between three and ten trees were harvested from each site. The selection was based on wood density, fibre length and fibre coarseness of individual trees, aiming at trees that were representative of average density and fibre morphology values of the site. Table 4 shows the fibre and density data for the chosen trees as well as average numbers for the respective site.

**Table 4.** Density and fibre properties of individual trees selected for harvest and comparison to site averages (site averages are based on 10 sample trees).

Site	Tree	LWFL [mm]*	Site average LWFL [mm]*	Coarseness [mg/m]*	Site average coarseness [mg/m]*	Density [g/cc]	Site average density [g/cc]
18-01 green	2	2.24	2.31	0.138	0.144	411	408
	5	2.43		0.134		403	
	10	2.30		0.158		383	
18-01 red	7	2.15	2.21	0.155	0.154	407	415
	8	2.21		0.139		409	
	9	2.25		0.150		434	
05-02	3	2.59	2.49	0.156	0.180	415	435
	10	2.51		0.207		419	
	11	2.44		0.186		399	
01-01	3	2.23	2.41	0.151	0.161	383	405
	6	2.404		0.187		387	
	7	2.805		0.161		410	

	1	2.35		0.169		377	
	2	2.25		0.119		349	
	3	2.24		0.138		410	
	4	2.19		0.140		360	
15-01	5	2.29	2.34	0.156	0.162	377	380
	6	1.87		0.151		377	
	7	2.62		0.208		387	
	8	2.42		0.191		406	
	9	2.51		0.169		423	
	10	2.66		0.177		334	
	1	2.58		0.199		423	
SPF-1 <sup>†</sup>	3	2.46	2.40	0.176	0.187	466	434
	7	2.54		0.181		402	
	1	2.27		0.158		423	
	2	2.42		0.156		400	
	3	2.44		0.173		367	
	4	2.84		0.231		446	
14-02	5	2.72	2.57	0.156	0.171	373	419
	6	2.79		0.196		414	
	7	2.74		0.150		403	
	8	2.70		0.203		367	
	10	2.12		0.135		419	
	2	2.29		0.154		437	
	3	2.46		0.148		365	
07-01	4	2.35	2.41	0.146	0.153	430	420
	5	2.53		0.163		419	
	6	2.79		0.178		386	
	8	2.45		0.143		445	
	8	2.50		0.178		385	
16-01	9	2.47	2.61	0.159	0.181	359	379
	10	2.77		0.188		381	
	3	2.70		0.209		419	
SPF-3 red <sup>†</sup>	4	3.07	2.68	0.172	0.187	413	417
	6	2.37		0.205		489	
	1	2.85		0.193		427	
SPF-3	9	2.68	2.68	0.201	0.187	413	417
	12	2.44		0.166		424	

\* These values are from the 60-80 year age class only.

<sup>†</sup> Harvested in 2004. Note that site averages of SPF-3 red and SPF-3 are the same as the site is the same.



### 3.4 Influence of attack stage on wood and fibre properties of selected sites

For the sites selected for harvest, new and previous core data can be combined to compare site-averaged wood and fibre properties of green, red, grey and late grey stage trees grouped by general subzone characteristics (dry – moist – wet) as per sample matrix. Main effect ANOVA analysis was used to quantify the influence of attack stage and subzone characteristics (Table 5). Note that core moisture and extractives are not included in the analysis, as only limited data is available for sample sites of previous projects, but the influence of TSD on moisture and extractives in general is discussed in section 3.2.

**Table 5.** Main effect ANOVA analysis of site and attack stage-influence on wood and fibre properties.

Property	Whole model results		Univariate results	
	p	R <sup>2</sup> <sub>adj.</sub>	p <sub>subzone</sub>	p <sub>attack stage</sub>
<b>SilviScan (60-80 years)</b>				
Wood density	0.072	0.054	0.25	0.071
Fibre diameter	<b>0.0009</b>	0.158	<b>0.0001</b>	0.20
Cell wall thickness	<b>0.044</b>	0.067	0.24	0.055
Wood fibre coarseness	<b>0.004</b>	0.126	<b>0.007</b>	<b>0.037</b>
Specific surface area (SSA)	<b>0.001</b>	0.151	0.10	<b>0.002</b>
Microfibril angle (MFA)	0.052	0.063	0.054	0.22
Collapsibility geometrical factor <i>G</i>	<b>0.048</b>	0.065	0.15	0.071
<b>FQA (60-80 years, after maceration)</b>				
Length weighted fibre length	<b>0.00009</b>	0.193	<b>0.00006</b>	0.066
Fibre coarseness	<b>0.0001</b>	0.19	<b>0.0007</b>	<b>0.017</b>

At a significance level of  $p = 0.05$ , many of the fibre properties are influenced by attack stage and/or subzone, however the correlation coefficients of such models are low, thus not much of the variability is explained. Univariate results that distinguish between the two factors identify an influence of subzone on fibre coarseness (of the wood fibres as well as after maceration), fibre length and fibre diameter. This is expected as growth conditions are known to influence fibre properties as discussed earlier. Looking at plots of these variables, an increase in fibre length, coarseness and diameter is seen going from dry to moist to wet sites (see Figure 15 for an example plot of fibre length and Appendix A for remaining plots).

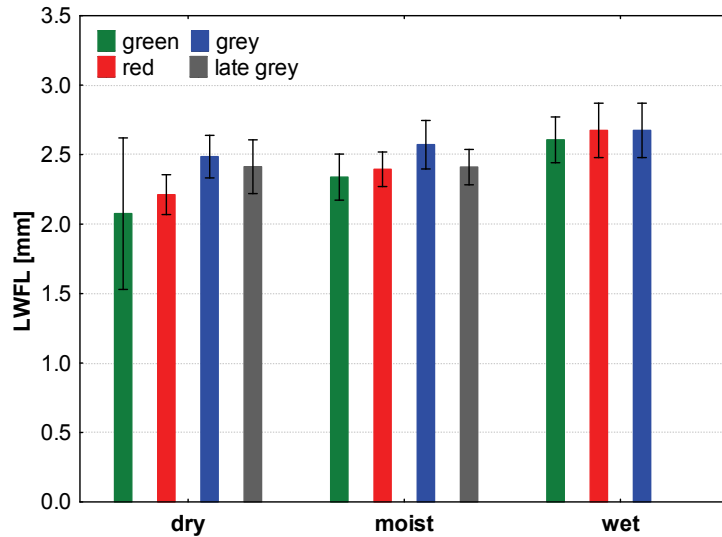


**Figure 15.** Average fibre length at sites selected for pulping trial compared by subzone.

An influence of attack stage is predicted for coarseness and specific surface area. Posthoc analysis, using the less conservative Fisher LSD, shows a difference between green sites and other sites for coarseness, with lower coarseness for green sites. However, the more conservative Scheffe posthoc test does not identify any significant differences between the attack stages. It is also not readily conceivable why wood fibres of MPB-attacked trees would have a higher coarseness. Thus this result should be seen cautiously. It should also be noted that SilviScan coarseness is an indirect measurement. It is calculated from fibre diameter and wood density, assuming a constant cell wall density of  $1500 \text{ kg/m}^3$ . Thus if any changes occur in cell wall density or wood chemistry, coarseness results would be affected.

For specific surface area (SSA), the predicted influence of attack stage, however, is significant and Scheffe posthoc analysis predicts differences between green trees compared to any of the MPB-attack stages, with specific surface higher for green trees. Fibre SSA in SilviScan analysis is calculated based on fibre perimeter and fibre coarseness. Fibre coarseness is an indirect measurement as discussed, thus SSA is actually calculated from fibre diameter (measured as radial and tangential diameter), wood density and cell wall density, which is assumed constant. As neither fibre diameter nor wood density show any influence from TSD, it can be questioned if the effect on SSA is real. The limitations of the calculation of SSA regarding the assumption of constant cell wall density could also play a role. Also, it is possible that TSD-effects on diameter or wood density exist but are masked by site effects.

Results for the selected sites can be compared to previous results of TSD influence on fibre properties (Trent et al. 2006) to further investigate any possible influence on TSD on wood and fibre properties. Wood and fibre properties from both Trent et al. 2006 and this study were combined and analyzed by main effect ANOVA. Attack stage was described as green, red, grey or late grey stage, while the site effect was included by using site index as an indicator (this was possible as site indices ranged from 9 to 24 for

the combined sample set, thus offering a wider range than has been the case for data of the current work only. Similar to results for the limited data set shown in Table 5, an effect of attack stage was predicted for coarseness measured by FQA ( $p_{\text{attack stage}} = 0.023$ ) and for specific surface area measured by SilviScan ( $p_{\text{attack stage}} = 0.010$ ), but not for coarseness by SilviScan analysis. Also, the influence of attack stage on coarseness from FQA was shown to only exist at higher site indices and is thus questionable. The effect on surface area, however, may be real. But more work would be needed to confirm this result, including a more detailed analysis of cell wall density, and a closer examination of actual core profiles.

An effect of site index using the combined data set is seen for significantly more variables than seen for the selected samples, likely due to the larger sample range (the selected sites of this study comprise only three different general subzones and only two different site indices). Variables that are influenced by site index are basic density ( $p_{\text{site index}} = 0.027$ ), fibre diameter ( $p_{\text{site index}} = 3 \cdot 10^{-5}$ ), coarseness ( $p_{\text{site index}} = 0$ ), wall thickness ( $p_{\text{site index}} = 1 \cdot 10^{-6}$ ) and specific surface area ( $p_{\text{site index}} = 2 \cdot 10^{-3}$ ) of the SilviScan variables, and length ( $p_{\text{site index}} = 3 \cdot 10^{-6}$ ) and coarseness ( $p_{\text{site index}} = 0$ ) of the FQA measurements.

### 3.5 Exact kill date determination for harvested trees

Results from the dendrochronology study showed that kill dates of trees in some cases were later than assumed from aerial overview data and tree and foliage indicators (Table 6). Particularly, site 14-02 would be classified as red stage by kill date, while the appearance of trees was classified as grey stage. In this report, we will report results within each subzone class by green/reed/grey/late grey stage as defined in Table 3 for all sites, but the limitations of actual TSD distribution between all sites should be kept in mind.

**Table 6.** Time-since-death (TSD) estimates compared to actual TSD as determined by dendrochronology (trees harvested in 2006).

Site	Attack stage (foliage indicators)	TSD estimate* [years]	Actual TSD† [years]
<b>“Dry” sites</b>			
18-01 green	Green	N/A	N/A
18-01 red	Red	2	2
05-02	Early grey	6	4-6
01-01	Late grey	17	30
<b>“Moist” sites</b>			
15-01	Green	N/A	N/A
SPF-1	Red	1-2	-
14-02	Early grey	3-4	2
07-01	Late grey	10	6-7
<b>“Wet” sites</b>			
16-01	Green	N/A	N/A
SPF-3 red	Red	1-2	-
SPF-3	Early grey	3-4	3

\* Estimated from aerial overview data, foliage and tree characteristics, MPB spread history or a combination thereof.

† Estimated from dendrochronology

### 3.6 Chip quality

Basic chip density, given as o.d. weight/green volume, is an important parameter in kraft pulping, as production is volume limited. Thus (depending also on yield), denser wood can result in higher production rates. However, very dense wood can be slow to impregnate and may result in uneven pulping. Packing (or bulk) density is important for kraft pulping for similar reasons. In general, basic and packing densities correlate well.

For samples in this study, main effect ANOVA (with site attribute = dry, moist or wet and attack stage = green, red, grey or late grey as main effects) showed that both site attribute ( $p_{\text{subzone}} = 0.019$ ) and attack stage ( $p_{\text{attack stage}} = 0.009$ ) are of significant influence on basic density at the selected level of significance of  $p = 0.05$ . Posthoc analysis, using the conservative Scheffe test, showed that differences exist between the dry and the moist subzones, and that samples in the late grey stage are significantly less dense than samples in the grey or red stage. Bulk density showed similar results, with  $p_{\text{subzone}} = 0.020$  and  $p_{\text{attack stage}} = 0.031$ . Posthoc analysis shows differences in packing density for dry subzones when compared to either moist or wet subzones, and between the red stage samples and late grey stage samples. Figure 16 shows a comparison of basic density grouped by subzones.

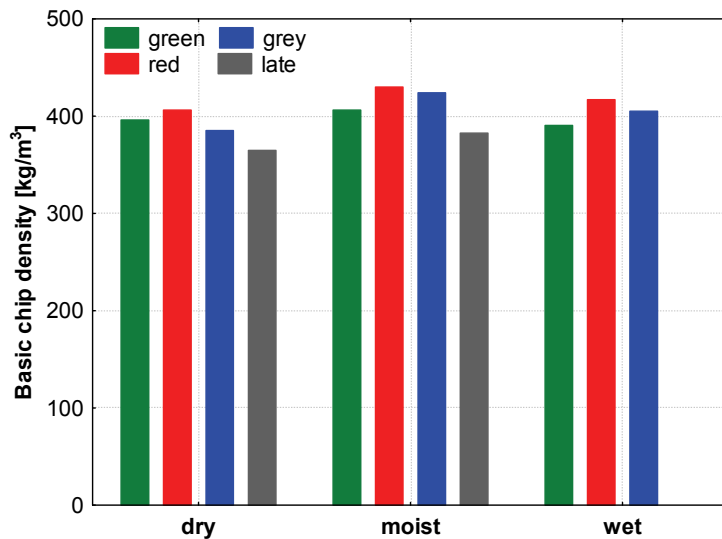


Figure 16. Basic density of chip samples by subzone attribute.

While differences in density are small, chip moisture content (or chip solids) differ noticeably between wood chips from green sites and from sites with dead wood, as expected ( $p_{\text{attack stage}} = 0.002$ ), but there is no difference between different subzones. The drop in moisture content is severe: From around 40% to 50% solids to between 70% and 90% solids (Figure 17), with most samples from dead wood being below fibre saturation point, which is commonly assumed at around 30% moisture on a dry wood basis (Skaar 1988), which translates to 23% moisture on a wet wood basis.

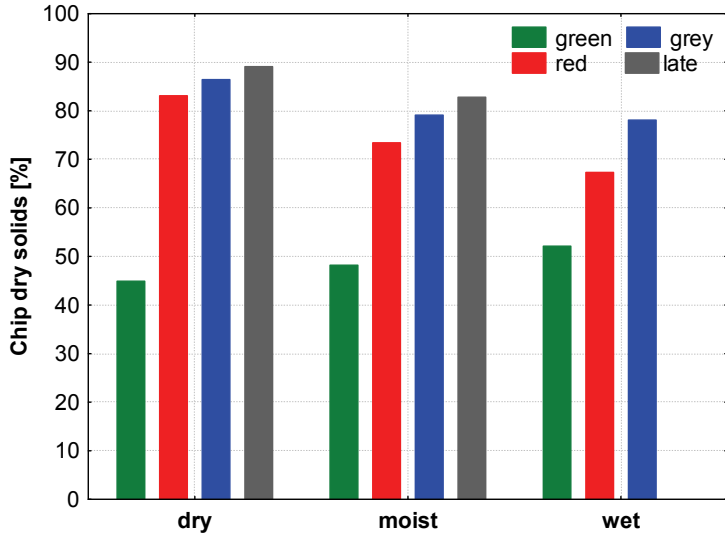


Figure 17. Chip dry solids content for all chip samples.

Chip size distribution was determined by Gradex and Rader screening (Appendix B). The chip size distribution determined by Gradex suggests that with increasing TSD, more pin chips and overthick chips and less accept chips are produced (Figure 18). Rader screening also results in higher numbers of thicker chips, for categories up to 4 mm slot size (Figure 19). To evaluate the significance of differences in distributions, we used the non-parametrical Kolmogorov-Smirnov two-sample test. Chip size distributions were averaged over the three sites for each TSD-category, as sample site was of no influence. Test statistics were significant ( $p < 0.1$ ) only when comparing the green chips to grey or late grey chips for the Rader screening. Thus, some indication exists that more oversized chips are produced, but results are ambiguous.

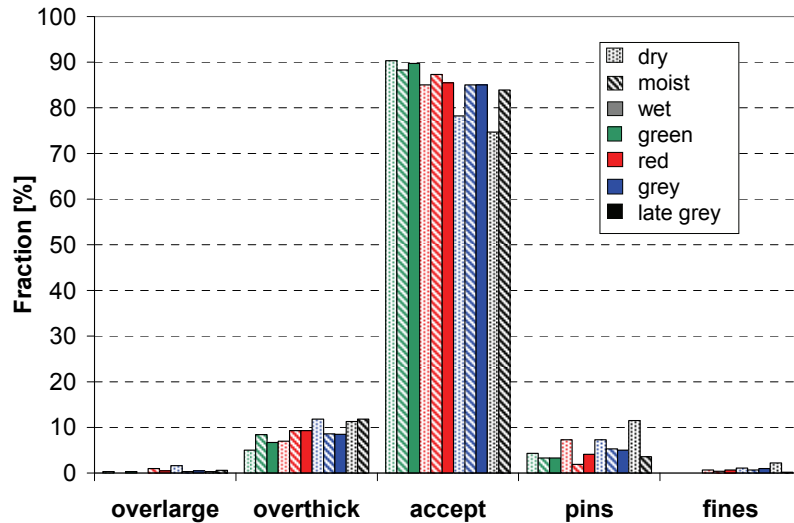


Figure 18. Chip size distribution by Gradex classification.

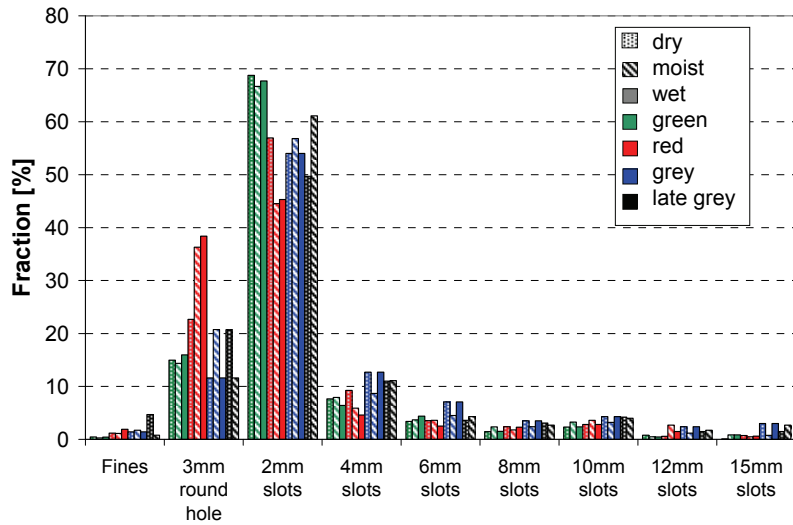


Figure 19. Chip size distribution by Rader classification.

### 3.7 Kraft pulping

#### 3.7.1 Pulping parameters

Monitoring of pulping parameters included kappa number, pulp yield and the effective alkali consumed during pulping as a function of H-factor. A plot of kappa number versus H-factor (Figure 20) shows that some wood samples pulp more easily than others (lower kappa number at the same H-factor), but the incremental drop in kappa number with increasing H-factor is similar. Also, the differences do not seem to be a function of either TSD or site series (see Figure 21 which compares H-factor at a kappa number of 30).

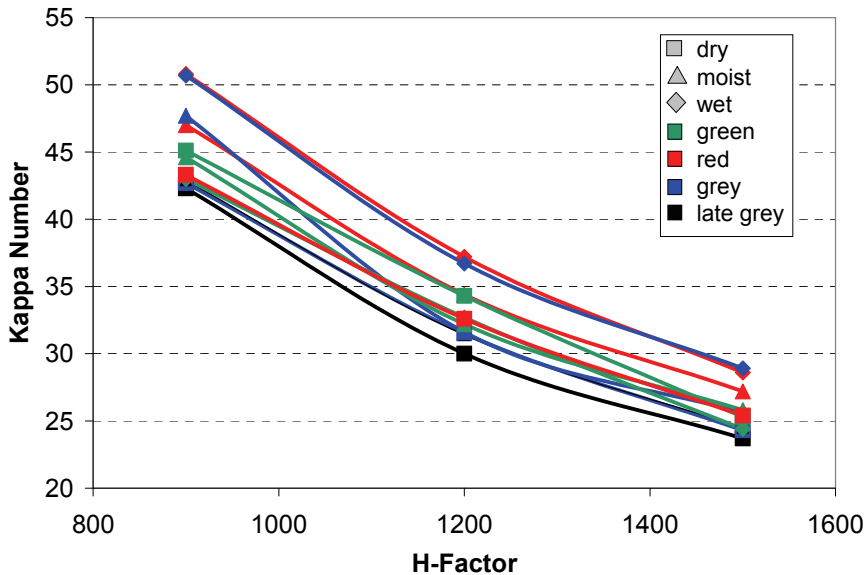
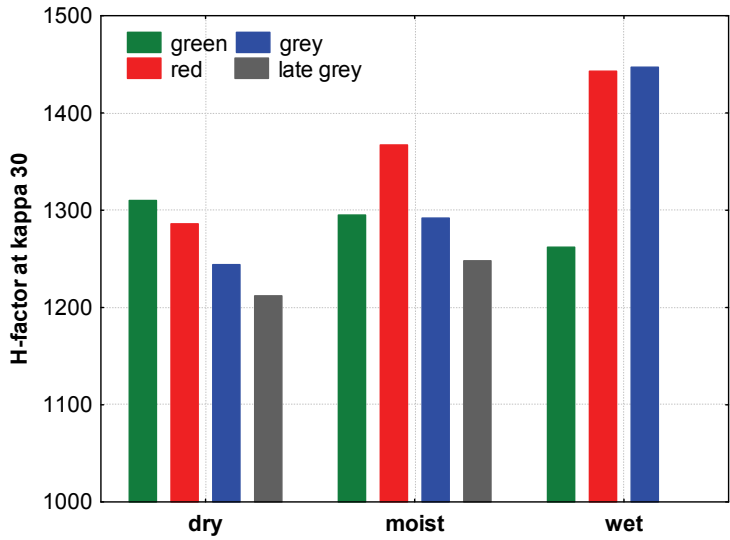
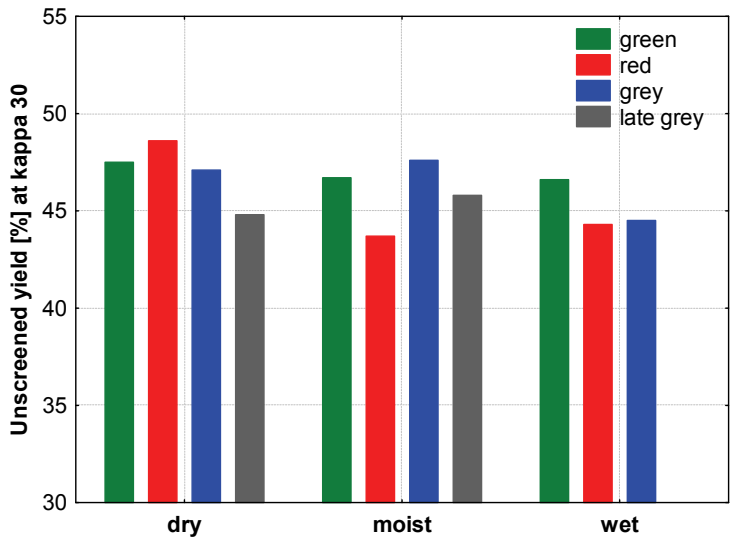


Figure 20. Kappa number versus H-factor for all pulp samples.



**Figure 21.** H-factor at kappa 30 for all pulp samples, grouped by subzone (site attribute).

Similarly, pulp yield shows absolute differences when plotted against kappa number or when compared at kappa 30 (Figure 22), but the incremental drop in pulp yield for increasing H-factor is similar, and neither TSD nor site attribute can explain the differences in pulp yield. Differences in pulp yield can be as high as 5% points and are likely site-related with other factors being important as well as just the general site attributes used to group sites for this study. The percentage of consumed effective alkali also does not show any influence of TSD or site attribute. See Appendix C for plots of pulping parameters versus kappa number and a table of pulping parameters at kappa 30.



**Figure 22.** Pulp yield at kappa 30 for all pulp samples, sorted by site attribute.

To confirm any influence of TSD or site attribute on pulping parameters, an ANOVA analysis with these two factors as main effects was performed using the pulping data at kappa 30. It confirmed that neither effect was significant at an alpha-level of  $p = 0.05$  in determining pulp yield, H-factor or consumed effective alkali ( $p > 0.25$  for all variables).

### 3.7.2 Pulp quality

Strength, structural and optical properties of handsheets made from pulps at all four PFI mill beating points showed little influence of site attribute or TSD. When compared at a standardized freeness of 400 ml CSF, none of the handsheet properties showed any influence from TSD (Appendix C). This was confirmed by main-effect ANOVA with TSD and site attribute as effects, setting the level of significance at  $p = 0.05$ . Site attributes had an influence only on opacity ( $p_{\text{subzone}} = 0.043$ ) and scattering coefficient ( $p_{\text{subzone}} = 0.035$ ). Examining plots for these variables showed that opacity and scattering coefficient are slightly lower at wetter sites, however the differences are small (opacity averaged for all wet sites (all attack stages) is about 1.2 to 1.5 ISO point lower than for dry and moist sites, and scattering coefficient of wet sites is about 5 to 15  $\text{g}/\text{cm}^2$  lower). Also, these variables have little importance for unbleached kraft pulps, but give some indication of sheet bonding.

There is a difference in tensile strength of about 12 Nm/g for green and red stage pulps within the “dry” sites (Figure 23). Experimental error has shown to be in the range of 5 Nm/g for pine kraft pulps (Dalpke et al. 2007), therefore the difference is real. This could be an indication that tensile may be effected from MPB attack, as these samples came from exactly the same site, thus site effects were eliminated as much as possible. However, a generalization of this observation is not possible, as it is based on only two samples. The overall ANOVA analysis did not show any effect of TSD on tensile strength.

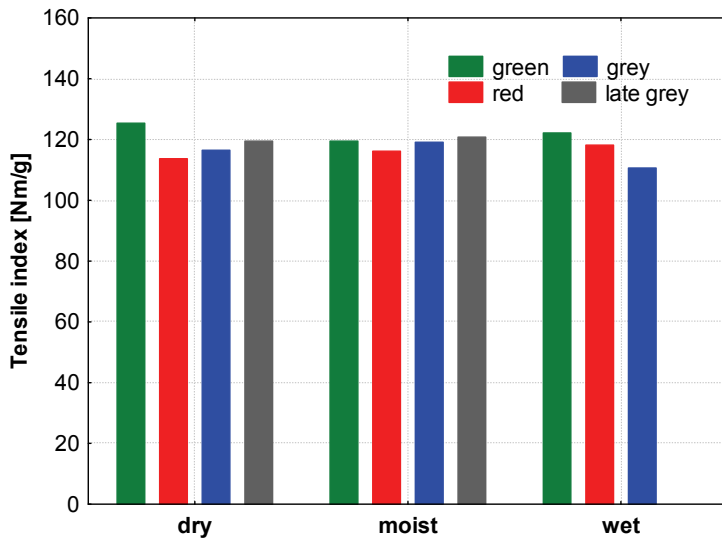


**Figure 23.** Tensile index of kraft pulps at CSF = 400 ml grouped by subzone (site attribute).



Fibre dimensions measured with the FQA are given in Table 7. Differences between samples exist, but are small. Results of an ANOVA analysis with site attribute and TSD as main effects are shown in Table 7. Length and coarseness are influenced by site attribute, as expected (with slightly longer and coarser fibres at the moist and wet sites compared to dry sites), but TSD is not of influence. Distribution plots for fibre length show only minor variability (Appendix C). The distributions are very similar in shape (with the exception of fibres from the moist, late grey site).

**Table 7.** Fibre quality data for kraft fibres

Site	Attack stage	Fibre length <sup>†</sup> [mm]	Fibre width [μm]	Fibre coarseness [mg/m]	Fibre curl <sup>†</sup>	Kink index [1/mm]
“Dry” sites						
18-01 green	Green	2.66	29.8	0.140	0.034	0.20
18-01 red	Red	2.58	28.7	0.137	0.036	0.30
05-02	Early grey	2.61	30.5	0.145	0.048	0.42
01-01	Late grey	2.56	30.8	0.140	0.042	0.35
“Moist” sites						
15-01	Green	2.74	30.2	0.177	0.041	0.23
SPF-1	Red	2.71	28.5	0.142	0.040	0.27
14-02	Early grey	2.84	29.6	0.170	0.044	0.32
07-01	Late grey	3.06	29.7	0.153	0.045	0.33
“Wet” sites						
16-01	Green	3.00	30.6	0.174	0.042	0.29
SPF-3 red	Red	2.98	28.6	0.162	0.052	0.37
SPF-3	Early grey	2.77	30.6	0.160	0.053	0.45

<sup>†</sup>Length weighted average

**Table 8.** Univariate results from main effect ANOVA analysis showcasing the influence of site attribute (subzone) and attack stage on kraft fibre quality.

Property	Site attribute influence	TSD influence
	P <sub>subzone</sub>	P <sub>attack stage</sub>
Fibre length, length weighted [mm]	<b>0.046</b>	0.68
Fibre width [μm]	0.24	<b>0.011</b>
Fibre coarseness [mg/m]	<b>0.039</b>	0.26
Fibre curl, length weighted	<b>0.069</b>	0.17
Kink index [1/mm]	<b>0.027</b>	<b>0.006</b>
Collapse index (G/E <sub>T</sub> )	0.11	<b>0.013</b>

Time-since-death influences fibre width and kink index as well as collapsibility factor according to ANOVA analysis. Note that kink index also shows an influence from site attribute. Posthoc analysis and an examination of average fibre widths show that kraft fibres from red stage wood have smaller diameters than other samples. However, differences are small, and the fibre width distributions (Appendix C) are very similar except that distributions for red stage fibres are slightly shifted towards lower diameters. At this time we are not able to explain the observation of smaller fibre diameters for red

stage fibres. Also, the differences in diameter do not translate into significant handsheet quality differences between red stage wood and other wood, thus are not of practical importance.

Collapsibility for kraft pulp fibres is estimated by calculating the geometrical factor  $G$  (Equation 3). Cell wall thickness after pulping is not readily available, thus we use a relationship proposed by Scallan and Green (1975) that describes the reduction of cell wall thickness during pulping for oven dry kraft fibres. Assuming that the given relationship holds also for wet fibres, and using SilviScan measurements of wood fibre wall thickness and kraft yield as input, kraft fibre wall thickness is calculated. The geometrical factor  $G$  is then calculated based on FQA-measured fibre diameter and estimated wall thickness. Actual collapse index is proportional to the geometrical factor and the inverse of the transverse modulus of elasticity  $G/E_T$  (Jang and Seth 1998), with the latter depending on microfibril angle and the principal compliance constants of the fibre wall (Jang 2001). For a wet fibre wall:

$$E_T(\Theta) = \frac{1 - 4 \sin^2 \Theta \cos^2 \Theta \left(1 - \frac{S_{11}}{S_{66}}\right)}{S_{11} \cdot \cos^4 \Theta} \quad (\text{Equation 4})$$

with  $\Theta$  = microfibril angle (MFA)  
 $S_i$  = principal compliance constants of the fibre wall

The ratio of  $S_{11}/S_{66}$  is set to 0.74 for softwood kraft at kappa 30 based on work by Page et al. (1977) and microfibril angle is known from SilviScan measurements. The ratio of  $G/E_T$  was calculated and numbers are compared in Table 9. Similarly to fibre width results, the collapse index ( $G/E_T$ ) of fibres from red stage wood is slightly lower. While this difference is significant according to ANOVA analysis (Table 8), the differences are likely too small to be of practical influence. The differences in collapse behaviour that exist are so small that microscope images of cross-sections also do not reveal obvious differences between red stage and other samples.

**Table 9.** Selected fibre morphology values and resulting collapse index as represented by  $G/E_T$ .

Site	Attack stage	Fibre wall thickness <sup>†</sup> [ $\mu\text{m}$ ]	Geometry factor $G$	MFA [ $^\circ$ ]	Transverse modulus $E_T$	$G/E_T$
“Dry” sites						
18-01 green	Green	1.5	9.3	11.7	1.043	8.9
18-01 red	Red	1.5	8.7	12.2	1.047	8.3
05-02	Early grey	1.5	9.2	9.1	1.025	8.9
01-01	Late grey	1.4	10.0	14.7	1.071	9.4
“Moist” sites						
15-01	Green	1.4	9.5	12.5	1.045	9.1
SPF-1	Red	1.6	7.9	11.8	1.044	7.6
14-02	Early grey	1.6	8.4	10.6	1.035	8.1
07-01	Late grey	1.5	9.1	10.8	1.036	8.7
“Wet” sites						
16-01	Green	1.4	9.7	10.7	1.036	9.4
SPF-3 red	Red	1.6	8.2	8.0	1.019	8.0
SPF-3	Early grey	1.6	8.8	10.1	1.032	8.5

<sup>†</sup>Calculated from wood fibre wall thickness and kraft pulp yield.

The strongest effect from attack stage in Table 8 is seen on kink index. Curl also increases with advancing attack stage, but the trend is not clear and according to ANOVA not significant. Kinks are fibre defects that can be introduced by various processes, particularly when pulp is handled at higher consistencies as is common in many parts of pulp and paper mills. Low consistency refining will counter this effect and straighten fibres to a certain degree. Kink and curl both are important parameters as highly kinked and curled fibres result in less strong paper than straight fibres. In the pilot plant pulping employed for this study, the only process that could introduce kink and curl is the thickening of brown stock by centrifuge, after the brown stock coming from the digesters was diluted and screened. Therefore, kink index of these pulps cannot be compared to mill values, but the relative increase in kink index with increasing TSD of up to 0.2/mm when comparing green and grey or late grey pulps is significant. As all pulps are handled in exactly the same way, an increasing kink index with attack stage could suggest that fibres are becoming more susceptible to damage with increasing TSD. However, it should be kept in mind that no significant influence on strength properties is seen with increasing TSD.

Micrographs of kraft handsheets (surface and cross-sections, at 0 and 12000rpm PFI mill refining) confirm that little differences should be expected. While some differences regarding the appearance of sheet consolidation, fibre coarsenesses and fibre collapsibility exist, these were very small, thus sheets were difficult to differentiate. We attempted to subjectively rank the images. No trend with attack stage was obvious for the ranked images, although all green sheets were ranked among the more consolidated sheets with most fibres being collapsed. Ranking before and after PFI mill refining was relatively similar within the constraints of such subjective ranking. Figure 24 shows selected cross-sections and surfaces where differences were perceived to be largest.

These images illustrate how small differences are. Also, note that even before PFI mill refining, the majority of fibres are collapsed and the sheets are well consolidated.



**Figure 24.** Cross-section and surface images of selected kraft handsheets before and after PFI mill refining.

### 3.8 Thermomechanical (TMP) pulping

#### 3.8.1 Energy-freeness relationship

In preliminary work, it was found that wood from pine trees that had been attacked and killed 3 years prior to harvest needed slightly less energy to pulp to the same freeness than wood that had been killed 1 or 2 years previously or was currently attacked (Watson 2006). Such an influence of TSD could not be confirmed in the current study. While a plot of freeness versus energy for all samples (Figure 25) suggests that red stage trees may need more energy to pulp to the same freeness than green, grey or late grey samples, this difference was not significant when compared at a standardized freeness of 100 ml CSF (data are given in Appendix D) by main effect ANOVA with site attribute and attack stage as factors. Spread overall can be large as illustrated by the green and grey samples from moist subzones, which require significantly lower energy to pulp to the same freeness than other samples.

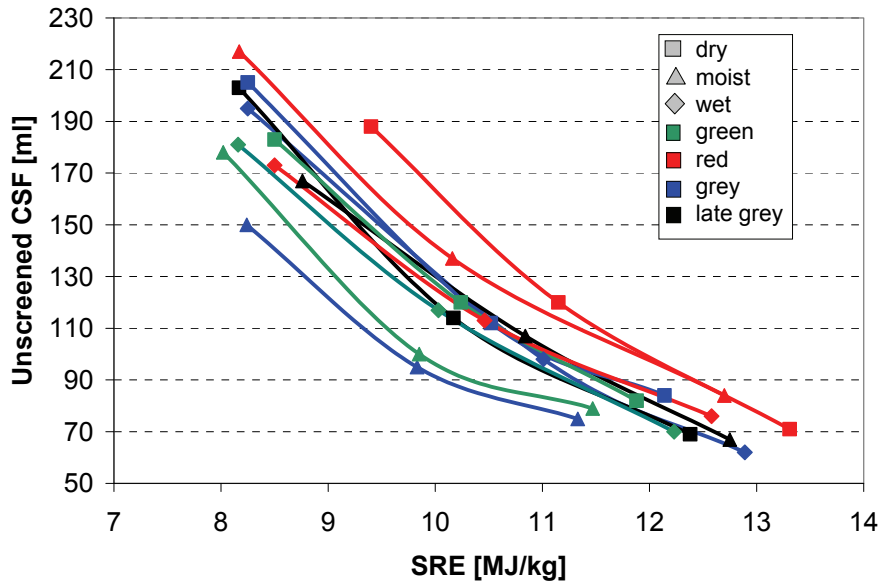


Figure 25. Freeness versus energy relationship for all pulp samples.

Given the lack of differences in refining energy for green and dead wood, moisture content (Figure 17) does not seem to influence the energy-freeness relationship. Equalization of moisture content in the pre-steaming stage could be one explanation for this. Other research has shown that chip moisture content does not influence TMP energy consumption if kept above fibre saturation point (Eriksen et al. 1981, Hartler 1986). Implications of wood moisture content on TMP pulping are investigated in more detail in a separate study (Hu et al. 2007A).

#### 3.8.2 Pulp quality

Pulp quality parameters include fibre properties, sheet structure and strength properties as well as optical properties. The raw data for the TMP pulps produced from 27 samples from different sites are shown in Appendix D. In order to facilitate data analysis and

discussion, the raw data were standardized by interpolation or extrapolation to a freeness of 100 mL CSF and a specific refining energy of 10.0 MJ/kg (Appendix D).

Data were examined as a function of CSF and also specific refining energy SRE. Additionally, interpolated values at 100 ml CSF as well as at 10 MJ/kg SRE were evaluated for differences due to site attributes and attack stage by main effect ANOVA. Results are shown in Table 10. At a significance level of  $p = 0.05$ , sheet density, roughness, opacity and brightness are influenced by the attack stage, for both a comparison at 100 ml CSF as well as at 10 MJ/kg SRE. Additionally, growth conditions (site attributes) have an effect on sheet density and long fibre fraction (R-28), but only when compared at 100 ml CSF. Also, scattering coefficient (at 100 ml CSF and 10 MJ/kg SRE) and tensile index (at 100 ml CSF only) are influenced by the attack stage when considering a significance level of  $p = 0.1$ .

**Table 10.** ANOVA analysis for TMP pulp and handsheet properties with site attribute and attack stage as main effects.

Property	At 100 ml CSF		At 10 MJ/kg SRE	
	$P_{\text{subzone}}$	$P_{\text{attack stage}}$	$P_{\text{subzone}}$	$P_{\text{attack stage}}$
SRE [MJ/kg]	0.369	0.158	N/A	N/A
CSF [ml]	N/A	N/A	0.302	0.219
LWFL (FQA) [mm]	0.546	0.502	0.413	0.183
R-28 fraction [%]	<b>0.031</b>	0.287	0.996	0.322
R-48 fraction [%]	0.767	0.541	<b>0.546</b>	0.393
P200 fraction [%]	0.426	0.496	0.146	0.568
Apparent density [kg/m <sup>3</sup> ]	<b>0.025</b>	<b>0.003</b>	0.606	<b>0.039</b>
Tensile index [Nm/g]	0.535	<b>0.082</b>	0.732	0.195
Tear index (4-ply) [mNm <sup>2</sup> /g]	0.646	0.829	0.913	0.548
Burst index [kPa·m <sup>2</sup> /g]	0.824	0.389	0.766	0.166
Sheffield roughness [SU]	0.263	<b>0.034</b>	0.493	<b>0.022</b>
Scattering coefficient [cm <sup>2</sup> /g]	0.369	<b>0.097</b>	0.388	<b>0.103</b>
ISO opacity [%]	0.593	<b>0.002</b>	0.664	<b>0.005</b>
Brightness [%]	0.702	<b>0.0006</b>	0.676	<b>0.0003</b>

### *Fibre Properties*

Average fibre length and long fibre fraction (either R-48 or R-28 BauerMcNett fractions) are not influenced by mountain pine beetle attack. This suggests that the shorter fibre lengths for increasing TSD found in an earlier study (Watson 2006) were likely due to site effects. The R-28 fraction shows some influence from subzone attributes. This may be related to the dependence of wood (macerated) fibre length on subzone that was discussed earlier (3.2.1). A plot of R-28 versus freeness (Figure 26) shows that while according to ANOVA there is no significant influence of TSD, there are still important differences between the different samples. Particularly, the late grey, dry subzone sample and also the grey, moist subzone sample show lower R-28 fraction which should have an influence on sheet strength. Whether the low R-28 fraction of the late grey, dry sample is related to the fact that this is the sample with the longest TSD (30 years) cannot be concluded for sure. However, it should be noted that the macerated wood fibres of the late grey trees were not shorter compared to the other samples within the dry subzone

sites, thus the late grey stage fibres may have been more susceptible to shortening during refining. Red stage pulps lie at the higher end of R-28 fractions found in this study.

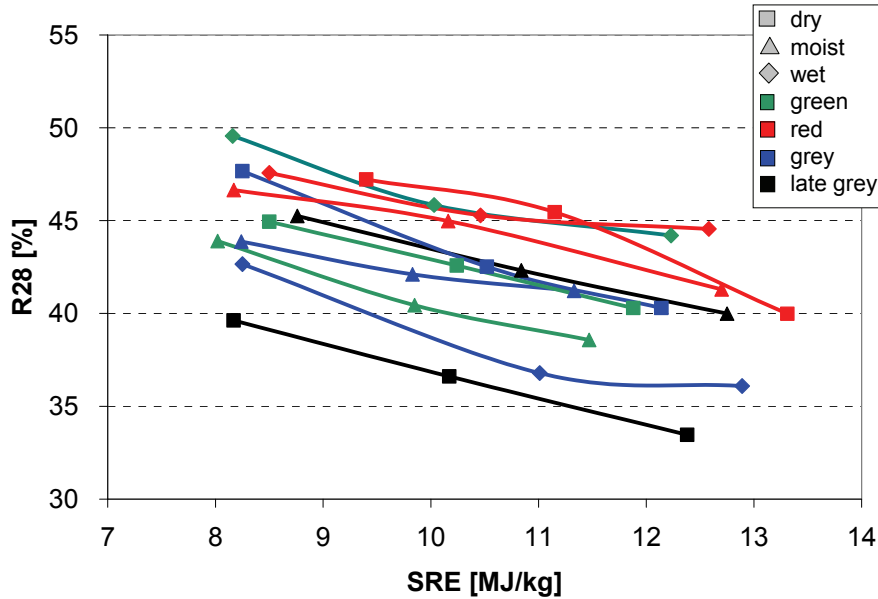


Figure 26. BauerMcNett R-28 (long fibre) fraction as a function of CSF for all samples.

Fines are an important characteristic of TMP pulp. Fibre fragments and small fibrils contribute to surface area, thus to sheet bonding. On the other hand, a large amount of ray cell material which does not bond well can be detrimental to sheet strength. A comparison of fines shows a trend of increasing fines with increasing TSD for the dry and wet subzones, but not the moist subzones (Figure 27). According to ANOVA analysis, the effect of TSD overall is not significant.

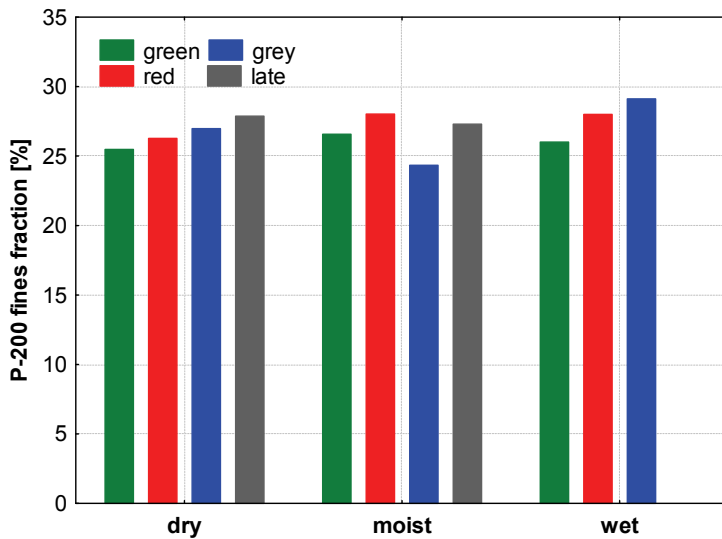


Figure 27. Fines (BauerMcNett P-200 fraction) at 100 ml CSF compared by subzones.

### Sheet consolidation and strength properties

Sheet density decreases with increasing freeness. Pulp from live trees makes denser handsheets at a given freeness than any of the dead tree samples (Figure 28). Green trees also result in higher sheet density when compared at a given refining energy. This effect of green versus MPB-killed wood is also confirmed by the ANOVA analysis. Posthoc tests (Scheffe) show that sheet density from green trees differs significantly from any other sample. The difference in sheet density is small (in the range of 10 to 40 kg/m<sup>3</sup>), however may be important as pulping to a lower freeness will be required if sheet density is to be maintained, which can result in drainage issues on the papermachine. According to ANOVA results, subzone also has a small influence on sheet density (Scheffe posthoc test: sheet density of samples from dry subzones differs from wet subzones).

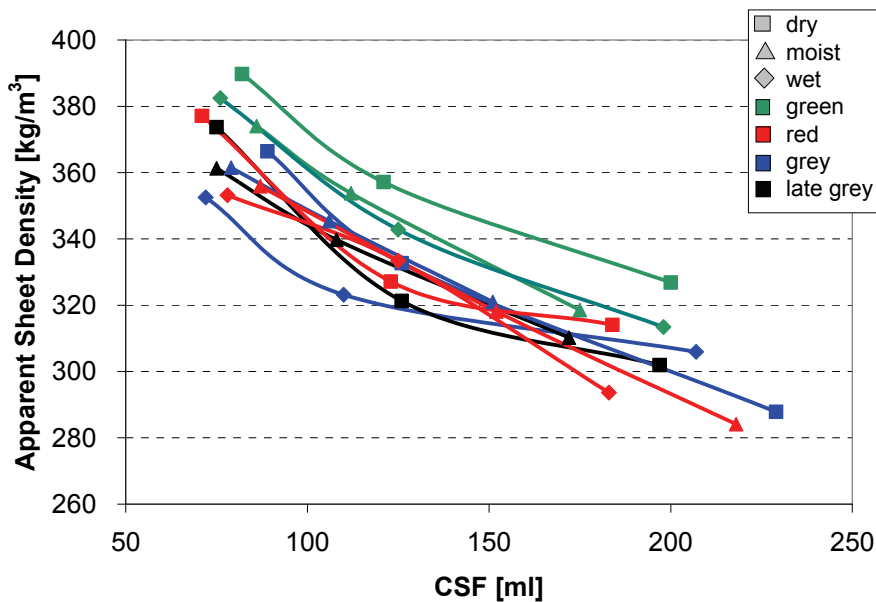
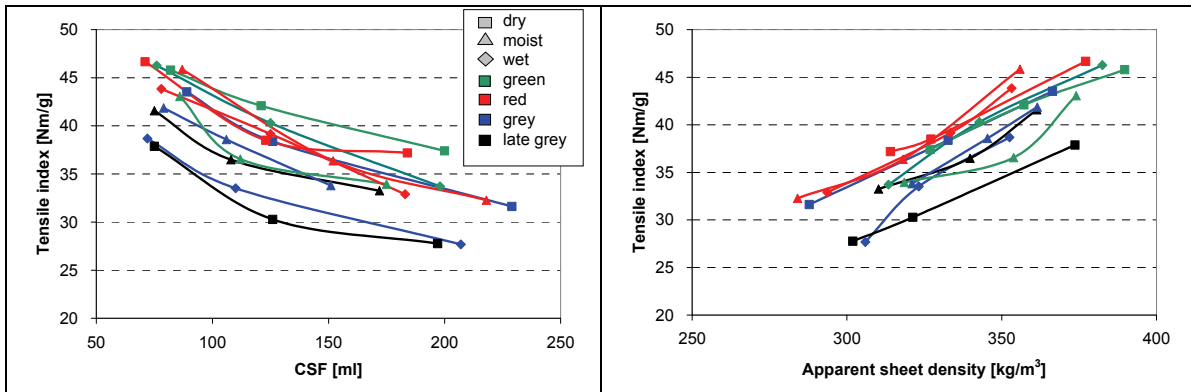


Figure 28. Sheet density as a function of CSF.

In general, higher sheet density at a given freeness results in improved strength properties. This is not obvious for these samples. While the ANOVA analysis shows some influence at the 90% significance level of attack stage on tensile index (at constant CSF only), posthoc analysis shows that this relates to the late grey samples being significantly lower in tensile than green or red attack samples. As discussed earlier, at least the late grey sample from a dry subzone has a significantly lower long fibre fraction so the lower tensile for this sample was expected. Overall, variability of tensile index is large. Also, while the green tree samples lie at the higher end of tensile index range when compared against freeness, this difference is less apparent when compared against sheet density (Figure 29). In fact, when compared at constant sheet density, the red stage samples show the highest tensile values. Note in these plots the low tensile for the late grey, dry subzone sample and grey, moist subzone sample, in agreement with their lower long fibre fraction.





**Figure 29.** Tensile index as a function of CSF (a), and of apparent sheet density (b)

Other strength properties (tear and burst index) did not show any influence from either attack stage or site attribute. Variability for these properties between sites can be high (up to 2.5 mNm<sup>2</sup>/g or 25 % for tear index, and up to 0.75 kPam<sup>2</sup>/g or 25 % for burst index), and the late grey, dry subzone and grey, moist subzone samples again show lower numbers than other samples.

#### *Sheet surface and optical properties*

The most obvious influence on pulp properties from MPB attack is on brightness. Figure 30 illustrates the decrease in brightness with attack stage within each subzone and compared at 100 ml freeness. ANOVA confirms the influence of attack stage on brightness. The decrease of up to 9% is very severe as bleaching of this pulp is difficult. Issues relating to brightness decrease and bleaching of pulp from MPB-killed wood are addressed in a separate study (Hu et al. 2007B).

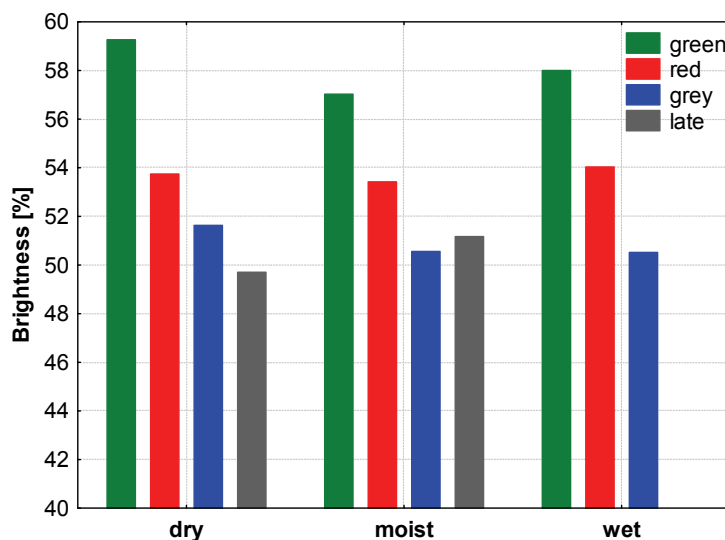


**Figure 30.** Brightness of TMP handsheets at 100 ml CSF.

Opacity shows a similarly obvious influence of attack stage, again confirmed by ANOVA (Figure 31). Opacity increases with MPB attack. Opacity is an important parameter for printing papers, thus an increase could be beneficial. However, opacity is influenced by scattering and absorption coefficients of the paper. Given that an influence of attack stage on scattering coefficient is much less obvious (Figure 32), it is likely that the increase in opacity is largely related to the lower brightness, thus differences may be much less after bleaching. ANOVA analysis of scattering coefficient shows a difference due to attack stage only at the 90% significance level, and only for green compared to late grey pulps. Whether attack stage influences scattering coefficient is therefore questionable. Scattering coefficient is related to the free surface in sheets, thus depends on the surface area of the pulp, and decreases with increasing sheet bonding.

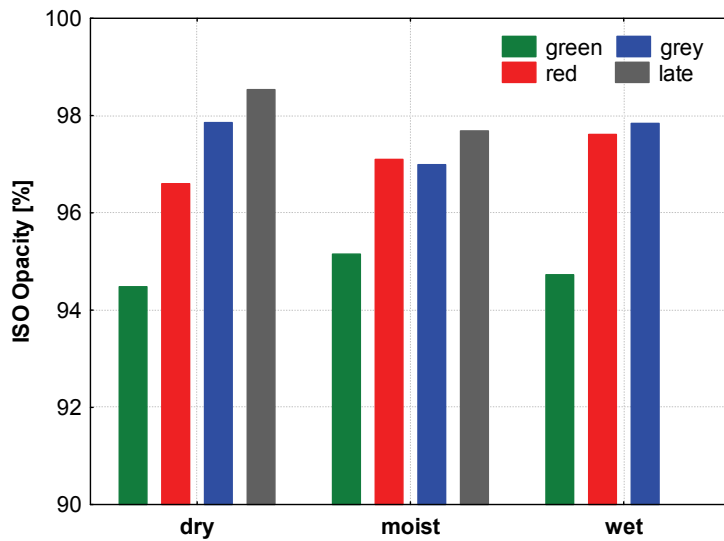


Figure 31. ISO opacity of TMP handsheets at 100 ml CSF.

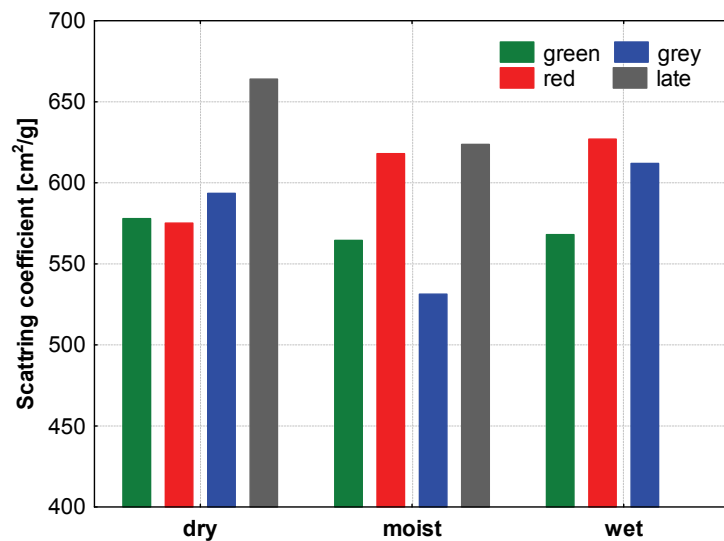


Figure 32. Scattering coefficient of TMP handsheets at 100 ml CSF.

Lastly, an influence of attack stage is also seen on the surface roughness. Surface properties are very important for TMP pulp, as they have a profound influence on printing properties, as well as processing issues during printing such as linting. Linting can also become an issue during papermaking. While the surface roughness of handsheets cannot be compared to the roughness of machine-made paper, relative differences between handsheets may be an indication of possible issues regarding the paper surface, thus should not be dismissed. For the samples in this study, surface roughness increases with TSD, thus may point towards an increased linting tendency, and a negative effect on print quality. The differences in roughness are confirmed by ANOVA, and posthoc analysis shows significant differences between green samples when compared to grey or late stage samples.

However, as a word of caution, it should be mentioned here that such a difference in surface roughness is only seen when measuring the smooth sides of handsheets which have been in contact with the metal drying plate (as is commonly done), but not when measuring on the rough side which have been in contact with the blotting paper (Figure 33). This illustrates that surface roughness is a complex property that not only depends on furnish, but also on the interaction with the backing material during sheet forming. Whether an influence on roughness from MPB-attack is seen likely will depend on the machine setup as well as forming fabric, press felts, and surface properties of drying cylinders that are used in any given papermachine.

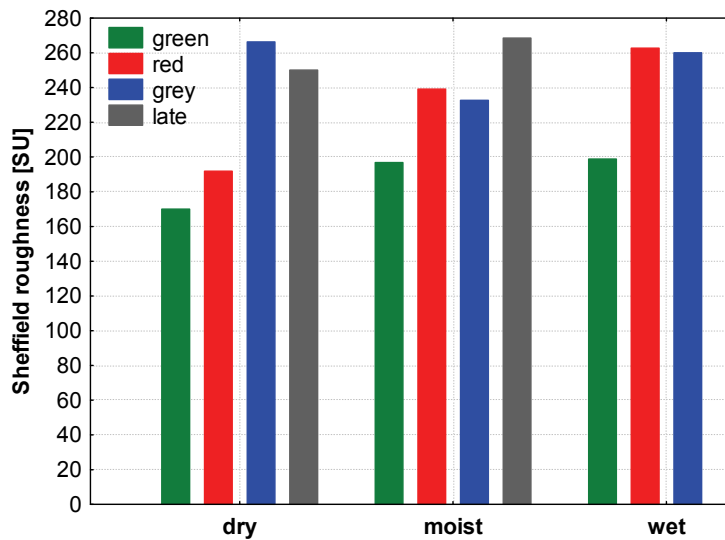
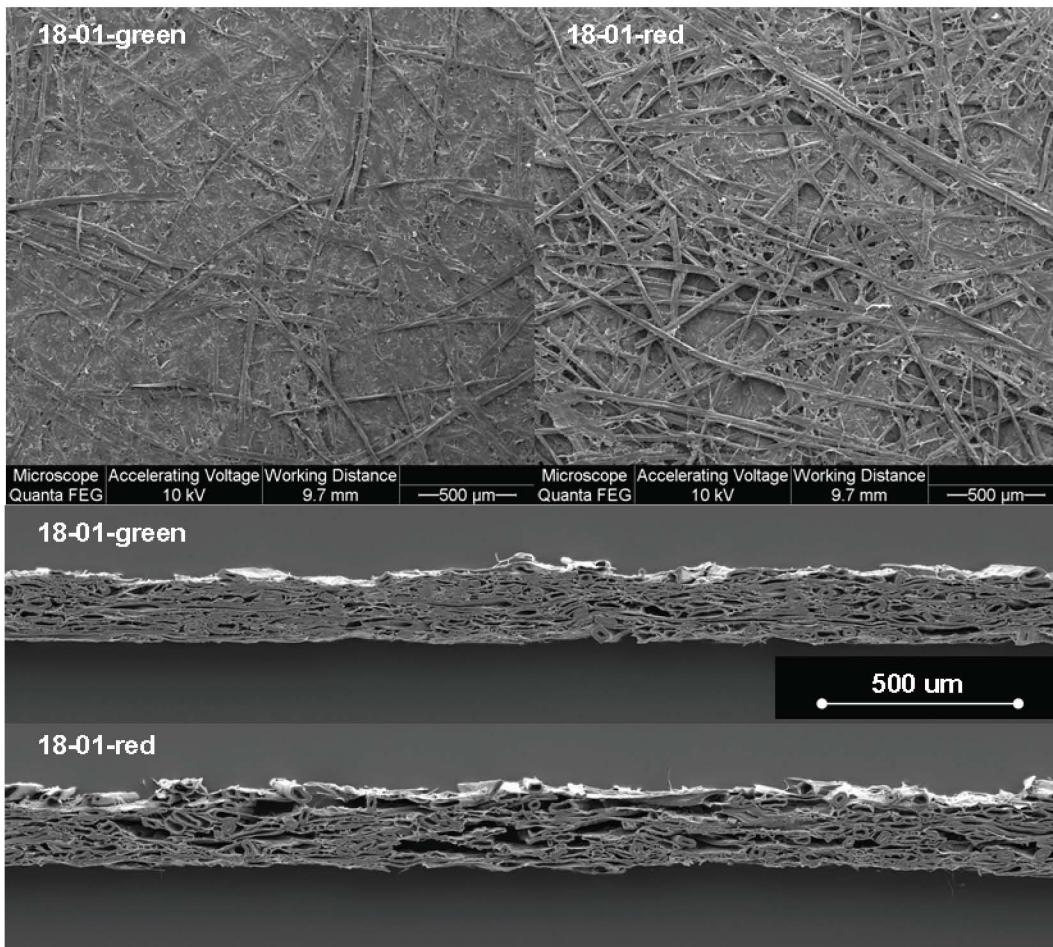


Figure 33. Surface roughness of smooth sides of TMP handsheets at 100 ml CSF.

#### *Micrographs of handsheet surface and cross-sections*

To further evaluate sheet structure and fibre morphology, handsheet cross-sections and surfaces were examined by ESEM. Handsheets refined to the lowest CFS were used. Sheets appear well closed in the surface images (showing the rough side of the handsheet), and while some differences regarding openness and consolidation exist, they are relatively small. An exception were handsheets from the dry/red stage site, which

appeared much coarser and less consolidated than other sheets, particularly when compared to handsheets made from trees from the same site but unattacked (dry/green). Ranking all sheets however, did not return any relationship of sheet surface appearance with attack stage. The cross-sections (rough handsheet side up) also did not show any obvious differences between different attack stages. While handsheets from green sites appear well consolidated, of constant caliper and smooth surface, the same is true for some of the handsheet from attacked stages, although others do look more irregular and less well consolidated. As before, a difference is seen between red and green trees from the dry site (see Figure 34 for surface and cross-sectional images of these two samples). Note that for kraft handsheets, such differences between red and green trees from the dry site were not apparent. All micrographs of TMP handsheets are shown in Appendix E.



**Figure 34.** Surface and cross-section images taken with the ESEM of unattacked and red attack samples from the “dry” site.

### 3.8.3 Calendering and calendered handsheets quality

The differences in surface roughness, together with mill reports about excessive linting and other printing issues with the use of MPB-killed wood, prompted us to do a preliminary evaluation of linting propensity of some of the samples of this study. The

samples from the dry subzone sites were selected for the linting study, as trends with increasing TSD were most obvious for this group of samples.

For the linting tests, calendered handsheets were needed. Larger amounts of pulp had to be produced to provide enough material for additional handsheet making. These pulps were produced with a target of 100 ml CSF. Handsheets were produced with standard methods and calendered to two target roughness numbers of 3.5 and 4  $\mu\text{m}$  PPS S10 roughness, measured on the rough side of the sheet. A calibration curve using a range of nip loads was produced initially to determine the required nip load for the target roughness. Results from the calibration are shown in Figure 35. The late grey sample required a lower nip load to reach a specified target roughness compared to green, red and grey samples which were rather similar in their calendering behaviour. Note that the late grey sample starts out with a slightly lower roughness, contrary to what was observed for the smooth side of the sheet.

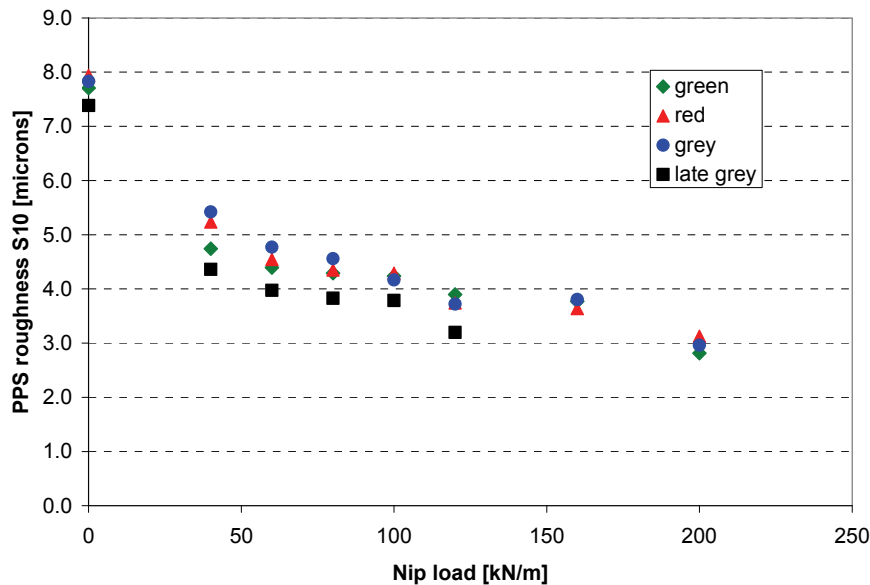


**Figure 35.** Handsheet smoothing with increasing calendering nip load for samples from the dry subzone sites.

Nip loads to reach the target roughness values are calculated from the calibration curves and are given in Table 11. Note that the required load to reach 3.5  $\mu\text{m}$  in the late grey sample is similar to the loads needed to reach 4.0  $\mu\text{m}$  in the other samples. Thus, it is also possible to compare calendering results at an approximately constant nip load.

**Table 11.** Required nip loads to reach set target PPS roughness values (dry site samples).

Site	Attack stage	Subzone attribute	Required nip load [kN/m]	
			PPS = 3.5 $\mu\text{m}$	PPS = 4.0 $\mu\text{m}$
18-01-green	Unattacked	Dry	172	115
18-01-red	Red	Dry	170	110
05-02	Grey	Dry	175	107
01-01	Late grey	Dry	110	60

Results of handsheet properties before and after calendering are given in Appendix D. With calendering, sheet density increases, thus bulk and caliper decrease, and strength properties decrease. The loss in strength properties is well known and is caused by breaking of bonds. It should also be noted that for the green, red and grey samples, the higher load required to reach a target PPS of 3.5  $\mu\text{m}$  caused some calender blackening, a defect that is related to excessive nip loads which the paper cannot tolerate. In calender blackening, selective densification of already dense spots occurs, and manifests itself in the appearance of glossy, black spots caused by crushing of fibres (Elbert et al. 1996).

When compared at similar roughness values, the late grey sample results in less dense handsheets compared to the other three samples (Figure 36). These differences however, are likely caused by the difference in required nip load to reach a certain roughness. When the 3.5  $\mu\text{m}$  handsheets of green, red and grey samples are compared to the 4.0  $\mu\text{m}$  handsheets of the late grey samples (see Appendix D), which were calendered at approximately similar loads, no significant differences are seen in sheet density. Air resistance, which is inversely related to sheet porosity, closely follows sheet density behaviour, thus is also lower for the late grey sample at a given roughness. Tensile of the late grey stage handsheets compared at 4  $\mu\text{m}$  roughness is higher than for the other samples, as expected, due to the lower required nip load, however drops more with continued calendering and is in the same range as the other samples at 3.5  $\mu\text{m}$  roughness (Figure 37). At similar sheet densities, the tensile of late grey stage wood is lower, as was the case for uncalendered sheets.

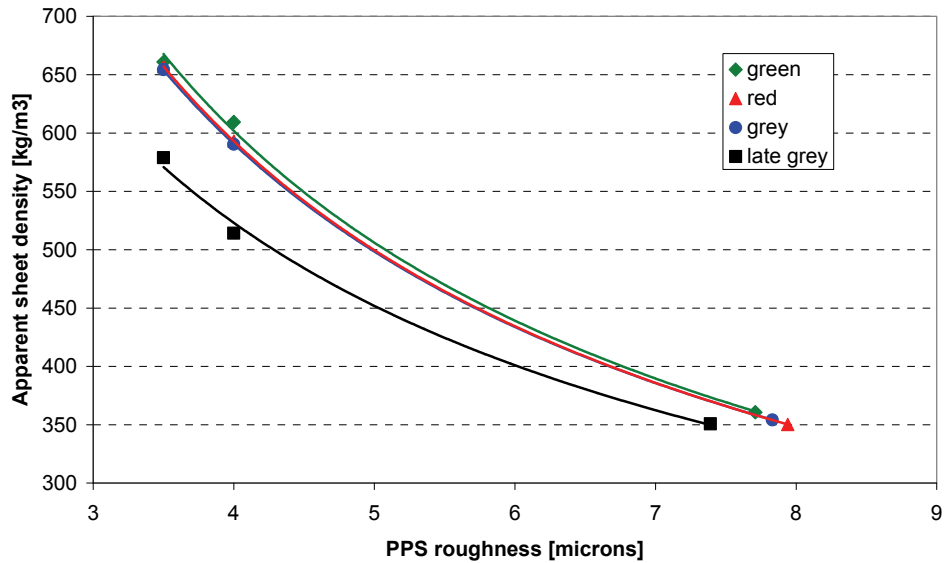


Figure 36. Sheet density as a function of PPS roughness for dry site samples.

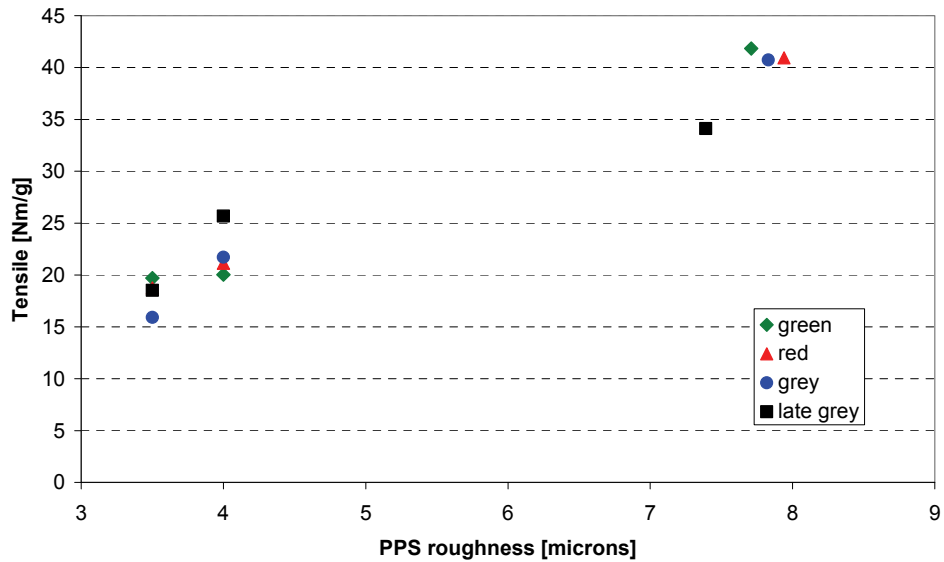
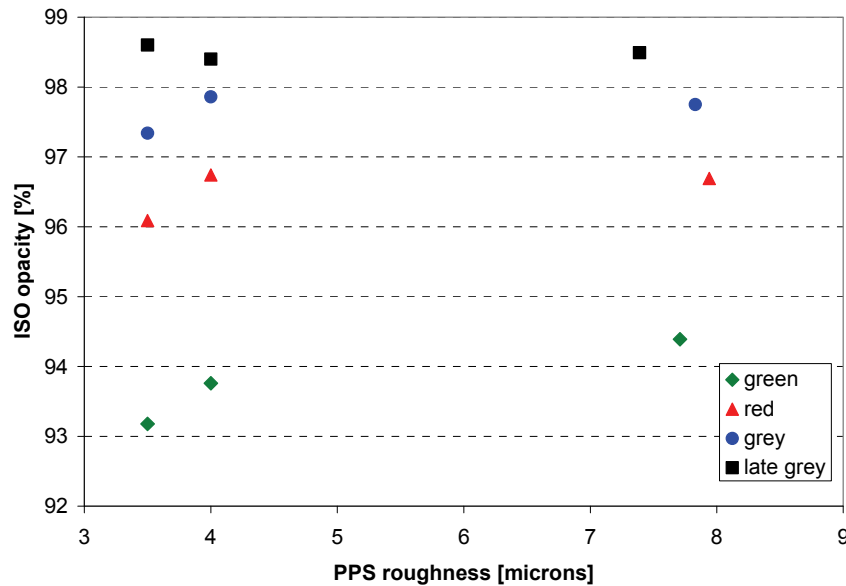


Figure 37. Tensile index as a function of PPS roughness for dry site samples.

The influence of calendering on optical properties is less obvious. Opacity and scattering coefficient, which are closely related, stay approximately constant with calendering. Differences in opacity (Figure 38) and scattering coefficient that exist for the uncalendered handsheets thus are preserved. For the green, red and grey samples, a small reduction in either property is seen at the lowest roughness value. This is likely related to the calender blackening that was seen for these points, as crushing of fibres will reduce the total air-fibre interface area. A small reduction in both properties is also seen for the green sample at the first calendering point when compared to uncalendered handsheets. A

decrease in opacity is often seen during supercalendering, even without blackening (Nesbakk and Helle 2002).



**Figure 38.** Opacity as a function of PPS roughness for dry site samples.

It was suspected that the differences in calendering behaviour of the late grey sample may be caused by differences in fibre morphology. Sheets made from finer fibres are generally easier to calender than sheets from coarser fibres. We thus determined the coarseness of the two longest BauerMcNett fibre fractions (R-14 and R-14/28). Differences between samples are not significant (Table 12). However, as observed earlier, the long fibre fraction (R-28) is lower for the late grey sample, thus these sheets contain less of these coarse, long fibres. While this may explain why a target roughness is reached with lower nip loads compared to the other samples, it would contradict the observation that the sheet density reduction is similar for all samples when using the same nip load. Clearly, more variables than long fibre fraction, fines fraction and coarseness contribute, and we have currently not enough information to explain the differences in calendering behaviour.

**Table 12.** Fibre morphology of R-14 and R-14/28 fractions for pulps from dry subzone sites at 100 ml CSF.

Site	Attack stage	Subzone attribute	Fibre coarseness [mg/m]		LWFL [mm]	
			R-14	R-14/28	R-14	R-14/28
18-01-green	Unattacked	Dry	0.331	0.263	3.05	2.33
18-01-red	Red	Dry	0.358	0.271	3.01	2.31
05-02	Grey	Dry	0.339	0.274	3.07	2.35
01-01	Late grey	Dry	0.322	0.257	3.03	2.52



While the calendering results of handsheets cannot be compared to actual machine-made paper, some conclusions can be drawn based on the relative differences between samples. Depending on the target properties during calendering, the use of late grey stage wood may have different impacts. If a certain roughness is targeted, using late grey stage wood will require lower nip loads, which will result in less decrease in strength properties and increased sheet bulk. Increased sheet bulk is beneficial for ease of sheet handling (higher stiffness), but means less paper on a roll, thus requires more roll changes in a printing press. If, on the other hand, bulk is targeted, the use of late grey stage wood will impact mostly the roughness, which will be lower for the late grey stage wood. Again, this can be beneficial as long as roughness values do not drop too low. In general, a combination of roughness and bulk is targeted in a mill. While the data we have for calendering are too few to draw firm conclusions, the results suggest that some changes may occur with using wood of increasing TSD, which could result in problems reaching target specifications. Thus the possible influence on roughness and calendering behaviour of MPB-killed wood should be followed up with more detailed studies.

### 3.8.4 Linting

Linting propensity was determined using two different methods, as explained in 2.4.4. It should be emphasized that for the tests, unbleached pulp was used. Also, the Paplint test was done on handsheets, which differ substantially from machine-made paper. Results from these tests are thus not directly comparable to results obtained from samples taken from paper mills. Still, they enable a relative comparison between the linting behaviour of the selected samples, and therefore may provide valuable information about the influence of increasing TSD of MPB-killed wood on the linting behaviour of paper made from TMP.

#### *Pulp linting propensity index (PLPI) test*

The pulp linting propensity index (PLPI) is a measure of the relative amount of low surface area material in a pulp. Such material, in general, bonds less well, thus is easily removed during printing if found at the paper surface, thus contributing to linting. The PLPI values found for the four selected samples in this study were between 45% and 60% (Table 13), which is very high. Values found for lodgepole pine in other work (Reza Amiri, personal communication) are in the range of 20% to 30% at similar refining energies (but made in a different refiner and with different refiner settings). Differences between the four tested samples are minor, although the red sample shows an 8% to 10% points higher value compared to other samples. However, values should be compared at constant refining energy, and the refining energy for the red samples was lower by 0.5 to 1 MJ/kg, which can result in a change of up to 10% PLPI at this energy level.

**Table 13.** PLPI numbers for samples from dry subzones at approximately 100 ml CSF.

Site	Attack stage	Subzone attribute	CSF [ml]	SRE [MJ/kg]	PLPI [%]
18-01-green	Unattacked	Dry	92	11.22	52
18-01-red	Red	Dry	100	10.66	60.5
05-02	Grey	Dry	94	11.56	48
01-01	Late grey	Dry	100	11.03	45

It is suspected that the refining conditions caused the high PLPI values found for these four samples. However, it is also possible that there is some site influence on linting, as all samples were from sites in rather dry subzones. However, at least for the four samples tested, no influence of MPB-killed wood on predicted linting propensity is apparent, with the exception of a slightly higher linting propensity of the red stage sample.

As the PLPI test has a high variability, data are too few to draw firm conclusions. If further PLPI lint testing on MPB-killed samples will be done, the influence of refiner and refining conditions should be investigated first by pulping the same chip samples in a different refiner, and by including a range of refining energies. Also, samples from different sites would have to be included to account for a possible site effect.

### *Paprican lint test*

While the PLPI test determines the amount of material that may contribute to linting, the Paprican lint test, or Paplint, is designed to simulate the actual printing action in a printing press, thus quantifies the actual amount of lint material that will be encountered. The Paplint test was done on the four dry site samples, each calendered to two different roughness targets, which enabled the evaluation of the effect of different nip loads on linting.

Results from the Paplint test are summarized in Table 14. Average accumulated length of removed fines, medium and long fibres are given, as well as overall accumulated fibre length, number of particles removed and average length of removed particles. For all samples, all numbers increase with increasing calendering (decreasing PPS roughness). This reflects the well known fact that increasing calendering not only causes a decrease in tensile, but also an increase in linting, due to the decrease in bonding. The increase in total accumulated fibre length of linting material with decreasing PPS roughness is illustrated in Figure 39.

**Table 14.** Results from Paplint testing for dry site samples.

Site	Attack stage	PPS [ $\mu\text{m}$ ]	$\text{La}_f$	$\text{La}_m$	$\text{La}_l$	$\text{La}_T$	$\text{L}_T$	N
18-01-green	Unattacked	3.5	31.2	12.0	49.2	<b>92.4</b>	<b>0.49</b>	<b>3058</b>
		4.0	25.1	7.5	28.6	<b>61.2</b>	<b>0.38</b>	<b>2605</b>
18-01-red	Red	3.5	26.9	8.8	30.6	<b>66.3</b>	<b>0.40</b>	<b>2667</b>
		4.0	25.5	8.4	27.1	<b>61.1</b>	<b>0.38</b>	<b>2641</b>
05-02	Grey	3.5	31.5	11.5	48.5	<b>91.5</b>	<b>0.43</b>	<b>3424</b>
		4.0	23.7	6.3	26.6	<b>56.6</b>	<b>0.32</b>	<b>2832</b>
01-01	Late grey	3.5	41.2	15.9	85.4	<b>142.5</b>	<b>0.50</b>	<b>4590</b>
		4.0	39.6	13.1	54.2	<b>107.0</b>	<b>0.40</b>	<b>4363</b>

$\text{La}_f$ : average cumulated fines length per unit of printed area,  $\text{m}/\text{m}^2$  (length < 0.85 mm)

$\text{La}_m$ : average cumulated medium fibre length per unit of printed area,  $\text{m}/\text{m}^2$  (length < 0.85 mm < 1.35 mm)

$\text{La}_l$ : average cumulated long fibre length per unit of printed area,  $\text{m}/\text{m}^2$  (length > 1.35 mm)

$\text{La}_T$ : average cumulated fibre length per unit of printed area,  $\text{m}/\text{m}^2$

$\text{L}_T$ : average fibre length (includes all 3 classes), mm

N: total number of fibres removed

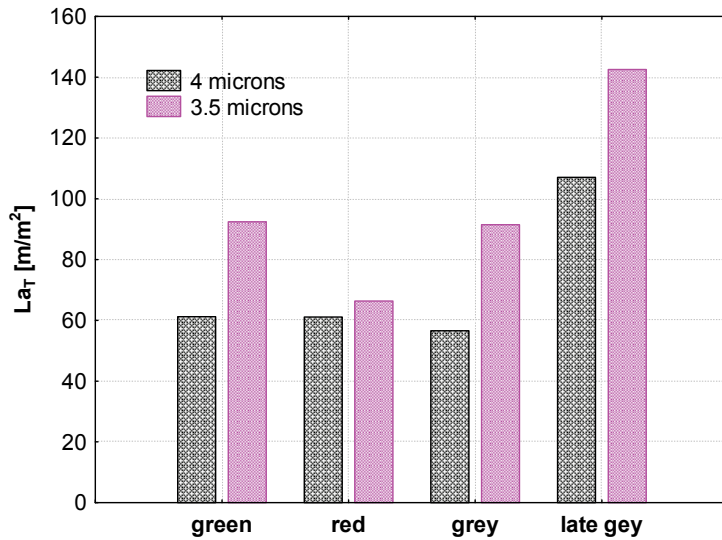


**Figure 39.** Accumulated fibre length  $La_T$  of linting material for dry site samples.

Figure 39 also illustrates that there is a noticeable difference in linting material removed from late grey samples compared to green, red and grey samples. The difference is caused by increased removal of all three length classes of fibres that are counted (long fibres, medium fibres and fines). Compared to the green sample, a 75% increase in accumulated fibre length for the late grey sample is seen at a PPS roughness of 4  $\mu m$ , and a 55% increase at 3.5  $\mu m$ . These numbers are significant. The numbers become even more significant when considering calendering at the same nip load, in which case the late grey sample at 3.5  $\mu m$  has to be compared to green, red and grey samples at 4  $\mu m$  PPS roughness. The increase in accumulated fibre length from green to late grey stage is 130% when comparing for a similar nip load, thus even higher than when comparing at constant surface roughness.

To evaluate whether the increased linting propensity of the late grey stage sample could be explained by differences in the different components of the pulp (e.g., high number of ray cells or similar), we collected the lint material of the samples calendered to 3.5  $\mu m$  PPS roughness and looked at them under the microscope. No differences in the composition of the lint material of all samples were found. However, it was noted that the lint material contains a high amount of long fibres, independent of attack stage of the samples. An example of the observed lint material is shown in Figure 40.

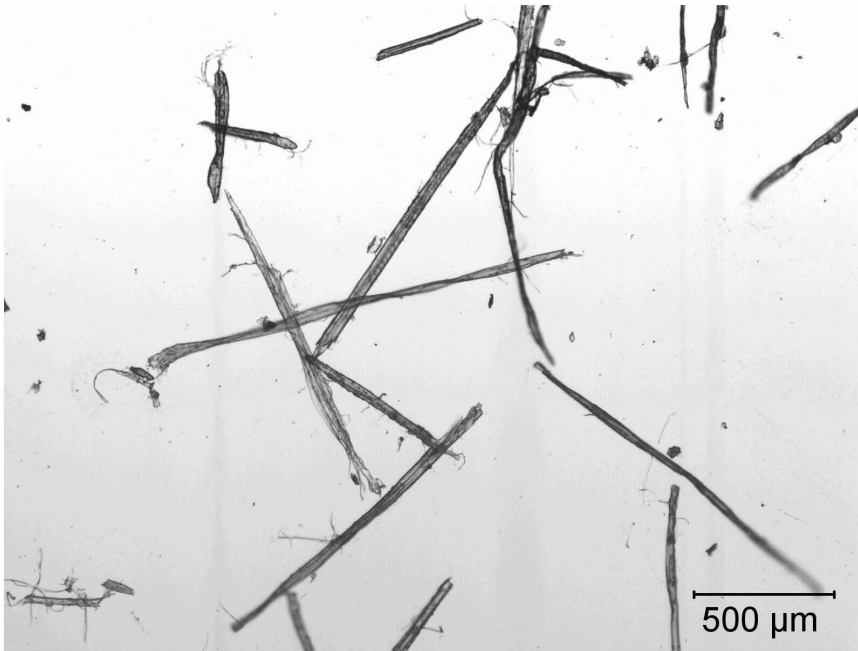


**Figure 40.** Lint material of the “dry”, late grey sample (site 01-01) calendered to 3.5  $\mu\text{m}$  PPS S10 roughness.

Linting propensity is influenced by a variety of factors including furnish and machine parameters. For furnish properties, fibre morphology (coarseness) and amount of fines are critical. However, for the samples used for the Paplint test, only small differences in coarseness and fines exist, thus they cannot explain the difference in linting propensity. When comparing sheet density and tensile (both indicators for sheet bonding) of the calendered handsheets at constant nip load, no differences were found between the late grey sample and other samples either. Thus there are no obvious differences in bonding ability. Given the effects on handsheet properties from calendering as well as results from both linting tests, it is, therefore, fair to conclude that while some influence of late grey stage wood on linting and calendering behaviour may exist, more information and a larger sample size are required to explain the behaviour and identify root causes.

#### **4 Conclusions**

The influence of TSD of MPB-killed lodgepole pine on pulping and pulp quality was investigated. Sampling for this study included sites from three different biogeoclimatic subzones in B.C. representing varying growth conditions, thus accounting for natural variability. Prior to pulping, fibre and wood quality were determined on core samples. Results confirmed findings of an earlier study that had shown little influence on fibre and wood properties from TSD except on wood moisture, which decreases rapidly. Some influence of TSD on specific surface area is also predicted, but needs further exploration. Site characteristics have an influence on fibre morphology (fibre length, coarseness and width), as has been shown in other studies, emphasizing the importance of proper sample control if the influence of TSD is to be distinguished from natural variability.

Chip quality is affected in a minor way, with lower accepts and a higher proportion of oversize chips, although these differences are not statistically significant. The kraft pulping data showed that MPB attack has little influence on either pulping or pulp quality variables. However, in other work it was shown that operational issues, including changes in tall oil recovery, exist (Allen et al. 2007). While variation in yield at constant kappa can be large (up to 5% points), there is no statistically relevant relationship between yield and TSD. While for one specific site, a small drop in tensile is seen going from unattacked to red attack trees, no effect on tensile or other strength properties is predicted when considering all sample sites. Regarding fibre quality, an increase in kink index with TSD was found, but not on fibre length, coarseness or diameter. While kink produced in a laboratory environment is not directly comparable to the mill environment, the differences in kink were significant, thus could suggest a possible effect of TSD on the susceptibility of fibres to damage that would result in kink.

No statistically significant effect of TSD on energy requirement and strength properties of TMP pulps was seen. Also, statistically, long fibre fraction was not affected, although one late grey and one grey sample showed a significantly lower R-28 fraction. For these samples, tensile was also noticeable lower. In general, tensile of grey and late grey attack wood appears, on average, lower than for green trees, however this effect was not statistically significant. While fines seem to increase slightly with TSD, the effect is also not statistically significant. Brightness decreases drastically (up to 9% points), largely due to the blue stain content, and with this opacity increases with TSD. Scattering coefficient does not show any consistent influence from TSD. A significant effect of TSD was found on sheet density and sheet roughness. The density of green trees was higher and roughness lower, although effects on roughness were only noted for the smooth side of the handsheets.

Owing to the possible effect of TSD on sheet surface and sheet structure, a preliminary investigation of the linting behaviour was done for selected samples. During calendering of handsheets for printing tests, the late grey sample needed a significantly lower nip load to reach target roughness. This is contrary to what is seen in some B.C. mills that report increased calendering needs, and may be due to the low long fibre fraction of this sample. Linting, however, was also much higher for this sample, even though the handsheets had been calendered at lower loads. Results from a second test for linting, the PLPI test, however did not show significant differences between samples. While these results have to be considered preliminary, particularly as the Paprican lint test was done on standard handsheets and not on machine-made paper, they do suggest that an effect of MPB-attack on resulting TMP paper printing quality may exist. These tests should thus be extended to include more samples and sheet forming conditions, that more closely simulate papermachine forming.

In summary, issues with the use of MPB-killed wood are likely largely related to the decreased moisture content. For kraft pulp, little influence of TSD is seen and at least from a fibre quality perspective, even late grey stage wood may be used without significant problems. For TMP pulp quality however, some differences in pulp quality due to MPB-attack are seen. These relate mostly to sheet structure and surface properties,

which are important parameters for printing papers, a main use of TMP pulp, thus should be followed up with more detailed studies of surface and printing behaviour.

## **5 Acknowledgements**

This project was funded by the Government of Canada through the Mountain Pine Beetle Initiative, a Program administered by Natural Resources Canada, Canadian Forest Service. Publication does not necessarily signify that the contents of this report reflect the views or policies of Natural Resources Canada – Canadian Forest Service.

The authors would like to thank the many individuals who provided services throughout this study. Brian Frenkel, John Baker (both Avison Management/Vanderhoof) and Steve Law (DWB/Lac La Hache) provided field services and Jim Chadbourn, Zach Ditoro, Mario Desrosier and Kyle Larden provided help with harvesting. The help of Stewart Pyper (BC Ministry of Forests and Range Chilcotin), Adam Caputa (BC Ministry of Forests and Range Vanderhoof), Wendi Knott (BC Ministry of Forests and Range Ndaina), Steve Harrison (BC Ministry of Forests and Range Fort St. James), Gerry Venos (BC Ministry of Forests Cariboo), Stacy Perkins (BC Ministry of Forests and Range Prince George) and Adam Veley (BC Ministry of Forests and Range Quesnel) in obtaining free use permits is greatly appreciated. Tennessee Trent provided invaluable help in the planning phase of the field work, and Maxwell McRae was a great help in conducting sampling and harvesting. Doug Thompson (University of Northern BC) provided kill date determinations for harvested trees by dendrochronology.

Our colleagues from Evalutree are gratefully acknowledged for their careful analysis of wood cores. We would like to thank Reza Amiri, Joe Aspler and Tony Manfred for fruitful discussions regarding the linting work, all their colleagues for their help with linting tests, and James Drummond for his patience in providing the many excellent micrographs. The advise and general guidance given by Paul Bicho throughout the study is much appreciated.

## 6 Literature Cited

- Allen, L.; Uloth, V. 2007. Operational Extractives Management from Mountain Pine Beetle Attacked Lodgepole Pine for Pulp and Papermaking. Natural Resources Canada, Canadian Forest Service, Pacific Forestry Centre, Victoria, BC. Mountain Pine Beetle Initiative Working Paper 2007-15. 45 p.
- Allen, P. 1999. "Sample preparation methods for determining the fibre length, coarseness and shape with the OpTest Fiber Quality Analyzer (FQA) Equipment". OpTest Inc.
- Banner, A.; Mac Kenzie, W.; Haeussler, S.; Thomson, S.; Pojar, J.; Trowbridge, R. 1993. A Field Guide to Site Identification and Interpretation for the Prince Rupert Forest Region. Land Management Handbook Number 26. BC Ministry of Forests, Research Branch. Victoria, B.C.
- Dalpke, B.; Hussein, A.; Trent, T.; Gee, W.; Johal, S.; Yuen, B.; Watson, P.A. 2008. Assessment of the economic (pulp and pulp quality) effects of increased lodgepole pine in SPF chip mixtures. Natural Resources Canada, Canadian Forest Service, Pacific Forestry Centre, Victoria B.C. Mountain Pine Beetle Initiative Working Paper 2007-08. 88 p.
- DeLong, C. 2003. A Field Guide to Site Identification and Interpretation for the Southeast Portion of the Prince George Forest Region. Land Management Handbook Number 51. BC Ministry of Forests, Forest Science Program. Victoria, B.C.
- Elbert, U.; Hoydahl, H.-E.; Martens, G.; Praast, H.; Weidenmuller, J. 1996. Image analysis of calender blackening. *Papier* 50(2): 53-59.
- Eriksen, J.T.; Hauan, S.; Gaure, K.; Mattans, A.L. 1981. Consequences of chip quality for process and pulp quality in TMP production. Preprints of the International Mechanical Pulping Conference, Oslo, Norway.
- Hartler, N. 1986. Wood quality requirements in mechanical pulping. *Nord. Pulp Paper Res. J.* 1(1): 4-10.
- Harvey, R.D. Jr. 1986. Deterioration of mountain pine beetle-killed lodgepole pine in northeast Oregon. USDA For. Serv. R6-86-13. Pacific Northwest Region, Portland, OR.
- Hatton, J.V. 1979. "Chip Quality Analytical Procedures". Chapter 14 in *Chip Quality Monograph*, Edited by Hatton, J.V., Joint Textbook Committee of the Paper Industry.
- Hatton, J.V.; Hunt, K. 1991. Managed lodgepole pine forests: I. Density and chemical properties of juvenile, mature and top wood. *Pulp and Paper Report PPR 890*. Paprican. Vancouver, B.C.

- Hatton, J.V.; Gee, W.Y.; Cisneros, H.A.. 1992. Managed logepole pine forests: II. Yield and quality of unbleached kraft pulps from juvenile, mature and top wood and their relationships with wood and fibre properties. Pulp and Paper Report PPR 966. Paprican. Vancouver, B.C.
- Holmes, R. 1983. Computer-assisted quality control in tree-ring dating and measuring. *Tree Ring Bull.* 43:69-78.
- Hsieh, E.; Uy, N.; Wallbacks, L. 2006. Development of a portable spectroscopic sensor to measure wood and fibre properties in standing mountain pine beetle-attacked trees and decked logs. Natural Resources Canada, Canadian Forest Service, Pacific Forestry Centre, Victoria, BC. Mountain Pine Beetle Initiative Working Paper 2006-16. 33 p.
- Hu, T., Omholt, I., Johal, S., Yuen, B., Zhao, M., Drummond, J. Miles, K.B., Stacey, M., Hellstern, M. and Watson, P. 2008. Pilot mechanical pulping assessment of dry blue-stained and grey-stage wood chips from beetle killed lodgepole pine. Natural Resources Canada, Canadian Forest Service, Pacific Forestry Centre, Victoria, BC. Mountain Pine Beetle Initiative Working Paper 2008-25. In press.
- Hu, T.; Williams, T.; Yazdi, S.; Wallbacks, L.; Watson, P.A. 2008. Overcoming the brightness ceiling for mechanical pulps prepared from blue-stained lodgepole pine chips. Natural Resources Canada, Canadian Forest Service, Pacific Forestry Centre, Victoria, BC. Mountain Pine Beetle Working Paper 2008-05. 29 p.
- Isenberg, I.H. 1980. Pulpwoods of the United States and Canada. Volume I – Conifers. The Institute of Paper Chemistry. Appleton, WS: 212.
- Jang, H.F. 2001. A theory for the transverse collapse of wood pulp fibres. 12<sup>th</sup> Fund. Res. Symp., Oxford: 193.
- Jang, H.F.; Seth, R.S. 1998. Using confocal microscopy to characterize the collapse behaviour of fibres. *Tappi J.* 81(5): 167.
- Keays, J.L; Bagley, J.M. 1970. Digester Assembly for Precision Pulping Studies. *Tappi*, 53(10): 1935-1940.
- Lawrence, V.; Woo, K. 2005. Silviscan: An Instrument for Measuring Wood Quality. Paprican Special Report PSR 550. Paprican. Vancouver, B.C.
- Lewis, K.; Thompson, D.; Hartley, I.; Pasca, S. 2006. Wood decay and degradation in standing lodgepole pine (*Pinus contorta* var. *latifolia* Engelm.) killed by mountain pine beetle (*Dendroctonus ponderosa* Hopkins: Coleoptera). Can. For. Serv. Mountain Pine Beetle Initiative Working Paper 2006-11. Victoria, B.C.



- Nesbakk, T.; Helle, T. 2002. The influence of the pulp fibre properties on supercalendered mechanical pulp handsheets. *J. Pulp Pap. Sci.* 28(12):406-409.
- Page, D.H.; El-Hosseiny, F.; Winkler, K.; Lancaster, A.P.S. 1977. Elastic modulus of single wood pulp fibres". *Tappi J.* 60(4):114.
- Pitts, S.; Bicho, P.; Watson, P. 2001. Rapid Prediction of Fibre Properties: Opportunities Using Forest Site Classification Methods. Pulp and Paper Report PPR 1532. Paprican. Vancouver, B.C.
- Reid, R.W. 1961. Moisture changes in lodgepole pine before and after attack by the mountain pine beetle. *For Chron.* 34:368-375.
- Scallan, A.M.; Green, H.V. 1975. The effect of pulping upon the dimensions of wood tracheids. *Wood and Fibre* 7(3):226.
- Shrimpton, D.M. 1972. Extractives associated with the wound response of lodgepole pine attacked by the mountain pine beetle and associated microorganisms. *Can. J. Bot.* 51:527.
- Shrimpton, D.M. 1973. Variation in the extractives from lodgepole pine. *North. For. Centr. Inf. Report NOR-X-18.*
- Skaar, C. 1988. Wood-water relations. Springer-Verlag, Berlin, Heidelberg, New York, pp. 35-41.
- Snyder, J.P. 1987. Map Projections: A Working Manual. U.S. Geological Survey Professional Paper 1395. United States Government Printing Office, Washington, D.C.
- Steen, O.A.; Coupé, R.A. 1997. A Field Guide to Forest and Site Identification for the Cariboo Forest Region. Land Management Handbook Number 39. BC Ministry of Forests, Research Branch. Victoria, B.C.
- Stokes, M.; Smiley, T. 1968. An introduction to tree-ring dating. University of Chicago Press, Chicago, IL. USA.
- Trent, T.; Lawrence, V.; Woo, K. 2006. A wood and fibre quality-deterioration model for mountain pine beetle-killed trees by biogeoclimatic subzone. Mountain Pine Beetle Initiative Working Paper 2006-10. Natural Resources Canada, Canadian Forestry Service, Victoria, B.C.
- Velmex, Inc. 1992. The velmex "TA" system for research and non-contact measurement analysis. Bloomfield, NY, USA.
- VoorTech Consulting. 2004. MeasureJ2X. Holderness, NH, USA.

- Watson, P. 2006. Impact of the mountain pine beetle on pulp and papermaking. 2006. Pages 255-275 (Chapter 10) *in* L. Safranyik and W.R. Wilson, editors. The mountain pine beetle: a synthesis of biology, management, and impacts on lodgepole pine. Natural Resources Canada, Canadian Forest Service, Pacific Forestry Centre, Victoria, British Columbia. 304 p.
- Woo, K.; Watson, P.; Mansfield, S. 2005. The effects of mountain pine beetle attack on lodgepole pine wood morphology and chemistry: Implications for wood and fibre quality. *Wood Fiber Sci.* 37(1): 112.
- Wood J.R.; Karnis A. 1992. "Linting Propensity of Mechanical Pulps". *Pulp and Paper Canada* 93(7):17-24.
- Wood J.R.; Karnis A. 1996. "The Determination of the Specific Surface of Mechanical Pulp Fines from Turbidity Measurements". *Paperi Jaa Puu* 78(4):181-186.

## **7 Contacts:**

Dr. Barbara Dalpke  
Pulp & Paper Res Inst. of Canada  
3800 Wesbrook Mall  
Vancouver, BC  
[bdalpke@paprican.ca](mailto:bdalpke@paprican.ca)  
(604) 222-3201 #366

## 8 Appendices

### Appendix A.

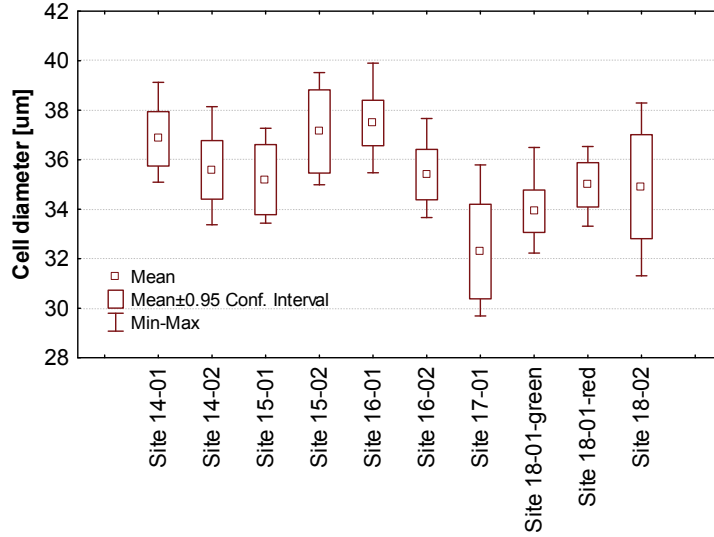


**Figure 41.** Average wood fibre diameter of trees from new sample sites (60 – 80 year age class), measured by SilviScan.

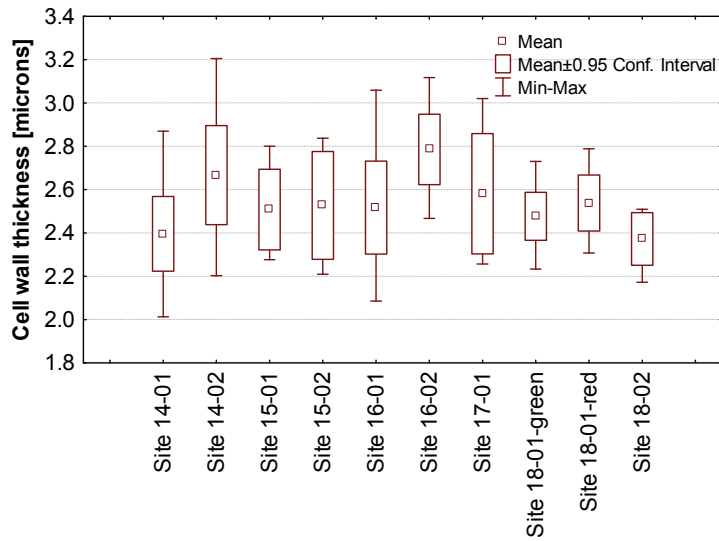


**Figure 42.** Average fibre wall thickness of trees from new sample sites (60 – 80 year age class), measured by SilviScan.

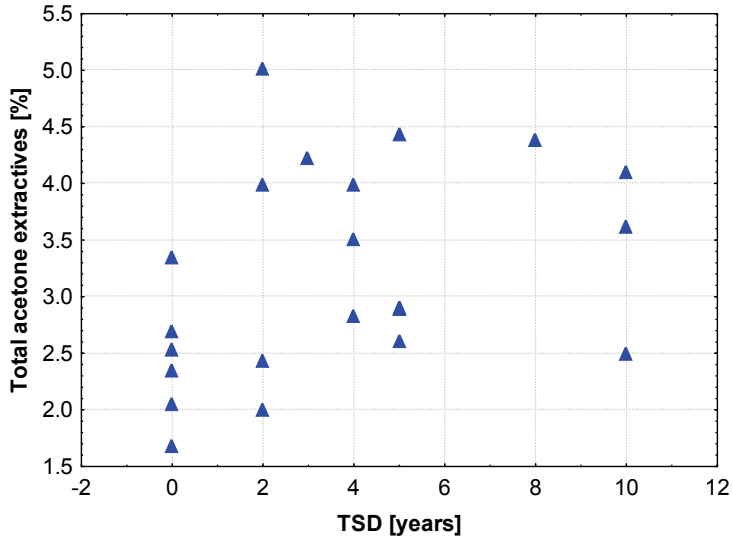


**Figure 43.** Total acetone extractives found at all sample sites of MPBI projects 8.15 and 8.65, as a function of TSD as estimated from tree appearance (extractive values shown are site averages).

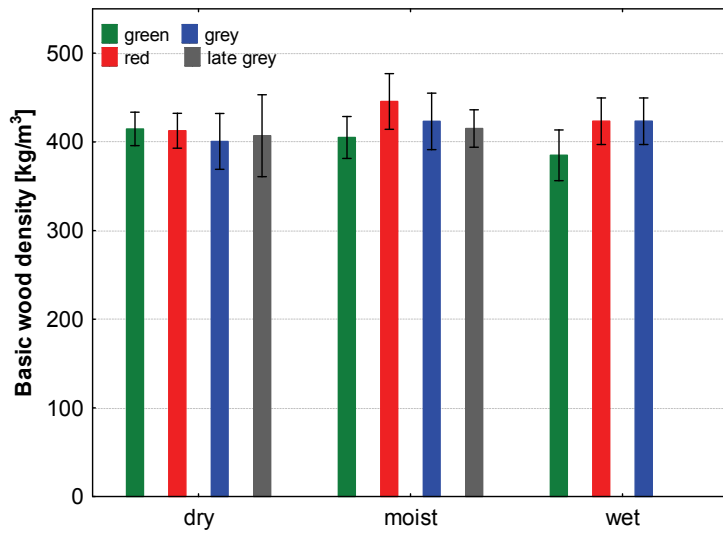


**Figure 44.** Basic wood density for the 60 – 80 years age class of sites selected for pulping trials, determined by SilviScan.

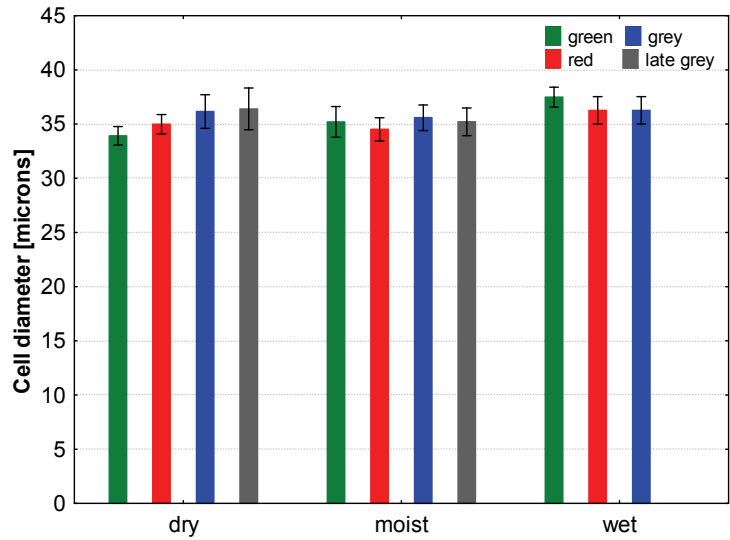


**Figure 45.** Wood fibre diameter for the 60 – 80 years age class of sites selected for pulping trials, determined by SilviScan.

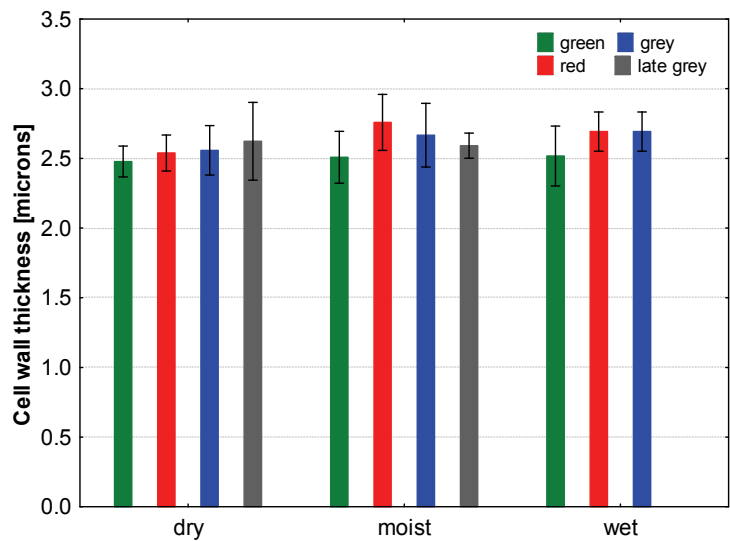


**Figure 46.** Wood fibre cell wall thickness for the 60 – 80 years age class of sites selected for pulping trials, determined by SilviScan.

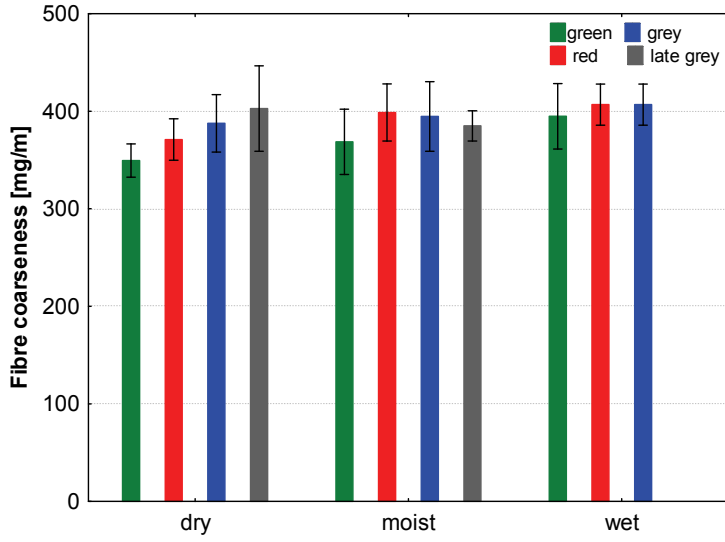


**Figure 47.** Wood fibre coarseness for the 60 – 80 years age class of sites selected for pulping trials, determined by SilviScan.

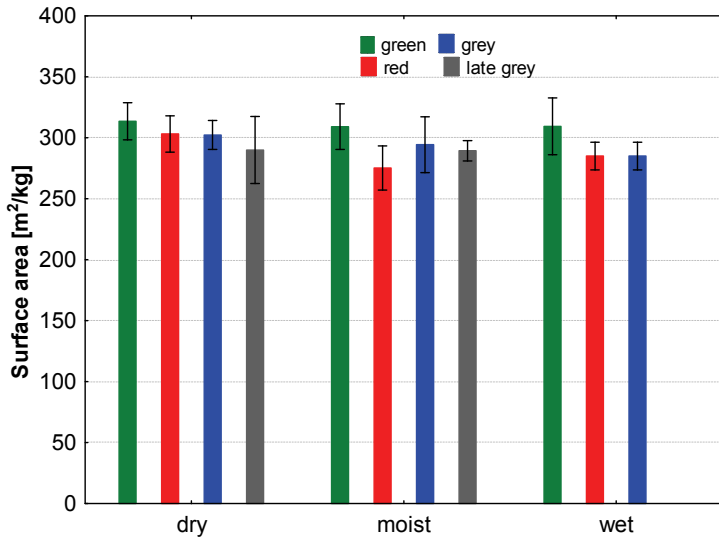


**Figure 48.** Specific surface area for the 60 – 80 years age class of sites selected for pulping trials, determined by SilviScan.

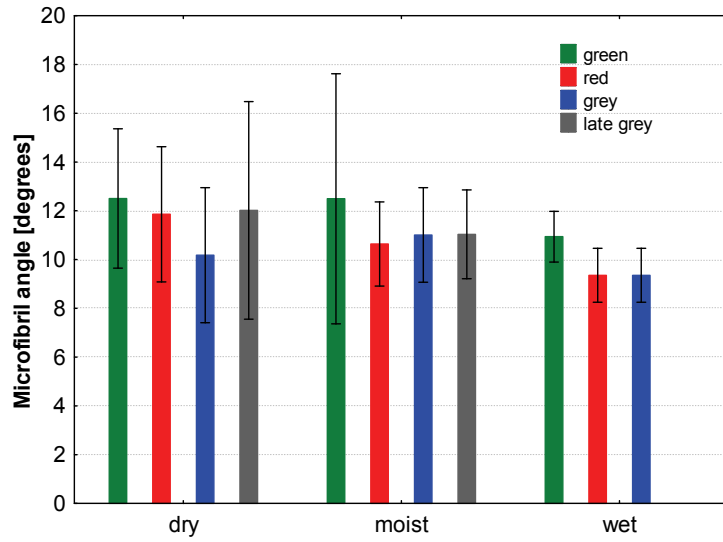


**Figure 49.** Microfibril angle for the 60 – 80 years age class of sites selected for pulping trials, determined by SilviScan.

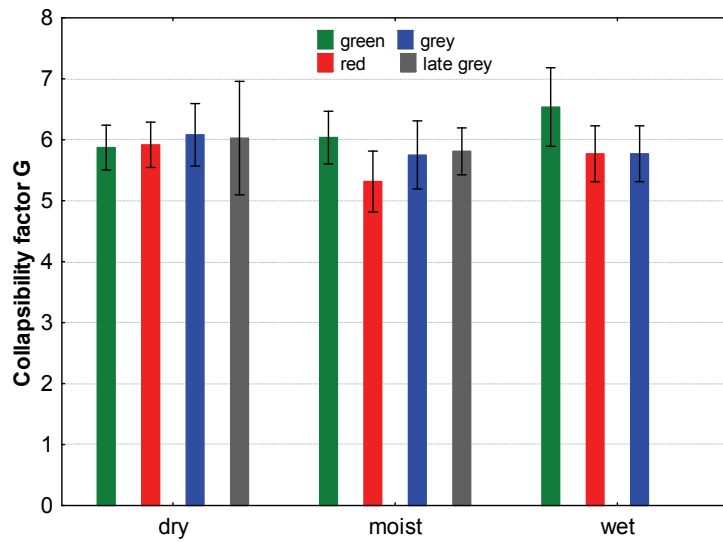


**Figure 50.** Collapsibility geometrical factor  $G$  for the 60 – 80 years age class of sites selected for pulping trials, determined by SilviScan.

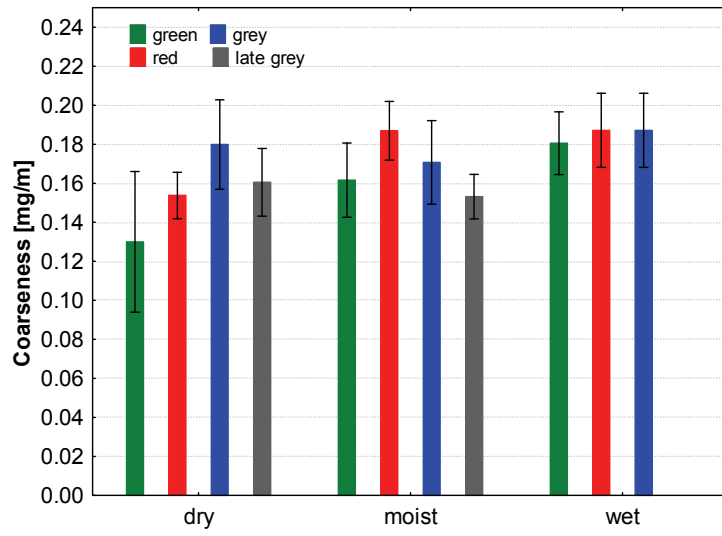


**Figure 51.** Fibre coarseness after maceration for the 60 – 80 years age class of sites selected for pulping trials, determined by FQA.



## Appendix B.

**Table 15.** Chip size distribution by sample sites, determined with the Gradex and Rader chip classifiers.

Site	18-01- green [%]	18-01- red [%]	05-02 [%]	01-01 [%]	15-01 [%]	SPF1 [%]	14-02 [%]	07-01 [%]	16-01 [%]	SPF-3- 2004 [%]	SPF-3- 2006 [%]
<b>Gradex</b>											
45mm - Round hole (over large)	0.3	0.0	1.6	0.3	0.0	1.0	0.3	0.6	0.3	0.5	3.2
10mm - Slot (overthick)	5.0	7.0	11.8	11.3	8.4	9.3	8.6	11.8	6.7	9.3	29.8
7mm - Round hole (accepts)	90.3	85.0	78.2	74.7	88.3	87.3	85.0	83.9	89.7	85.5	55.7
3mm - Round hole (pins)	4.3	7.3	7.3	11.5	3.3	1.9	5.3	3.6	3.3	4.1	10.0
Pan - Fines	0.0	0.7	1.1	2.2	0.0	0.4	0.7	0.2	0.0	0.7	1.4
<b>Rader</b>											
Fines	0.5	1.2	1.4	4.7	0.3		1.7	0.8	0.4		1.4
3 mm - Round hole (pins)	15.0	22.7	11.6	20.7	14.4		20.7	11.6	16.0		11.6
2 mm slots	68.8	56.9	54.0	49.7	66.7		56.8	61.1	67.7		54.0
4 mm slots	7.7	9.3	12.7	11.0	7.9		8.7	11.1	6.4		12.7
6 mm slots	3.4	3.5	7.1	3.6	3.7		4.5	4.3	4.4		7.1
8 mm slots	1.5	2.4	3.5	3.1	2.4		2.4	2.7	1.5		3.5
10 mm slots	2.3	2.8	4.3	4.2	3.3		3.2	4.0	2.4		4.3
12 mm slots	0.8	0.6	2.4	1.5	0.5		1.2	1.7	0.5		2.4
15 mm slots	0.1	0.7	3.0	1.5	0.8		0.8	2.7	0.8		3.0

**Table 16.** Chip densities and moisture contents by sample site.

Site	18-01- green [%]	18-01- red [%]	05-02 [%]	01-01 [%]	15-01 [%]	SPF1 [%]	14-02 [%]	07-01 [%]	16-01 [%]	SPF-3- 2004 [%]	SPF-3- 2006 [%]
Chip packing density [kg/m <sup>3</sup> ]	396	205	385	365	406	430	424	382	390	417	405
Chip basic density [kg/m <sup>3</sup> ]	202	406	205	193	212	219	218	205	202	222	219
Chip moisture [%]	44.9	83.1	86.4	89.1	48.2	73.4	79.1	82.8	52.1	67.3	78.1

Appendix C.

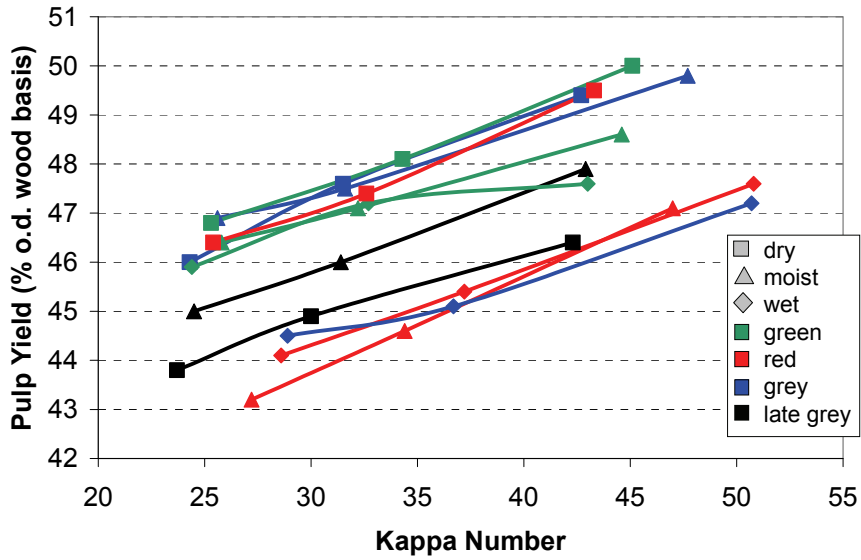


Figure 52. Pulp yield as a function of kappa number for all pulp samples.

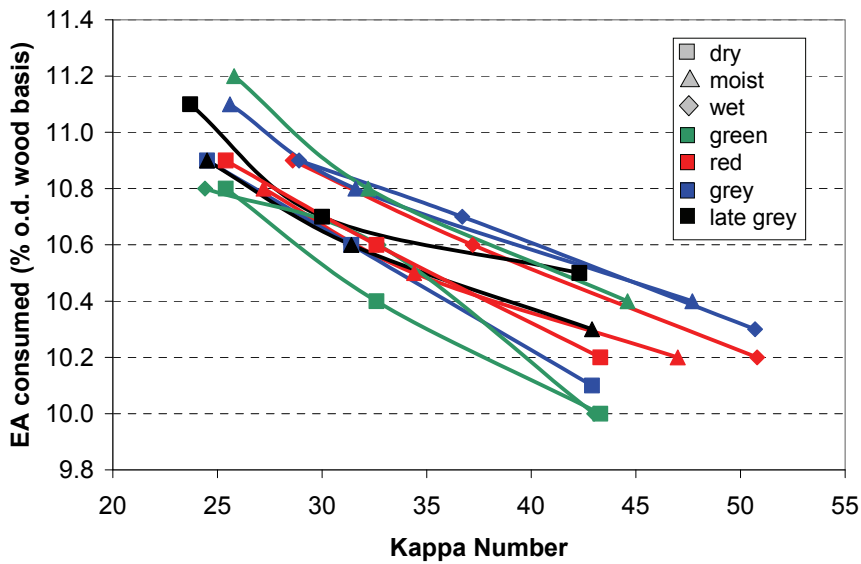
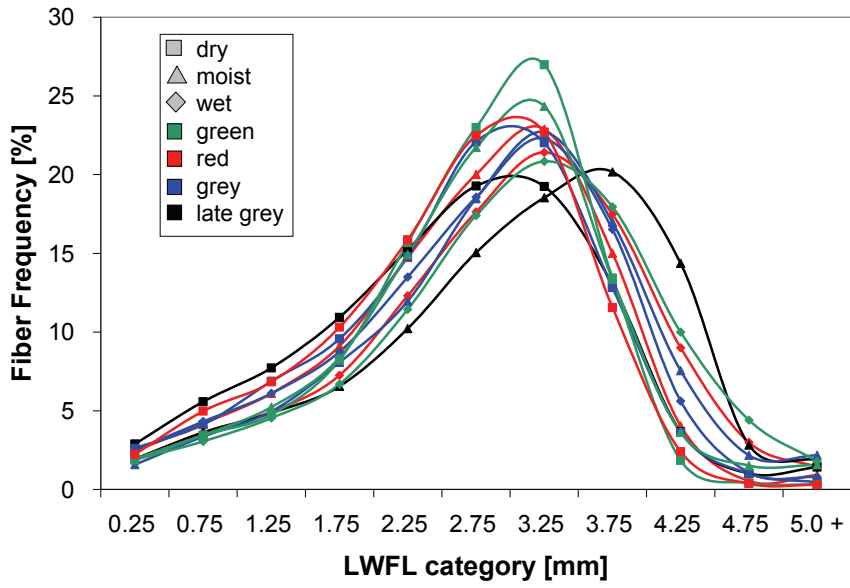
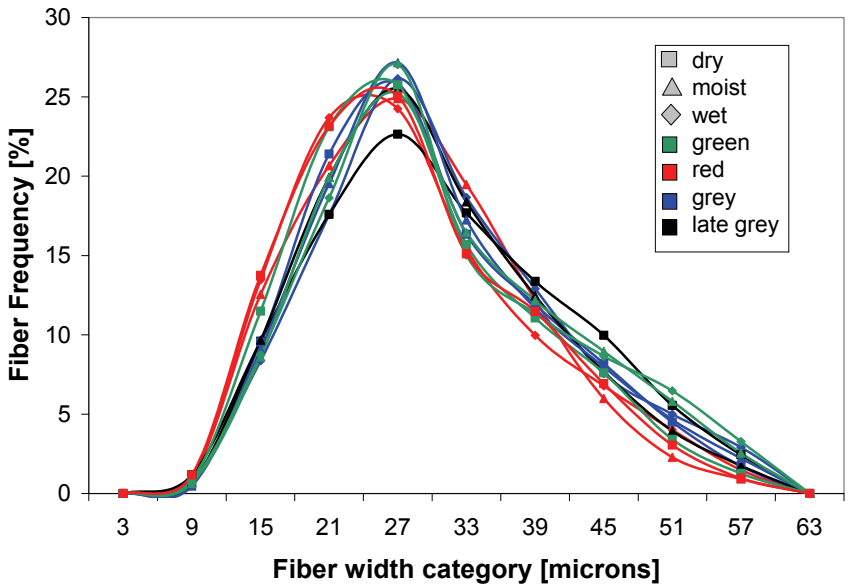


Figure 53. Consumed effective alkali as a function of kappa number for all pulp samples



**Figure 54.** Fibre length distribution (length weighted fibre length) of all pulp samples at kappa 30 and before PFI mill refining.



**Figure 55.** Fibre width distribution of all pulp samples at kappa 30 and before PFI mill refining.

**Table 17.** Kraft pulping data by sample site at kappa 30 (estimated by interpolation/extrapolation).

Site	18-01-green		18-01-red		05-02		01-01		15-01		SPF1		14-02		07-01		16-01		SPF-3-2004		SPF-3-2006			
	0	3000	6000	12000	0	3000	6000	12000	0	3000	6000	12000	0	3000	6000	12000	0	3000	6000	12000	0	3000	6000	12000
Unscreened yield [%]	47.5	48.6	48.6	47.1	44.8	46.7	43.7	45.8	46.6	44.3	44.5	44.3	44.3	44.3	44.3	44.3	44.3	44.3	44.3	44.3	44.3	44.3	44.3	44.3
H-Factor	1310	1286	1286	1244	1212	1295	1367	1248	1262	1443	1447	1443	1443	1443	1443	1443	1443	1443	1443	1443	1443	1443	1443	1447
Effective alkali consumed [%]	10.6	10.7	10.7	10.6	10.8	11.0	10.7	10.9	10.6	10.8	10.9	10.6	10.7	10.6	10.7	10.6	10.6	10.6	10.6	10.8	10.8	10.8	10.8	10.9

**Table 18.** Kraft pulp and handsheet data as a function of PFI refining.

	Site 18-01-green				Site 18-01-red				Site 05-02				Site 01-01			
	0	3000	6000	12000	0	3000	6000	12000	0	3000	6000	12000	0	3000	6000	12000
PFI Rev.	701	660	579	385	703	667	582	406	710	664	569	342	692	661	581	389
Screened CSF [ml]	532	625	649	664	533	630	647	672	540	636	658	675	564	661	692	703
Apparent Density [kg/m <sup>3</sup> ]	6.2	9.5	10.4	11.0	5.5	8.3	9.5	9.9	5.8	8.9	9.9	10.8	6.6	9.0	10.1	10.8
Burst Index [kPa·m <sup>2</sup> /g]	8.3	11.6	12.5	12.8	7.9	10.0	11.1	11.6	7.7	9.6	11.8	12.1	8.6	10.3	10.7	11.3
Breaking Length [km]	81.1	113.7	123.0	125.6	77.3	98.3	109.3	113.6	75.4	94.1	115.5	119.1	84.3	101.2	104.7	111.0
Tensile Index [N·m/g]	1.61	3.01	3.23	3.52	1.70	2.52	3.14	3.28	1.55	2.43	3.31	3.45	2.04	3.14	3.17	3.36
Stretch [%]	17.2	15.8	14.7	13.0	15.6	15.4	12.7	11.8	17.1	15.1	13.5	11.1	13.8	12.9	11.4	10.3
Tear Index 1-ply [mN·m <sup>2</sup> /g]	19.1	15.5	14.2	13.1	17.2	14.9	12.4	11.9	17.7	14.7	12.3	11.5	13.9	12.2	11.6	10.3
Tear Index 4-ply [mN·m <sup>2</sup> /g]	18.0	18.5	19.5	19.2	20.1	19.9	20.1	20.1	18.0	18.3	18.1	17.6	18.0	17.0	16.5	17.7
Zero Span Breaking Length [km]	2.1	5.1	10.3	39.9	1.8	4.3	8.4	27.9	2.2	5.3	10.0	46.2	5.5	9.6	18.9	44.4
Gurley Air Resistance [sec/100 ml]	257	237	213	147	264	240	218	163	272	254	233	136	234	209	175	124
Sheffield Roughness [SU]	96.5	93.7	92.6	91.8	97.4	94.5	91.9	91.5	97.3	94.0	91.8	90.7	98.6	95.5	94.4	91.8
Opacity [%]	271	195	172	161	266	192	162	152	272	186	163	149	317	208	179	158
Scattering Coefficient [cm <sup>2</sup> /g]																

Kraft pulp and handsheet data as a function of PFI refining.

	Site 15-01			Site SPF-1			Site 14-02			Site 07-01						
	0	3000	6000	12000	0	3000	6000	12000	0	3000	6000	12000				
PFI Rev.	700	671	580	350	691	647	553	339	722	693	606	353	718	678	590	359
Screened CSF [ml]	546	622	653	675	560	663	681	707	507	620	641	648	534	630	654	685
Apparent Density [kg/m <sup>3</sup> ]	6.0	9.0	10.3	11.3	7.1	9.5	10.8	11.5	4.9	8.1	9.0	9.9	6.2	9.0	10.0	11.0
Burst Index [kPa·m <sup>2</sup> /g]	8.9	10.8	11.4	12.4	8.8	11.0	11.7	12.3	6.7	8.7	10.2	12.3	8.7	10.4	12.1	12.2
Breaking Length [km]	87.5	105.5	111.9	121.6	86	108	115	120	65.9	85.4	99.7	120.3	85.0	102.0	118.3	119.7
Tensile Index [N·m/g]	1.77	2.86	2.91	3.35	1.52	2.71	3.03	3.07	1.27	2.18	2.75	3.15	1.74	2.65	3.33	3.23
Stretch [%]																
Tear Index 1-ply [mN·m <sup>2</sup> /g]	16.8	16.9	14.3	12.7	15.8	12.2	10.9	10.4	17.9	15.5	15.0	13.7	17.3	15.8	14.9	12.0
Tear Index 4-ply [mN·m <sup>2</sup> /g]	16.4	15.9	13.6	12.8	15.0	11.6	10.8	10.2	20.0	15.3	13.0	13.4	18.3	14.7	13.0	11.8
Zero Span Breaking Length [km]	20.6	20.1	20.9	19.4	18.1	16.3	15.6	16.4	19.6	20.2	19.4	20.5	18.8	17.3	18.5	18.7
Gurley Air Resistance [sec/100 ml]	1.7	4.4	8.7	41.6	0.0	7.1	12.6	56.5	1.0	2.2	5.1	31.5	2.2	4.4	9.6	44.8
Sheffield Roughness [SU]	268	260	228	127	232	218	200	103	310	286	268	159	265	257	224	121
Opacity [%]	96.3	94.1	91.8	91.5	97.2	93.7	91.5	90.9	97.1	94.1	91.6	90.7	96.6	93.9	92.4	91.5
Scattering Coefficient [cm <sup>2</sup> /g]	248	178	149	142	272	185	162	148	246	168	145	141	263	194	167	149

Kraft pulp and handsheet data as a function of PFI refining.

PFI Rev.	Site 16-01				Site SPF-3-2004				Site SPF-3-2006			
	0	3000	6000	12000	0	3000	6000	12000	0	3000	6000	12000
Screened CSF [ml]	709	678	573	349	699	668	564	356	717	675	576	358
Apparent Density [kg/m <sup>3</sup> ]	529	628	649	664	524	625	642	680	516	626	648	674
Burst Index [kPa·m <sup>2</sup> /g]	5.6	8.6	9.8	10.7	6.4	8.6	10.1	10.5	5.3	9.0	9.9	10.3
Breaking Length [km]	8.1	10.5	11.8	12.7	9.4	10.7	11.3	12.0	7.6	10.5	10.8	12.5
Tensile Index [N·m/g]	79.2	103.2	115.3	124.2	93	105	111	118	74.5	102.6	106.3	122.1
Stretch [%]	1.55	2.58	2.93	3.08	1.54	3.02	3.00	3.29	1.64	2.69	2.70	3.40
Tear Index 1-ply [mN·m <sup>2</sup> /g]	19.3	16.7	14.1	12.8	18.1	16.8	14.3	13.2	18.6	13.8	13.0	11.7
Tear Index 4-ply [mN·m <sup>2</sup> /g]	20.7	15.8	13.9	12.2	18.9	16.3	14.1	13.0	19.2	13.7	12.5	11.2
Zero Span Breaking Length [km]	20.4	19.3	17.9	18.1	18.5	17.7	18.7	19.1	19.4	19.3	18.4	19.0
Gurley Air Resistance [sec/100 ml]	1.8	4.8	10.1	48.4	0.0	4.3	8.3	56.6	1.6	4.4	9.9	49.0
Sheffield Roughness [SU]	285	265	236	138	278	262	232	121	289	263	225	126
Opacity [%]	95.9	92.7	90.5	89.1	96.1	93.4	90.3	89.7	97.9	94.0	92.7	90.4
Scattering Coefficient [cm <sup>2</sup> /g]	254	173	148	139	250	178	155	149	267	172	151	130

**Table 19.** Kraft pulp and handsheet properties at 400 ml CSF (estimated by interpolation/extrapolation).

Site	18-01- green	18-01- red	05-02	01-01	15-01	SPF1	14-02	07-01	16-01	SPF-3- 2004	SPF-3- 2006
PFI Rev.	11536	12205	10467	11656	10696	10384	10885	10935	10634	10731	10844
Screened CSF [ml]	663	673	671	703	670	697	647	680	661	672	669
Apparent Density [kg/m <sup>3</sup> ]	11.0	9.9	10.6	10.7	11.1	11.5	9.7	10.8	10.5	10.4	10.2
Burst Index [kPa·m <sup>2</sup> /g]	12.8	11.6	12.0	11.3	12.2	12.2	11.9	12.2	12.5	11.8	12.1
Breaking Length [km]	125.4	113.7	118.1	110.6	119.4	119.8	116.5	119.5	122.2	116.2	119.1
Tensile Index [N·m/g]	3.50	3.29	3.42	3.35	3.25	3.35	3.08	3.21	3.05	3.23	3.26
Stretch [%]	13.2	11.8	11.7	10.4	13.1	10.9	13.9	12.5	13.1	13.5	12.0
Tear Index 1-ply [mN·m <sup>2</sup> /g]	13.2	11.9	11.7	10.3	12.9	10.7	13.5	12.0	12.6	13.2	11.5
Tear Index 4-ply [mN·m <sup>2</sup> /g]	19.2	20.1	17.7	17.8	19.7	17.3	20.7	18.7	18.2	19.2	19.1
Zero Span Breaking Length [km]	37.7	28.5	36.9	42.9	34.4	43.6	26.6	38.5	39.7	46.4	41.5
Gurley Air Resistance [s/100 ml]	152	161	161	126	149	138	179	139	160	144	145
Sheffield Roughness [SU]	91.9	91.5	91.0	91.9	91.5	90.9	90.9	91.7	89.4	89.9	90.9
Opacity [%]	162	151	152	159	143	151	141	152	141	150	134
Scattering Coefficient [cm <sup>2</sup> /g]	11536	12205	10467	11656	10696	10384	10885	10935	10634	10731	10844

## Appendix D.

Table 20. Properties of TMP (raw data).

	Site 18-01 green dry/green		Site 18-01 red dry/red		Site 05-02 dry/grey		Site 01-01 dry/late					
Unscreened CSF [ml]	82	120	183	71	120	188	84	112	205	69	114	203
Specific Refining Energy [MJ/kg]	11.9	10.2	8.5	13.3	11.2	9.4	12.1	10.5	8.3	12.4	10.2	8.2
Screened CSF [ml]	82	121	200	71	123	184	89	126	229	75	126	197
Reject [% o.d. pulp]	0.0	0.0	0.1	0.0	0.0	0.1	0.0	0.0	0.2	0.0	0.0	0.1
Apparent Sheet Density [kg/m <sup>3</sup> ]	390	357	327	377	327	314	366	333	288	374	321	302
Burst Index [kPa•m <sup>2</sup> /g]	2.9	2.6	2.2	2.7	2.3	2.2	2.6	2.3	1.8	2.3	1.8	1.5
Tensile Index [N•m/g]	46	42	37	47	39	37	44	38	32	38	30	28
Stretch [%]	1.73	1.77	1.64	1.76	1.65	1.71	2.02	1.79	1.55	1.61	1.58	1.47
Tear Index, 4 ply [mN•m <sup>2</sup> /g]	8.1	8.2	8.7	7.2	8.3	8.5	7.8	8.9	9.6	6.6	7.4	7.6
Brightness [%]	59	60	59	53	54	54	52	52	51	49	50	49
ISO Opacity [%]	94.8	94.1	92.8	97.2	95.9	95.5	98.1	97.4	96.4	98.7	98.4	97.6
Scattering Coefficient [cm <sup>2</sup> /g]	585	570	538	598	552	533	603	572	524	676	657	593
Sheffield Roughness [SU]	145	200	239	163	231	252	264	273	312	217	276	289
<i>Bauer/McNett fractions</i>												
R 14 [%]	9.5	11.4	12.4	9.8	13.1	13.9	9.6	11.1	15.1	5.8	7.3	9.1
R 14/28 [%]	30.8	31.2	32.6	30.2	32.3	33.4	30.7	31.4	32.5	27.7	29.3	30.5
R 28/48 [%]	18.1	18.1	18.4	17.3	17.1	17.1	17.4	17.3	16.6	19.7	19.4	18.9
R 48/100 [%]	9.9	10.0	9.9	8.4	8.8	8.5	9.5	9.4	8.6	11.7	11.5	11.0
R 100/200 [%]	5.3	5.1	4.5	5.6	4.9	4.4	5.2	5.0	4.2	6.5	5.6	4.9
Pass 200 [%]	26.5	24.2	22.3	28.8	23.8	22.8	27.6	25.8	22.9	28.7	26.9	25.5
R - 48 Fraction [%]	58.4	60.7	63.4	57.3	62.6	64.3	57.7	59.8	64.3	53.1	56.0	58.5
R - 28 Fraction [%]	40.3	42.6	44.9	40.0	45.5	47.2	40.3	42.5	47.7	33.5	36.6	39.6
<i>FQA</i>												
W. Weighted Fibre Length [mm]	2.19	2.24	2.25	2.20	2.25	2.29	2.24	2.26	2.37	2.08	2.14	2.19
L. Weighted Fibre Length [mm]	1.57	1.61	1.64	1.56	1.62	1.66	1.58	1.60	1.70	1.43	1.48	1.51
Arithmetic Fibre Length [mm]	0.66	0.67	0.70	0.61	0.64	0.66	0.61	0.62	0.66	0.57	0.59	0.59



Properties of TMP (raw data)

	Site 15-01 green moist/green		Site SPF-1 moist/red		Site 14-02 moist/grey		Site 07-01 moist/late				
Unscreened CSF [ml]	79	100	84	137	217	75	95	150	67	107	167
Specific Refining Energy [MJ/kg]	11.5	9.9	12.7	10.2	8.2	11.3	9.8	8.2	12.8	10.8	8.8
Screened CSF [ml]	86	112	87	152	218	79	106	151	75	108	172
Reject [% o.d. pulp]	0.0	0.1	0.0	0.1	0.1	0.1	0.1	0.1	0.0	0.0	0.1
Apparent Sheet Density [kg/m <sup>3</sup> ]	374	354	356	318	284	361	345	321	361	340	310
Burst Index [kPa•m <sup>2</sup> /g]	2.6	2.3	2.9	2.3	2.0	2.7	2.2	2.0	2.5	2.3	1.9
Tensile Index [N•m/g]	43	37	45.9	36.4	32.3	42	39	34	42	36	33
Stretch [%]	1.65	1.47	1.77	1.56	1.51	1.73	1.60	1.49	1.85	1.56	1.59
Tear Index, 4 ply [mN•m <sup>2</sup> /g]	7.7	7.9	8.1	9.1	10.1	7.5	7.9	8.3	7.8	8.7	9.0
Brightness [%]	57	57	53	54	53	50	51	51	51	51	51
ISO Opacity [%]	95.7	94.5	97.2	96.7	95.9	97.3	96.8	96.5	98.0	97.5	97.0
Scattering Coefficient [cm <sup>2</sup> /g]	579	548	620	600	552	537	527	524	641	618	580
Sheffield Roughness [SU]	184	211	227	279	315	217	244	259	263	273	277
<i>Bauer/McNett fractions</i>											
R 14 [%]	8.7	9.6	12.0	14.9	16.9	10.9	11.1	12.4	10.9	12.6	15.0
R 14/28 [%]	29.9	30.9	29.3	30.1	29.7	30.3	31.1	31.5	29.1	29.8	30.3
R 28/48 [%]	18.5	18.2	15.8	15.4	15.1	18.3	18.8	18.9	16.9	16.6	16.3
R 48/100 [%]	10.0	10.0	8.8	8.5	8.5	9.7	10.0	9.9	9.4	9.2	8.8
R 100/200 [%]	5.8	5.1	5.7	5.0	4.6	5.4	5.3	4.9	5.3	5.4	4.4
Pass 200 [%]	27.2	26.1	28.5	26.1	25.2	25.4	23.9	22.5	28.4	26.6	25.2
R - 48 Fraction [%]	57.1	58.7	57.1	60.4	61.7	59.6	60.9	62.8	56.9	58.9	61.6
R - 28 Fraction [%]	38.6	40.5	41.3	45.0	46.7	41.2	42.1	43.9	40.0	42.3	45.3
<i>FQA</i>											
W. Weighted Average Fibre Length [mm]	2.16	2.21	2.40	2.41	2.42	2.26	2.28	2.33	2.35	2.42	2.50
L. Weighted Average Fibre Length [mm]	1.52	1.56	1.81	1.83	1.85	1.56	1.57	1.63	1.60	1.67	1.72
Arithmetic Average Fibre Length [mm]	0.61	0.63	0.93	0.95	0.96	0.60	0.60	0.63	0.59	0.62	0.63

Properties of TMP (raw data)

	Site 16-01 green wet/green		Site SPF-3-2004 wet/red		Site SPF-3-2006 wet/grey	
Unscreened CSF [ml]	70	117	181	76	113	173
Specific Refining Energy [MJ/kg]	12.2	10.0	8.2	12.6	10.5	8.5
Screened CSF [ml]	76	125	198	78	125	183
Reject [% o.d. pulp]	0.0	0.1	0.3	0.0	0.1	0.3
Apparent Sheet Density [kg/m <sup>3</sup> ]	383	343	313	353	333	294
Burst Index [kPa•m <sup>2</sup> /g]	2.8	2.5	2.1	2.9	2.5	2.2
Tensile Index [N•m/g]	46	40	34	43.8	39.2	32.9
Stretch [%]	1.77	1.68	1.45	1.69	1.65	1.49
Tear Index, 4 ply [mN•m <sup>2</sup> /g]	8.1	8.7	9.8	8.1	9.0	9.7
Brightness [%]	57	59	58	53	54	54
ISO Opacity [%]	95.2	94.2	93.1	97.8	97.4	96.5
Scattering Coefficient [cm <sup>2</sup> /g]	575	562	532	639	616	566
Sheffield Roughness [SU]	179	225	276	250	276	302
<i>Bauer/McNett fractions</i>						
R 14 [%]	14.7	15.5	19.0	15.5	15.1	17.0
R 14/28 [%]	29.5	30.4	30.6	29.1	30.2	30.6
R 28/48 [%]	16.0	15.4	15.3	14.9	14.6	14.5
R 48/100 [%]	8.2	8.1	7.5	7.8	7.8	7.8
R 100/200 [%]	5.1	4.9	4.5	5.4	4.6	4.2
Pass 200 [%]	26.5	25.7	23.1	28.4	27.6	25.9
R - 48 Fraction [%]	60.2	61.3	64.9	58.4	59.9	62.1
R - 28 Fraction [%]	44.2	45.8	49.6	44.6	45.3	47.6
<i>FQA</i>						
W. Weighted Average Fibre Length [mm]	2.46	2.47	2.50	2.42	2.48	2.53
L. Weighted Average Fibre Length [mm]	1.69	1.73	1.76	1.86	1.91	1.93
Arithmetic Average Fibre Length [mm]	0.62	0.64	0.66	0.96	0.98	0.98
				2.20	2.22	2.40
				1.47	1.48	1.60
				0.58	0.58	0.62

**Table 21.** TMP data interpolated to 100 ml CSF.

	SRE [MJ/kg]	R-48 [%]	R-28 [%]	P-200 [%]	LWFL [mm]	Sheet density [kg/m <sup>3</sup> ]	Tensile index [Nm/g]	Tear index [mNm <sup>2</sup> /g]	Sheff. Rough. [SU]	Scatt. Coeff. [cm <sup>2</sup> /g]	Brightn. [%]	ISO Opacity [%]
Site 18-01 green	11.1	59.4	41.9	25.5	1.59	375	44	8.2	170	578	59	94.5
Site 18-01 red	12.1	59.8	43.3	26.3	1.59	353	43	7.9	192	575	54	96.6
Site 05-02	11.1	58.4	41.0	27.0	1.59	354	42	8.2	266	593	52	97.9
Site 01-01	10.8	54.5	34.7	27.9	1.45	349	35	7.1	250	664	50	98.5
Site 15-01	9.9	57.9	39.6	26.6	1.54	364	40	7.8	197	564	57	95.2
SPF-1	11.8	58.1	42.6	28.0	1.81	348	43	8.3	239	618	53	97.1
Site 14-02	9.7	60.6	42.0	24.3	1.57	350	40	7.8	233	531	51	97.0
Site 07-01	11.3	58.2	41.4	27.3	1.64	346	38	8.5	268	624	51	97.7
Site 16-01	10.9	60.8	44.5	26.0	1.71	364	43	8.4	199	568	58	94.7
SPF-3-2004	11.4	59.1	44.5	28.0	1.89	344	42	8.5	263	627	54	97.6
SPF-3-2006	11.0	53.7	36.4	29.1	1.48	336	36	7.8	260	612	51	97.8

**Table 22.** TMP data interpolated to 10 MJ/kg specific refining energy.

	CSF [ml]	R-48 [%]	R-28 [%]	P-200 [%]	LWFL [mm]	Sheet density [kg/m <sup>3</sup> ]	Tensile index [Nm/g]	Tear index [mNm <sup>2</sup> /g]	Sheff. Rough. [SU]	Scatt. Coeff. [cm <sup>2</sup> /g]	Brightn. [%]	ISO Opacity [%]
Site 18-01 green	128	61.1	42.9	23.9	1.61	353	41	8.2	200	562	59	93.8
Site 18-01 red	161	64.0	46.9	22.8	1.64	318	38	8.4	245	539	54	95.6
Site 05-02	128	60.7	43.5	25.2	1.64	323	37	9.1	286	559	51	97.1
Site 01-01	120	56.3	36.9	26.8	1.48	326	30	7.4	279	653	50	98.2
Site 15-01	100	58.5	40.2	26.3	1.56	354	37	7.9	211	548	57	94.9
SPF-1	142	60.5	45.1	26.0	1.83	314	36	9.3	280	599	53	96.5
Site 14-02	90	60.7	42	24.0	1.57	345	39	7.9	244	527	51	96.9
Site 07-01	127	59.9	43.5	26.0	1.69	326	35	8.7	274	600	51	97.3
Site 16-01	117	61.3	45.9	25.7	1.73	343	40	8.7	225	562	58	94.1
SPF-3-2004	125	60.3	45.7	27.3	1.91	326	37	9.2	282	607	54	97
SPF-3-2006	126	55.2	38.3	27.9	1.54	320	32	8.0	275	586	50	97.3

**Table 23.** Properties of calendered TMP handsheets (dry subzone samples).

	Site 18-01 green		Site 18-01 red		Site 05-02		Site 01-01		
	Dry, green		Dry, red		Dry, grey		Dry, late grey		
PPS S10 roughness [ $\mu\text{m}$ ]	7.7	4	3.5	7.9	4	3.5	7.4	4	3.5
Calendering nip load [ $\text{kN/m}$ ]		115	172		110	170		60	110
Unscreened CSF [ml]	92			100			94		100
Specific Refining Energy [ $\text{MJ/kg}$ ]	11.2			10.7			11.6		11.0
Screened CSF [ml]	94			105			91		101
Reject [% o.d. pulp]	0.1			0.1			0.1		0.0
Apparent Sheet Density [ $\text{kg/m}^3$ ]	361	610	661	350	593	657	354	591	654
Burst Index [ $\text{kPa}\cdot\text{m}^2/\text{g}$ ]	2.5	1.2	0.8	2.3	1.1	0.8	2.5	1.2	0.8
Tensile Index [ $\text{N}\cdot\text{m/g}$ ]	42	20	20	41	21	19	41	22	16
Stretch [%]	1.63	0.67	0.66	1.48	0.70	0.59	1.65	0.74	0.53
Tear Index [ $\text{mN}\cdot\text{m}^2/\text{g}$ ] [4 Ply]	7.8	3.9	2.5	7.6	3.8	2.8	7.6	4.2	3.0
Brightness [%]	59			53			52		49
ISO Opacity [%]	94.4	93.8	93.2	96.7	96.7	96.1	97.8	97.9	97.3
Scattering Coefficient [ $\text{cm}^2/\text{g}$ ]	590	565	533	564	555	497	571	574	522
Sheffield Roughness [Rough side] [SU]	382	93	86	389	109	100	388	94	86
Sheffield Roughness [Smooth side] [SU]	189						257		213
Air Resistance [Gurley] [sec/100mL]	60	211	268	N/A	152	312	75	212	313
<i>BauerMcNett fractions</i>									
R 14 [%]	6.3			5.6			10.5		6.4
R 14/28 [%]	31.6			31.2			32.6		29.8
R 28/48 [%]	20.6			20.1			17.8		19.7
R 48/100 [%]	10.9			10.2			8.7		10.7
R 100/200 [%]	6.9			6.5			5.9		7.2
Pass 200 [%]	23.8			26.3			24.5		26.2
R-48 fraction [%]	58.4			56.9			60.9		55.9

## Appendix E.

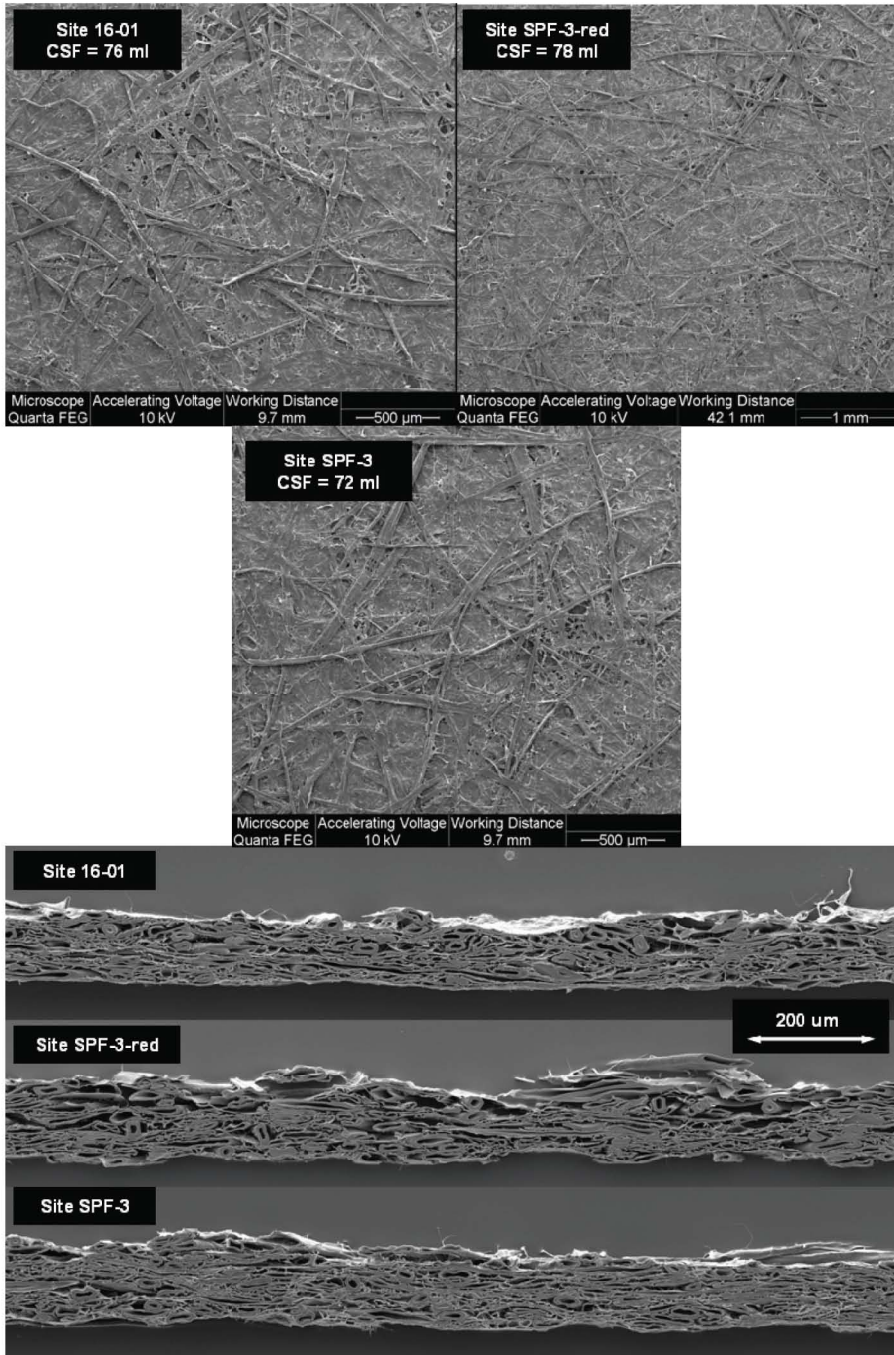
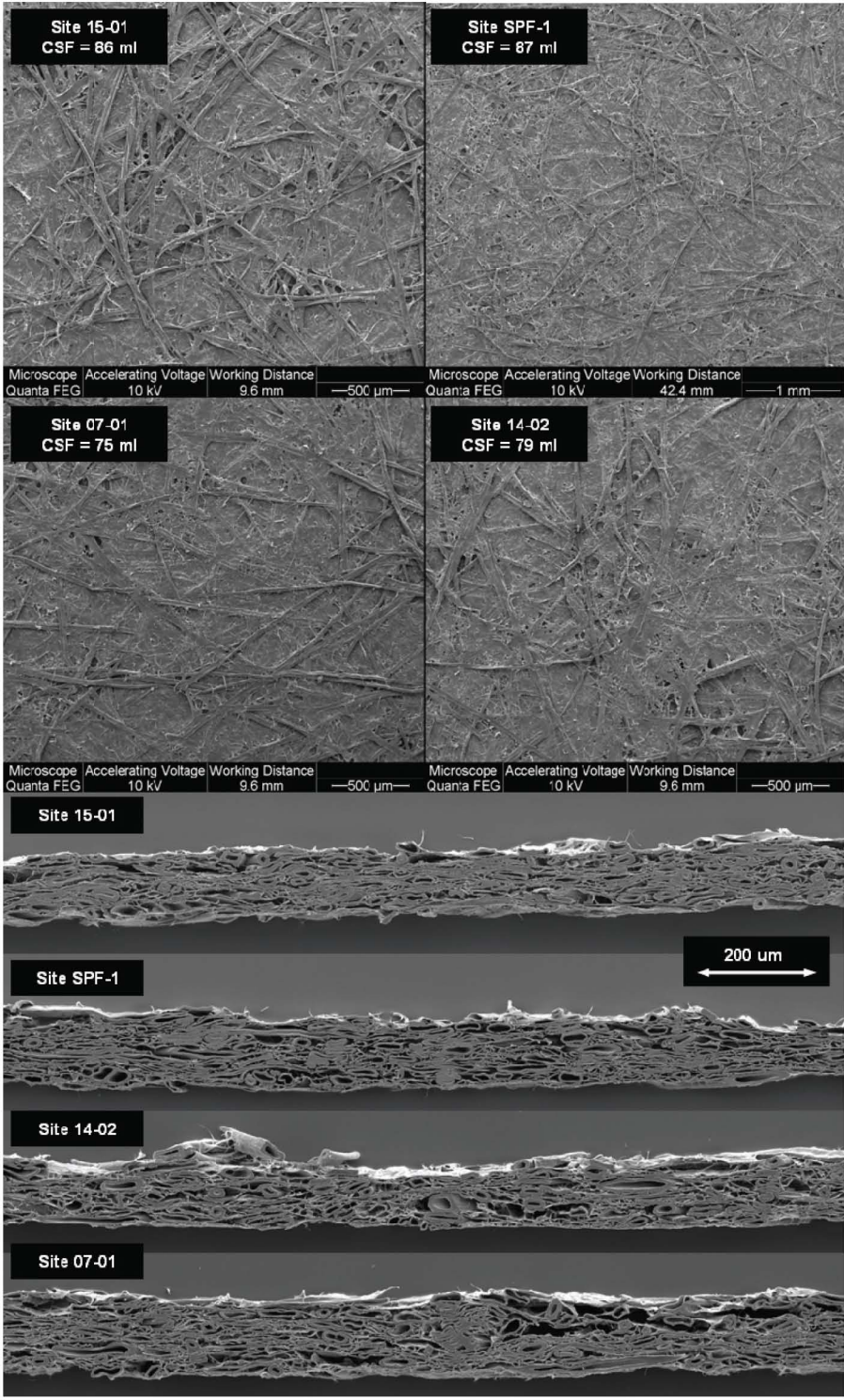
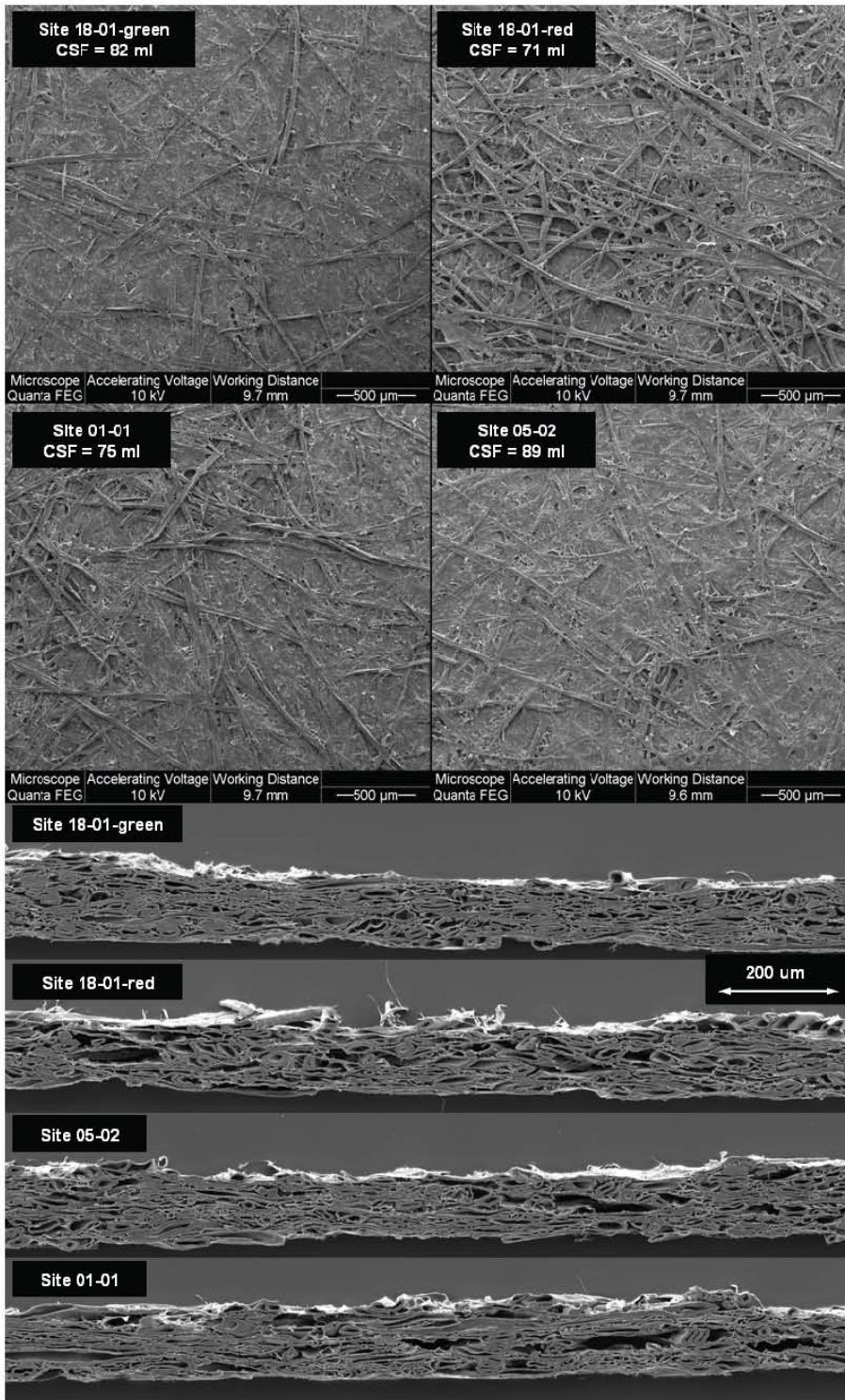


Figure 56. Surface and cross-section images of TMP sheets from "wet" sites.



**Figure 57.** Surface and cross-section images of TMP sheets from “moist” sites.



**Figure 58.** Surface and cross-section images of TMP sheets from “dry” sites.